3-10-2010

Nuclear Forensics: Measurements of Uranium Oxides Using Time-of-Flight Secondary Ion Mass Spectrometry (TOF-SIMS)

Wesley A. Schuler

NUCLEAR FORENSICS: MEASUREMENTS OF URANIUM OXIDES USING TIME-OF-FLIGHT SECONDARY ION MASS SPECTROMETRY (TOF-SIMS)

THESIS

Wesley A. Schuler, MSgt, USAF

AFIT/GWM/ENP/10-M03

DEPARTMENT OF THE AIR FORCE
AIR UNIVERSITY

AIR FORCE INSTITUTE OF TECHNOLOGY

Wright-Patterson Air Force Base, Ohio

The views expressed in this thesis are those of the author and do not reflect the official policy or position of the United States Air Force, Department of Defense, or the United States Government.

AFIT/GWM/ENP/10-M03

NUCLEAR FORENSICS: MEASUREMENTS OF URANIUM OXIDES USING TIME-OF-FLIGHT SECONDARY ION MASS SPECTROMETRY (TOF-SIMS)

THESIS

Presented to the Faculty

Department of Engineering Physics

Graduate School of Engineering and Management

Air Force Institute of Technology

Air University

Air Education and Training Command

In Partial Fulfillment of the Requirements for the

Degree of Master of Science in Combating Weapons of Mass Destruction

Wesley A. Schuler, BS

MSgt, USAF

March 2010

APPROVED FOR PUBLIC RELEASE; DISTRIBUTION UNLIMITED

AFIT/GWM/ENP/10-M03

NUCLEAR FORENSICS: MEASUREMENTS OF URANIUM OXIDES USING TIME-OF-FLIGHT SECONDARY ION MASS SPECTROMETRY (TOF-SIMS)

Wesley A. Schuler, BS

MSgt, USAF

Approved:

Larry W. Burggraf	10 Mar 2010
Larry Burggraf, Professor (Chairman)	Date
	10 Mar 2010
James Petrosky, Professor (Member)	Date
Daniel L Felker	10 MAR 2010
Daniel Felker (Member)	Date

Abstract

Over the past decade, law enforcement, governmental and public agencies have been stymied by the threat of the trafficking of nuclear materials. During this time span, reports from the International Atomic Energy Agency of illicit trafficking have increased eightfold from 20 to 160. For this reason, nuclear forensics is a burgeoning science focused on the identification of seized special nuclear materials. Identification of these materials is based upon the wealth of information that can be obtained by applying multiple analytical and measurement technologies. All of the information gained from each sample can then be used to further characterize other samples culminating in the inclusion of all of the collected data into a central database.

Information must be reported in a timely manner as actionable results need to be presented as quickly as possible if there is to be any attribution for trafficking of nuclear material. Identification parameters such as uranium content, isotopic composition, and levels of impurities can be measured simultaneously in an effort to completely characterize a sample. All of these measurements combined can offer information as to the source of the material and its intended use. Many of the current analytical techniques used in nuclear forensics require extensive sample preparation and offer minimal amounts of information about the sample. Time-of-Flight Secondary Ion Mass Spectrometry (TOF-SIMS) is presented as a rapid analytical technique that provides many of these identification parameters with minimal sample preparation.

TOF-SIMS spectra were collected on eight different standard reference materials covering a range of stoichiometries and levels of enrichment. Samples included UO_2, UO_3 and U_3O_8 stoichiometries ranging from slightly depleted (0.5% ^{235}U) to highly enriched (90.0% ^{235}U) uranium. Spectra were simulated in an effort to deconvolve composite peaks resulting from the protonation of cluster ions. The levels of protonation were quantified through the solutions of series of simultaneous equations. Spectra were then reassessed with a hydrocarbon subtraction from the $^{235}UO_2^+$ and $^{238}UO_2^+$ peaks to provide extremely accurate isotopic measurements. Analysis of the results revealed that actionable information could be determined rapidly with minimal sample preparation.

To my wife

Acknowledgments

First and foremost, I would like to thank my father, God, for the many blessings He has bestowed upon me and my family. My wife deserves more thanks than I am capable of giving for her patience, support and sacrifice over the past 18 months. Without her continued support, encouragement, and acting as a general sounding board, this entire experience would have been lost. Thank you to Maj LaVern Starman and Dr. Andrew Terzuoli for the contributions of silicon wafers for use as the sample mounting material. Thank you to Mr. Rick Patton for the SEM images of the cerium oxide samples. Thank you to Mr. Chris Anthony for all of the help with the radioactive material packaging and shipment guidance. Thank you to Mr. Eric Taylor for all of your help with the sample preparation and expertise in the laboratory. Thank you to Dr. Daniel Felker for all of your help, guidance and direction over the course of this project. Thank you to Dr. Larry Burggraf for all of your patience, understanding and quest for knowledge. It is a wealth of encouragement to know that people like you exist in this world with your capacity of understanding, intelligence and expectations of greatness. Special thanks go out to the collaborators at the State University of New York. Without the use of the TOF-SIMS instrument and further reprocessing of the data, none of this research would have been possible.

MSgt Wesley A. Schuler

Table of Contents

Page

Page

Page

List of Figures

Figure Page

Figure Page

Figure Page

List of Tables

Table Page

List of Acronyms

Acronym		Page
CRM	Certified Reference Material	29
SUNY	State University of New York	33
AFRL	Air Force Research Laboratory	34
FWHM	Full Width at Half Maximum	47
ALARA	As Low As Reasonably Achievable	83
PRSO	Permit Radiation Safety Officer	85
AFIT	Air Force Institute of Technology	86
WPAFB	Wright Patterson Air Force Base	86
RSO	Radiation Safety Office	86
LMIG	Liquid Metal Ion Gun	119
CC	Charge Compensation	120

NUCLEAR FORENSICS: MEASUREMENTS OF URANIUM OXIDES USING TIME-OF-FLIGHT SECONDARY ION MASS SPECTROMETRY (TOF-SIMS)

I. Introduction

1.1 Motivation for Nuclear Forensics

In his "Atoms for Peace" address to the general assembly of the United Nations (UN) on 8 December, 1953, United States (US) President Dwight D. Eisenhower laid the foundation for the creation of the International Atomic Energy Association (IAEA) (Fischer, 2007). The Statute, which was the defining document that developed the framework and structure of the IAEA, was approved by 81 nations in October, 1956 (Fischer, 2007). The original structure of the IAEA was based on three pillars: these are nuclear verification and security, safety, and technology transfer (Gale, 2007). The IAEA was born the next year as a result of the growing fear and concern of the threat of the use of nuclear technology as a weapon (Fischer, 2007).

The ensuing years showed a political climate that was in turmoil and a technology boom that has still not ebbed to this day (Fischer, 2007). By 1958, the political climate had made such a turn that many of the tasks outlined in the original Statute become impossible to perform (Fischer, 2007). To aid in the vast development of nuclear technology, the IAEA opened a laboratory in Seibersdorf. During the same time, the IAEA began the work which led to the eventual creation of the Marine Environment Laboratory to study contamination effects from nuclear weapons testing (Gale, 2007). The Cuban missile crisis in 1962 provided an impasse for the US and former Soviet

Union to begin seeking a means for both arms control and the reduction of nuclear weapons inventories (Fischer, 2007).

As more countries were becoming nuclear weapons states, France in 1960 and China in 1964, there was public concern about the spread of this technology (Fischer, 2007). The original Statute of the IAEA only covered nuclear power plants and fuel and had no purview over the control of the proliferation of nuclear weapons (Gale, 2007). This lack of control led to strong support for international controls to prevent the proliferation of nuclear weapons and safeguards to ensure their spread as well as a reduction to the current national stockpiles (Gale, 2007). The approval of the Treaty on the Non-Proliferation of Nuclear Weapons (NPT) in 1968 put into effect such a means of control (Fischer, 2007).

Throughout the 1970's, the NPT gained support by almost the entire industrialized world as well as many of the rapidly-developing nations of the era (Fischer, 2007). Nuclear power was seen as the answer to the needs of global power production, especially in light of the oil crisis in 1973 (Fischer, 2007). As technology continued to improve, the functions of the IAEA continued to grow in an effort to control arms proliferation while providing nuclear power to all areas of the world (Gale, 2007). Nuclear power was becoming ever more commercially available and the NPT was to be the source document for its rapid growth (Fischer, 2007).

The rapid gain in popularity of nuclear technologies reached its peak in the early 1980's (Fischer, 2007). Its demise can be blamed on the Three-Mile Island (TMI) incident in 1979 and the Chernobyl accident in 1986 (Fischer, 2007). Efforts to promote

the now seemingly horrible use of nuclear materials were evidenced in 1988 when the IAEA and UN joined forces to develop a program to eradicate New World Screwworm, a deadly livestock disease (Gale, 2007). Other efforts by the Seibersdorf laboratory to promote the use of nuclear technology have included the use of radiation as medical treatments, radiography of aerospace industry parts and continued research into power production (Gale, 2007).

In the early 1990's, the once powerful Soviet Union collapsed and gave rise to a new crime: the illicit trafficking of Special Nuclear Material (SNM) (Mayer and others, 2007). Title I of the Atomic Energy Act of 1954 defines SNM as isotopes of plutonium, uranium-233, and uranium enriched in the isotopes uranium-233 or uranium-235 (NRC, 2007). 1991 brought the clandestine nuclear weapons program of Iraq to the world stage (Fischer, 2007). This event along with the discovery of North Korea's ongoing research efforts into nuclear weapons created doubt into the safeguards protocols of the IAEA and the organization's ability to limit the proliferation of nuclear weapons (Fischer, 2007).

These findings and the safety concerns over accidents like TMI and Chernobyl led to the development of tighter safety and security programs within the IAEA (Gale, 2007). Since then, the IAEA has recorded more than 800 such cases (Mayer and others, 2007). The Strategic Arms Reduction Treaties of 1991 and 1993 resulted in the dismantlement of numerous nuclear weapons by both the former Soviet Union and the United States. The surplus nuclear materials from the dismantled weapons increased the availability of SNM to rogue nations and advanced the threat of nuclear weapons proliferation (Grant

and others, 1998). From the consequences of these actions emerged a completely new science: nuclear forensics (Mayer and others, 2007).

1.2 Applications of Nuclear Forensics

Identification of materials from the nuclear forensics point of view insists that there is a large quantity of material of which to sample (Chivers and others, 2008 and Ferguson, 2006). In many instances this is simply not the case and scientists must rely on analytical techniques to uncover the proverbial needle in the haystack (Erdmann and others, 2009). Table 1 indicates many of the laboratory techniques currently being used to identify SNM by today's forensic scientists (Wallenius and Ray, 2006). A rapid, sensitive technique is needed to identify exactly which particles are of interest to further study (GAO, 2009). Time will simply not allow a researcher to fully characterize each and every particle present in some complex matrix (Bürger and Riciputi, 2009). Table 2 illustrates the typical timeline for the forensics investigation of intercepted nuclear material (APS, 2008). While there are many techniques available, there is no singular technique that provides all of the answers to our questions (Hou and Roos, 2008).

Table1. Information that can be obtained from nuclear material (adapted from Wallenius and Ray, 2006).

Parameter	Information	Analytical Technique
Appearance (Morphology)	Material type (powder, pellet)	Optical Microscopy
Dimensions (pellet)	Reactor type	Database
U Content	Chemical composition	Titration, HKED, IDMS
Isotopic Composition	Enrichment→intended use	HRGS, TIMS, ICP-MS, SIMS
Impurities	Production process; geolocation	ICP-MS, GDMS, SIMS
Age	Production date	AS, TIMS, ICP-MS
$^{18}O/^{16}O$ ratio	Geolocation	TIMS, SIMS
Surface roughness	Production plant	Profilometry
Microstructure	Production process	SEM. TEM

Table 2. Timeline for a nuclear forensic investigation of intercepted material (adapted from APS, 2008).

Techniques/Methods	24-Hours	1-Week	1-Month
Radiological	Estimated total activity Dose Rate (alpha, gamma, n) Surface Contamination		
Physical Characterization	Visual Inspection Radiography Photography Weight Dimension Optical Microscopy Density	SEM (EDS) XRD Organics	TEM (EDS)
Traditional Forensic Analysis	Fingerprints, Fibers		
Isotope Analysis	alpha-spectroscopy gamma-spectroscopy	Mass Spectrometry (SIMS, TIMS, ICPMS)	Radiochemical Separations Mass spec. for trace impurities: Pb Stable isotopes
Elemental/Chemical		ICP-MS XRF ICP-OES	GC/MS

1.3 Fields of Study for Nuclear Forensics

In the past, it has taken an entire suite of techniques such as alpha, beta and gamma spectroscopy (Hou and Roos, 2007), X-ray photoelectron spectroscopy (XPS), scanning electrochemical spectroscopy (SECM) (Broczkowski and others, 2006), Auger electron spectroscopy (AES) (Bonino and others, 2001), Fourier transform infrared spectroscopy (FTIR) (Zhu and others, 2001) and TIMS (Jakopič and other, 2009) in order to obtain all of the information in a chemical fingerprint. Figure 1 highlights many of the fields of study where such information is collected and exploited (Becker, 2003).

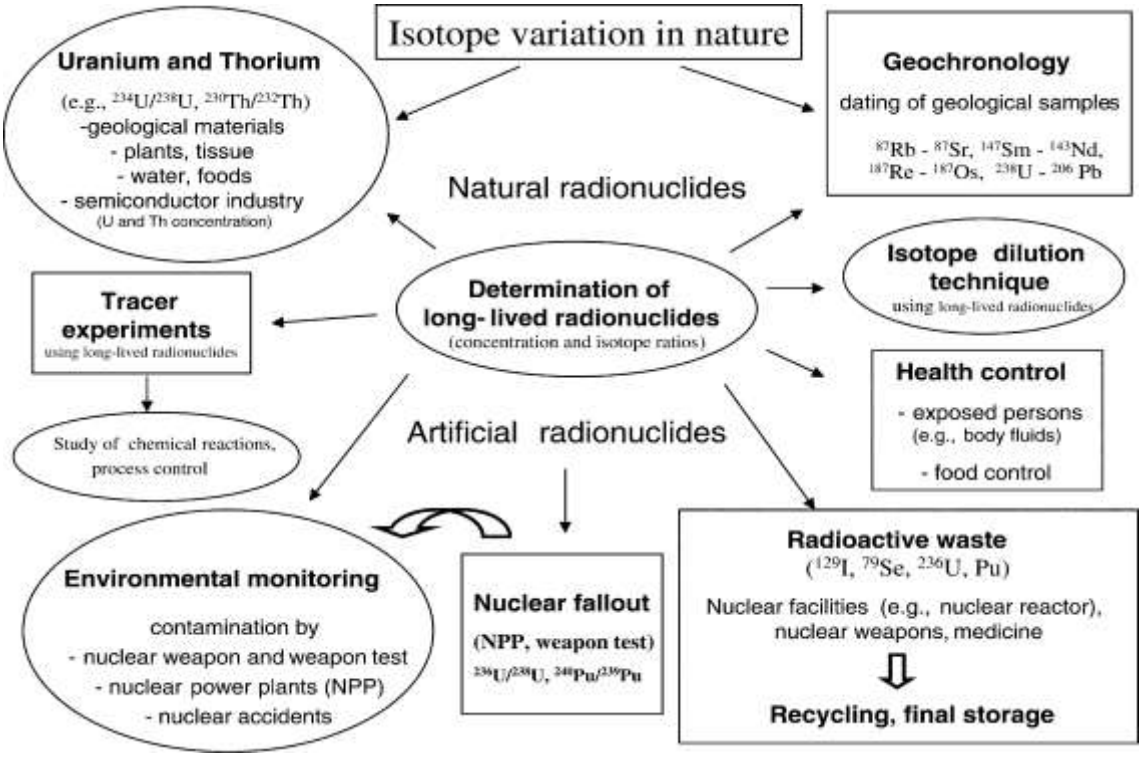

Figure 1. Overview of applicable fields of study for various nuclear forensics techniques (adapted from Becker, 2003).

A joint working group of the American Physical Society and the American Association for the Advancement of Science authored the current model of nuclear forensics analyses (APS, 2008). The report generated from their study highlights the relevant information and the widely varied scientific analysis techniques required to perform nuclear forensics investigations (APS, 2008). Figure 2 depicts the model action plan for a nuclear forensics analysis (APS, 2008). Much of this information can be provided using the singular technique of TOF-SIMS (Pajo, 2001 and Gerstmann and others, 2008).

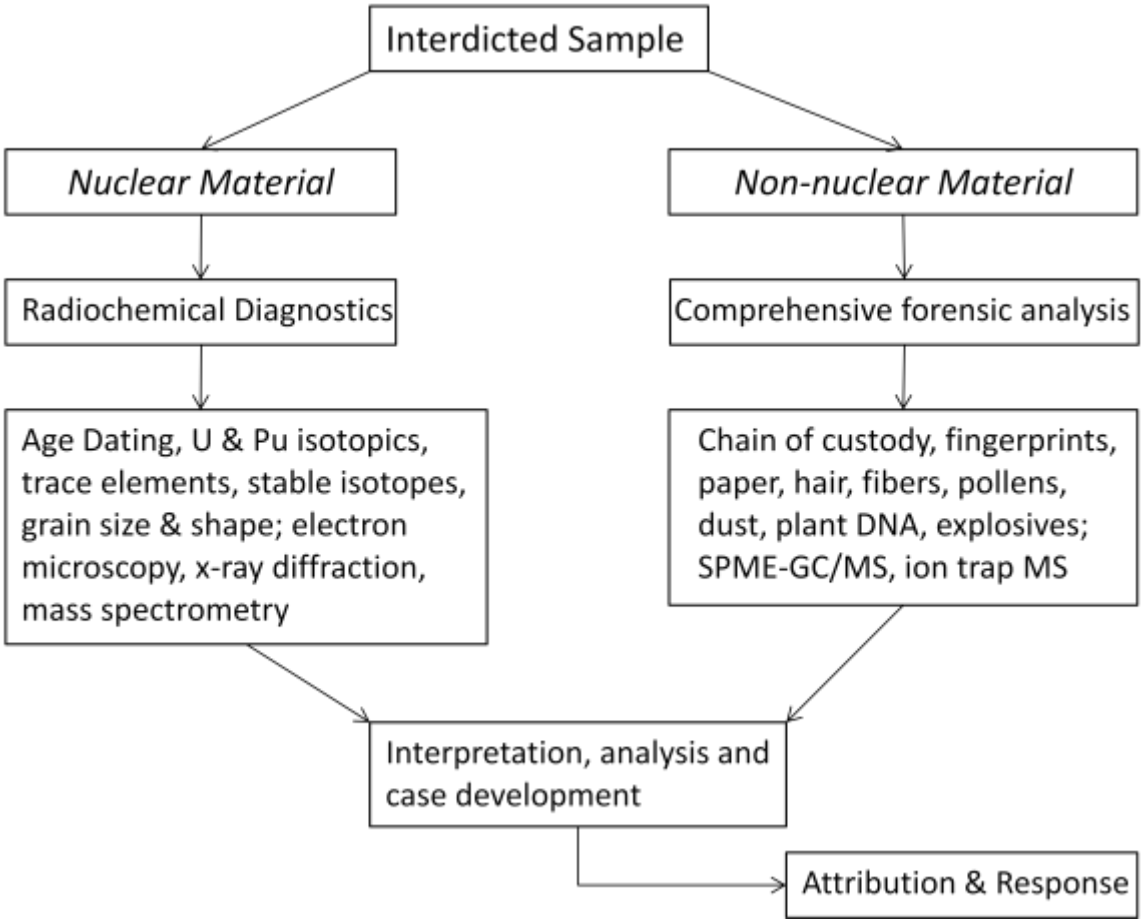

Figure 2. Model action plan for nuclear forensic analysis (adapted from APS, 2008).

II. Background

Over the past three decades, instances of illicit trafficking of nuclear materials have plagued law enforcement, public and governmental officials (Grant and others, 1998). This has given rise to the employment of nuclear forensics, the object of which is to quickly identify the composition and origin of materials obtained from traffickers (Mayer and others, 2007). Like most branches of forensics, the more we learn about techniques from past experience, the better we can classify, quantify and identify unknown materials (Halverson and Beals, 1999). Traditional laboratory techniques have been applied to nuclear materials identification using previous results such as impurities via mass spectrometry and mass spectroscopy and surface roughness via profilometry (Hou and Roos, 2008). In order to fully characterize any sample, several techniques can be applied to any given sample (Wallenius and Ray, 2006). From the wealth of data collected, a database containing data from many different measurements from many techniques can be constructed to help identify unknown materials (Pajo, 2001).

2.1 Uranium Forensics Characterization

Of specific interest in the nuclear forensics community is the study of uranium in its many varied forms (Pajo, 2001, Gnos, 2004, Allison, 2005 and Gerstmann and others, 2008). Ratios of isotopes, elemental impurities, and chemical form in given samples can provide information relating to the origins of the samples as well as chemical and physical processing (Betti and others, 1999). Uranium is a key component in nuclear weapons and it is imperative to determine any rogue states that wish to pursue a nuclear weapons program (Allison, 2005). Dose assessment is also of major concern to the

public at large, and measurements must be conducted to determine any risks associated with depleted, natural and enriched uranium in the environment (Gerstmann and others, 2008).

Uranium exists in a multitude of metallic and oxide forms, which leads to a wide range of stoichiometric and non-stoichiometric forms (Schueneman, 2001) and is found in all rocks and soils (Eisenbud and Merril, 1997). The partial pressure of oxygen in a given environment will determine the oxide form (Ohashi, 1974). Each of these oxide forms are very ionic and exist in valence states of U^{4+} and U^{6+} (Schueneman, 2001). Past studies of corrosion products from depleted uranium artillery shells has indicated the mean oxidation state of 4.6, suggesting a mixture of the U^{4+} and U^{6+} oxidation states (Gerstmann and others, 2008). Uranium also appears as inclusions in minerals, rocks and in the compositions of various alloys (Gnos, 2004). The trace and bulk measure of elemental abundances, isotopic composition and oxidation states provide a chemical fingerprint of the material being analyzed (Bürger and others, 2006). These chemical fingerprints can provide insight into the exact composition of unknown particles, where the particle originated and chemical processes that have occurred to the material (Nicolaou, 2006).

2.2 Inorganic Mass Spectrometry

Isotopic abundances of major and trace elements can reveal considerable information about the origin, age, intended purpose, as well as manufacturing and chemical processing of many different materials (Bürger and others, 2003). Plutonium and uranium isotopic values provide indications as to the source of the material as well as

nuclear fuel cycle activities; whereas trace elements such as strontium, neodymium, oxygen and other stable isotopes provide details relating the geographical source and provenance (Becker, 2003). This isotopic information has been referred to as an 'isotope fingerprint' (Keegan and others, 2008), and emerged as a powerful tool to gain critical nuclear forensics intelligence. Such information can readily be applied to numerous fields such as: investigations of nuclear accidents or illicit trafficking of nuclear materials, non-proliferation control, nuclear safeguards, and bioassay (Becker, 2003 and Bürger and others, 2006). Most recently, ultratrace analysis (defined as parts per billion) has been applied to environmental monitoring for radionuclides (Becker and Dietze, 2003).

An effective nuclear forensics program must be able to provide the identification of nuclear material in a timely and definitive manner (Allison, 2005.) Inorganic mass spectrometry has long been used to determine elemental and isotopic compositions at ultratrace levels (Becker, 2003). Figure 3 outlines the fields of application of inorganic mass spectrometry (Becker and Dietze, 2000). Thermal Ionization Mass Spectrometry has been the technique of choice for extremely accurate isotopic measurements but is being replaced by other methods (Becker, 2003). One of the major disadvantages of TIMS is that the technique requires the identification of individual particles of interest via fission track analysis, which requires irradiation of samples in a nuclear reactor (Esaka and others, 2008). SIMS has been used to characterize plutonium and highly enriched uranium (HEU) particles since the late 1990's and requires little or no sample preparation (Betti and others, 1999).

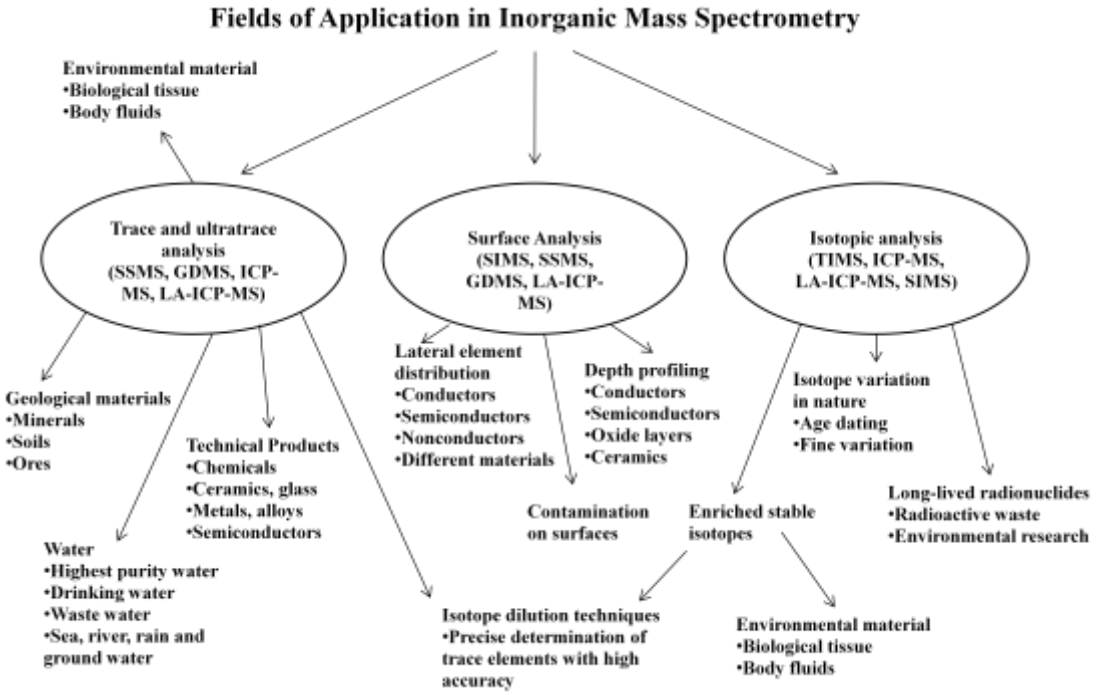

Figure 3. Fields of application in inorganic mass spectrometry (adapted from Becker and Dietze, 2000).

2.3 Mass Spectrometers

Thermal ionization mass spectrometry has long been the gold-standard by which isotopic abundances of heavy metal solids can be characterized (Hou and Roos, 2008 and Becker, 2003). TIMS instruments employ a completely destructive technique where an individual particle of interest is heated to vaporization, ionized and accelerated into a flight tube (MSU, 2009a). Individual isotopes are then separated by extremely large magnetic sectors and counted via an electron multiplier tube (MSU, 2009a). TIMS instruments can operate over only a very small mass range, require a great deal of sample preparation prior to analysis and can only analyze one particle at a time (Hou and Roos, 2007). Secondary ion mass spectrometry, especially in the light of time of flight techniques are now quickly approaching the precision and accuracy of the TIMS

instruments as shown in Figure 4 with a mass resolution of 10^{-3} to 10^{-4} amu (Crompton, 2008). Several benefits of TOF-SIMS over the TIMS include: TOF-SIMS instruments do not rely on costly and timely fission-track analysis for particle isolation, can operate over a wide range of masses (0-10,000 amu), require little or no sample preparation and can provide extremely useful images and depth profiles of samples (Pajo, 2001, MSU, 2009a and Crompton, 2008).

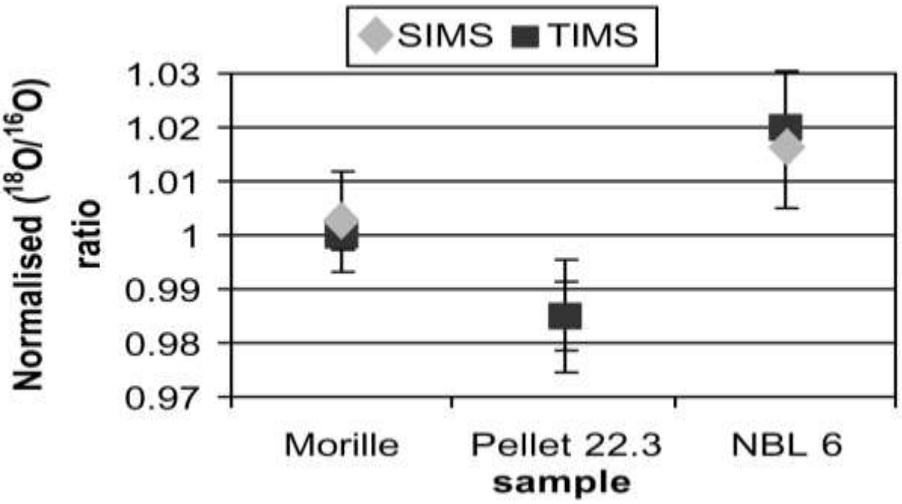

Figure 4. Normalized oxygen isotopic ratios of three uranium oxide samples by SIMS and TIMS (Pajo and others, 2001).

2.4 Motivation for the Application of SIMS

Since 1996, the IAEA has employed SIMS as a research tool to uncover clandestine nuclear weapons operations by rouge nations (Donohue and others, 2008). Many independent studies have been conducted in an effort to fully exploit the capabilities of SIMS instruments in the area of nuclear forensics. Donohue and others conducted SIMS experiments on spherical particles of uranium and plutonium. This is an extremely delicate operation due to deflection of the secondary ions (Donohue and others, 2008). Other studies centered on finding uranium isotopic abundances of

individual particles captured on cotton swipes (Esaka and others, 2004, Esaka and others, 2006 and Kips and others, 2007). The studies conducted by Esaka and others have proven the reproducibility of SIMS measurements as highlighted in Figure 5 (Esaka and others, 2004).

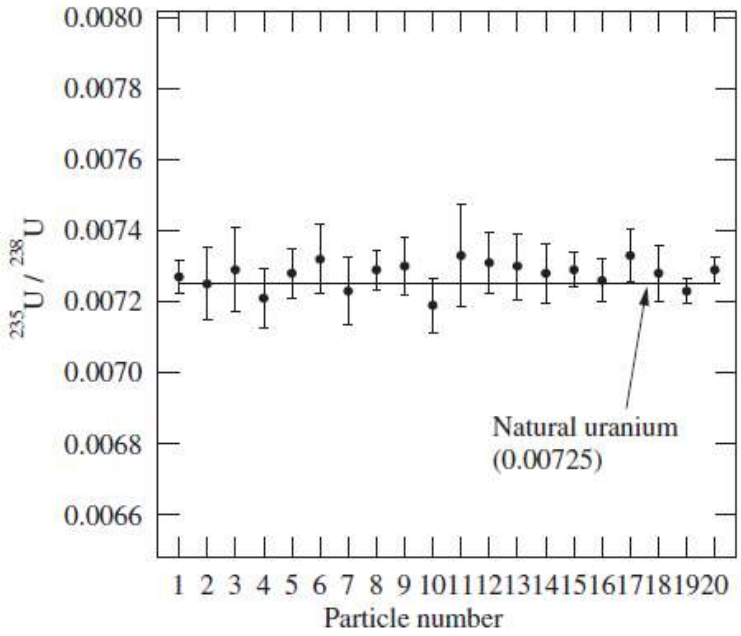

Figure 5: Isotope ratios of individual particles recovered from swipe samples (Esaka and others, 2004).

2.5 SIMS Mass Analyzers

Mass analyzers for SIMS instruments fall into three basic categories which specify the type of each instrument (Portier and others, 2007). The quadrupole-type analyzer was the first used in SIMS and uses a combination of direct current and a radio-frequency electric field to separate ions according to their mass to charge ratio (Beninghoven and others, 1987). The second mass analyzer is a multiple-focusing device, in which combinations of electrostatic and magnetic sectors are used for the

separation of masses (Wilson and others, 1989). The third type of mass analyzer is the TOF which relies on the time it takes an ion to drift down a flight tube before being counted (Portier and others, 2007). There are many advantages of using a TOF analyzer including: parallel detection of ions, extremely high mass resolution, the unlimited mass range, and its extreme sensitivity. The sensitivity, mass range and resolution are extremely important to this research in our effort to fully characterize higher order cluster ions. The performance features of the three types of mass analyzers are compared in Table 3.

Table 3. Performance of different types of mass analyzers for SIMS instruments (adapted from Portier and others, 2007).

Parameter	Quadrupole	Double-	Time-of-
Ion detection mode	Sequential	Sequential	Parallel
Mass resolution	<400	300-2500	5,000-10,000
Mass range	<1000	2000	Unlimited
Transmission (%)	<1	<50	80
Relative Sensitivity	1	10-30	<0.1

2.6 SIMS Studies

Much effort has been focused into method development for the determination of oxygen isotopic ratios by SIMS over the past two decades (Tamborini and others, 2002 and Pajo and others, 2001). The isotopic ratios of ^{16}O, ^{17}O and ^{18}O vary in natural particulates which has lead to an isotopic signature of various materials (Pajo, 2001). Studies have been conducted on UO_2 and U_3O_8 (Pajo and others, 2001 and Schueneman, 2001) as well as UO_3 (Schueneman and others, 2003) to determine the $n(^{18}O)/n(^{16}O)$ ratio as a direct application for nuclear forensics (Pajo, 2001). The precision of SIMS measurements on test samples was 0.05% which correlates well with similar TIMS

measurements with a precision of 0.04% (Pajo and others, 2001). The SIMS data cannot provide quantitative measurements of the oxidation states of the particles but does provide a qualitative assessment of the oxygen isotopic as well as the uranium and oxygen ratios (Schueneman and others, 2003 and Tamborini and others, 2002).

Many of the SIMS studies are focused on the isolation of individual particles of interest using an SEM equipped with an Energy Dispersive X-ray (EDX) analyzer to locate uranium or plutonium-containing particles (Donohue and others, 2008, Esaka and others, 2004, Esaka and others, 2006, Kips and others, 2007, and Keegan and others, 2008). These techniques have required rigorous protocols to be developed and are extremely time consuming (Donohue and others, 2008). The major drawbacks to these methods are that particles can be lost and only a few particles of interest were isolated after all of the manipulation (Donohue and other, 2008). Donohue and others' method is outlined below and graphically represented in Figure 6 (Donohue and others, 2008).

1. The sample is collected using a 10cm X 10cm cotton swipe
2. Sub-samples are collected using double-sided carbon tape affixed to an SEM stub
3. Reference marks are added to the SEM stub in the form of copper grids
4. Particles of interest were located using the EDX spectrometer of the SEM
5. Particles of interest were located under an optical microscope for removal
6. Proprietary software allowed for the location of the particles of interest
7. Particles were removed from the SEM stub via a tungsten needle
8. The only viable transferred particle was analyzed via SIMS

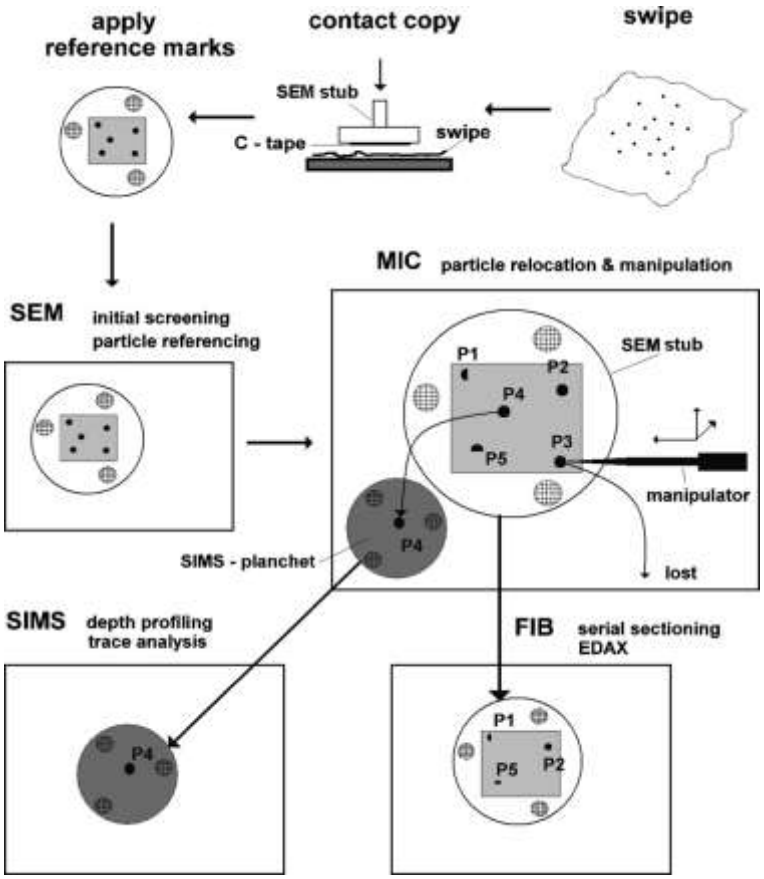

Figure 6. Particle transfer from swipe, screening, particle manipulation and characterization via SEM-EDX and SIMS (adapted from Donohue and others, 2008).

Researchers at the National Institute of Standards Technology (NIST) and the Department of Terrestrial Magnetism have worked to develop techniques using SIMS instruments to automatically search for particles of interest (Simons and others, 1998 and Nittler and others, 2003). There are several major drawbacks to such research including: techniques are specific to individual instruments, each was designed with proprietary software, and the techniques are not portable to other instruments. This illustrates the

need for a presumptive technique to rapidly locate particles of interest that does not rely on other instruments or instrument-specific techniques.

2.7 Complementary Surface Sciences

Many different techniques can be applied to determine trace-elemental compositions of materials. Auger electron Spectroscopy (AES), X-ray photoelectron spectroscopy (XPS) and TOF-SIMS are three of the most widely used techniques in today's analyses (Kohli and Mittal, 2008). Each technique has its own unique characteristics that can be applied to analyze surface compositions of particles in the sub-micron range (Kohli and Mittal, 2008). TOF-SIMS has several advantages over AES and XPS with its extremely small analysis spot size, sampling depth of as little as one monolayer, its detection limit in the parts-per-billion range and rapid imaging and depth profile capabilities (Kohli and Mittal, 2008). While TOF-SIMS does have several advantages over AES and XPS, both of the other surface sciences offer much simpler quantitation than current TOF-SIMS methodologies (Kohli and Mittal, 2008). An overview of selected properties for each of the methods is presented in Table 4.

Table 4. Overview of selected properties for surface analytical methods (adapted from Kohli and Mittal, 2008).

Method	AES	TOF-SIMS	XPS
Material	Conducting or semi-conducting solids. Insulators are very difficult	Any solid	Any solid
Information	Elemental. Oxidation state or chemical bonding in select cases	Molecular Weight, chemical bonding, elemental an isotopic	Chemical bonding, oxidation state, and elemental
Quantitative Analysis	Yes, but with standards	Only with standards	Yes, but with standards

Minimum Analysis Size	10nm diameter	1μm diameter for organic analysis, 50nm diameter for inorganic analysis	10μm diameter
Sampling Depth	5-25 monolayers	1-3 monolayers	5-25 monolayers
Detection Limit	0.1-1.0 at.%	1 ppma, $1X10^8$ atom/cm^2	0.01-1.0 at.%
Imaging	Yes	Yes, rapid	Yes
Depth Profiling	Yes	Yes, rapid	Yes
Major Limitations	Electron beam damage. Charging of insulating samples	Ion yields vary by orders of magnitude. Standards needed for quantitative analysis	Relatively large analysis area. Analysis is often time consuming

Francis and others conducted a study on the corrosion processes of steam generator tubing in a Canadian Deuterium Uranium (CANDU) reactor. The group chose TOF-SIMS as their primary analytical technique due to its sensitivity, acquisition efficiency, depth resolution and imagining capabilities (Francis and others, 2001). Results from XPS and AES measurements were compared to TOF-SIMS measurements and were found to be in good agreement (Francis and others, 2001). Many advantages were noted by the group: depth profiles were much quicker and more precise with the TOF-SIMS, the TOF-SIMS samples required much less preparation prior to analysis, and TOF-SIMS offers the ability to provide isotopic abundance (Francis and others, 2001).

TOF-SIMS can be used to measure trace elemental abundances in samples in order to provide information such as: chemical processing, a history of the sample, as well as a determination of natural versus anthropogenic processes of which the particle has been subjected (Bürger and others, 2009). TOF-SIMS can also provide measurements of bulk chemical processing signatures that relate to a sample's

stoichiometric ratios (Skoog and others, 2006). TOF-SIMS can further provide the isotopic ratios of uranium species in order to determine enrichment, depletion or nuclear reactor processes (Pajo and others, 2001). The last piece of the puzzle, oxidation states, cannot be directly measured via TOF-SIMS however, TOF-SIMS measurements do provide metal/oxygen compositions which, assuming equilibrium, measure the average oxidation state (Schueneman and others, 2003 and Gerstmann and others, 2008).

2.8 Time-of-Flight Secondary Ion Mass Spectrometry

Relatively new in the analysis of SNM is TOF-SIMS due partly to its young age as a surface science as well as deficiencies in the science itself. Deficiencies exist due to: varying secondary ion yields, matrix effects, reactive elemental surface contaminants, angle of incidence of the primary beam with respect to the sample, angle of emission of secondary species, mass bias of the instrument, and detector efficiency (Betti, 2005). These deficiencies make absolute intensity measurements problematic (Betti, 2005). Many of these deficiencies can be overcome due to the fact that relative measurements important for nuclear forensics can be reliably determined with TOF-SIMS (Betti, 2005, Francis and others, 2002, and Betti and others, 1999).

2.8.1 TOF-SIMS Operation

A TOF-SIMS instrument uses a pulsed primary beam of ions to ionize and sputter secondary ion species from a sample's surface (Benninghoven and others, 1987). These secondary ions are then accelerated into a mass spectrometer where individual ion masses can be separated based upon the time it takes the ion to leave the sample surface and

arrive at the detector (Crompton, 2008). Figure 7 illustrates the impact of the primary ion beam and resultant cloud of secondary ions (MSU, 2009b).

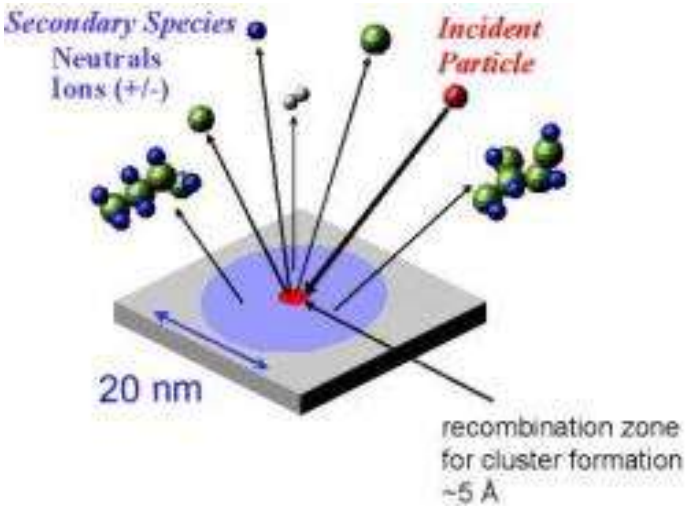

Figure 7. Illustration of incident particles (primary ions) and resultant secondary species being sputtered from the sample's surface (MSU, 2009b).

TOF-SIMS instruments have three distinct modes of operation: 1) mass spectra can be acquired to obtain isotopic and molecular species abundances with an average mass resolution on the order of 10,000 (Morrall and others, 2006); 2) images can be acquired with a resolution of 120 nm (MSU, 2009b) to visually determine the distribution of elemental and molecular species contained in the sample; and 3) depth profiles with a resolution of 1 nm (Kohli and Mittal, 2008) can determine the distribution of isotopic and molecular species as a function of depth from the surface of the sample (PHI, 2009b).

In TOF-SIMS, the secondary ions all have approximately the same kinetic energy because each species is accelerated over a very short distance in an extraction field (Vickerman and others, 1989). Equation 1 defines the kinetic energy of the secondary ions as they enter the drift tube where E_k is the ion kinetic energy, v is the velocity and m

is the mass. Ion selection will be based on the fact that ions of varying mass will have varied velocities and traverse the drift tube at varying times (Benninghoven and others, 1987). The time is takes a given ion to traverse the drift tube can be calculated by equation 2 where t is the arrival time of the secondary ion at the detector, t_0 is the time the ion enters the drift tube, L is the length of the drift tube (Schueneman, 2001). Variability in resolution due to the variance in the kinetic energy of the extracted ions is several orders of magnitude ranging from 100 to 10000 (MSU, 2009).

$$Ek = \frac{1}{2}mv^2 \qquad 1$$

$$t - t_0 = L\sqrt{m/2Ek} \qquad 2$$

TOF-SIMS is considered to be a semi-destructive technique (Betti, 2005) in that only the first few surface layers of atoms are sputtered away and ionized (Benninghoven and others, 1987). If sample preservation is at issue, much care must be taken during analysis to ensure that enough of the sample will remain for further characterization (Skoog and others, 2006). Also of note is the fact that inhomogeneous samples could provide spurious data and the information collected on the sample will depend upon which portion of the sample was analyzed (Benninghoven and others, 1987). The benefit of using TOF-SIMS lies in its sensitivity and the fact the each ion produced will be counted at the detector (Crompton, 2008). In conventional mass spectrometers, sensitivity is diminished due to the instrument only having the capability of counting one mass channel per unit time (Coakley, 2005). As time progresses, more and more of the sample is burned away as the spectrometer selects and counts each mass channel.

2.8.2 Calibration

Mass calibration of the TOF-SIMS must be completed in order to provide accurate spectra of the secondary species being counted. In situ calibration can be performed by measuring the secondary species of known standards (Wilson and others, 1989). A good laboratory best practice involves measuring a range of masses that include your species of interest as well as above and below your mass of interest (Pajo, 2001). As with most spectrometers, TOF-SIMS has the tendency to identify certain species with more probability than others (Hou and Roos, 2008). Some species will be easier to ionize than others and some will have a higher extraction potential. This higher extraction potential leads to a mass bias which must also be considered in any calibration routine (Crompton, 2008). Once standards are chosen, equation 3 can be used to determine a calibration curve based on a least squares fit of the data where the constants *a* and *b* are determined based on the time, *t* it takes mass, *m* to traverse the drift tube (Schueneman, 2001).

$$m = at^2 + b \qquad 3$$

Recent publications insist that there is lack of reference materials that are specific to the needs of the science of nuclear forensics (Lamont and others, 2008 and Inn and others, 2008). It has been proven that matrix effects can distort elemental and isotopic evaluations performed by SIMS instruments (Kohli and Mittal, 2008). The DOE, FBI, DTRA, NPL, and IAEA have all reported deficiencies in their certification programs (Lamont and others, 2008). The NIST has proposed three possible materials for

certification of instruments: Rocky Flat Soil-2 (SRM 4353A), NIST Peruvian Soil (SRM 4355A), and NIST Columbia River Sediment (SRM 4350B) (Inn and other, 2008). In any case, the materials chosen as reference materials need to be heterogeneous in order to limit the extent of matrix effects in measurements (Inn and others, 2008).

2.8.3 Quantification

Quantification of the SIMS data is further complicated with the application of relative sensitivity factors (RSF) in the conversion from ion intensity to concentration as shown below in equation 4 (Gunther, 2005):

$$C_E = \frac{RSF_E * I_E * C_M}{I_M} \qquad 4$$

where

C_E is the concentration of the element, E (the element of interest)

RSF_E is the relative sensitivity factor for element, E

I_E is the secondary ion intensity for element, E

C_M is the concentration of matrix element, M

I_M = secondary ion intensity for matrix element, M

Since the concentration is dependent upon all of the above factors, an RSF must be calculated and measured for each analyte of interest in matrices resembling those of unknown samples. Samples with known amounts of SRM's must either be purchased or developed for this purpose (Benninghoven and others, 1987). There has been extensive work in the calculation of RSF's for a wide range of materials in various matrices (Phinney, 2006).

2.8.4 Static SIMS

Static SIMS is applied in the spectroscopic and imaging modes, where only the outermost (1-3) atomic layers of the sample are ionized and accelerated toward the detector (Kohli and Mittal, 2008). Figure 8 shows how the primary ions impact the sample surface and desorb the surface material from the sample's surface via a "collision cascade" (PHI, 2009b). A high voltage potential is then applied between the sample surface and mass analyzer to extract the excited secondary ions into the TOF analyzer (Benninghoven and others, 1987). A pulsed primary ion source (on the order of 1ns) is used to produce the TOF-SIMS spectra, Figure 9 shows an example spectrum (Kips and others, 2007). For each pulse of primary ions, a mass spectrum on the range of masses of interest can be obtained by performing a time to mass conversion based upon the arrival times of the secondary ions at the detector (Crompton, 2008).

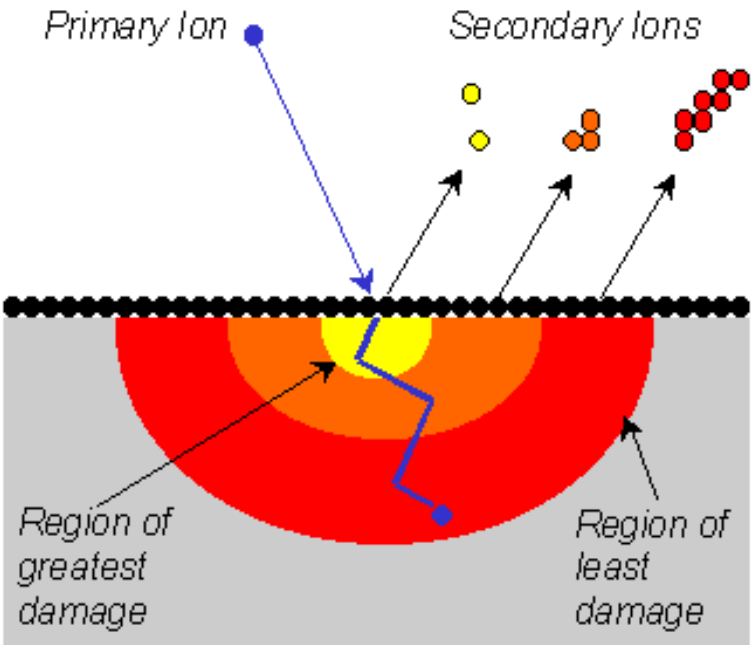

Figure 8. Cutaway of sample surface showing primary ion interaction and secondary ion excitation (PHI, 2009b).

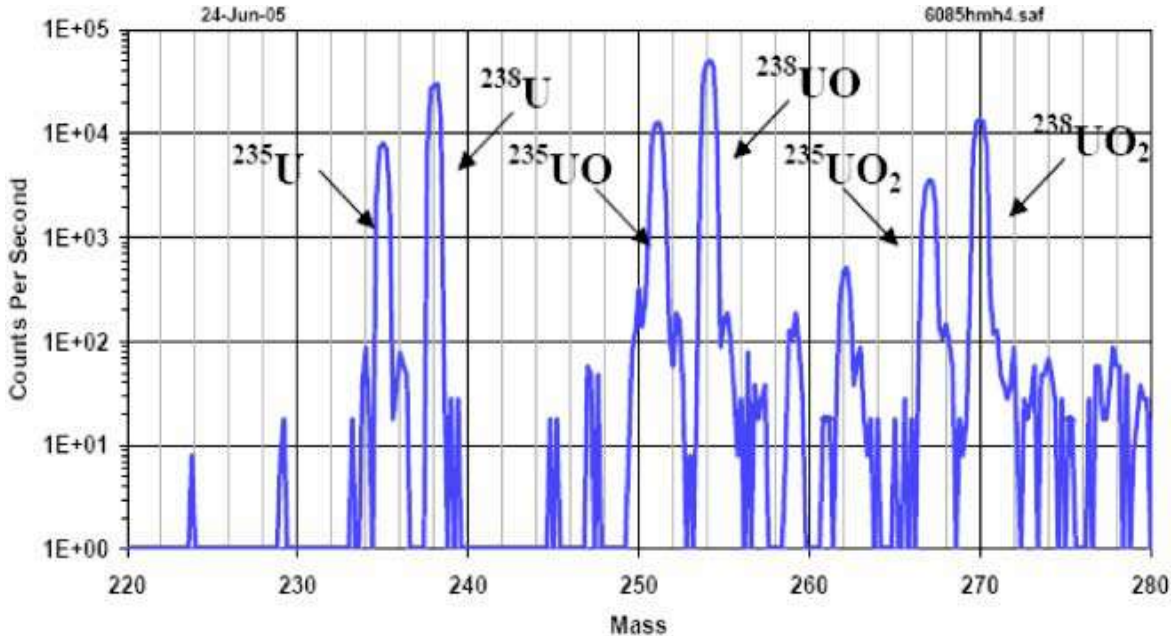

Figure 9. Sample mass spectrum of UO_2 to demonstrate the data one might receive from a TOF-SIMS analysis with major fragments and isotopes highlighted (Kips and others, 2007).

2.8.5 Chemical Imaging

Chemical images can be generated by rastering a finely focused primary ion beam across the sample's surface and collecting a mass spectrum at each pixel (Wilson and others, 1989). The entire mass spectrum or only a portion thereof can be acquired from each pixel from the region of interest within the sample. The secondary ion images coupled with each pixel's mass spectrum can be combined to determine the exact composition of the sample's surface (Benninghoven and others, 2006). Figures 10a-d on the following page show the images generated from secondary ion and molecular species from a cross-section of a sheet of coated paper. Figure 10a, the total ion image, contains the summation of every secondary species identified at each individual pixel. Figure 10b

contains just the $C_3H_7O^+$ peak, which is an organic fragment of cellulose. Figure 10c contains an image of the sodium (Na^+) peak, which is from the clay coating on the paper. Figure 10d contains the iron (Fe^+) peak information and is assumed to have been a contamination due to the razor blade used to cut the paper. Figure 10d is illustrative the extremely high sensitivity of the TOF-SIMS instrument in that even a slight contamination can provide a substantial signal (PHI, 2009b).

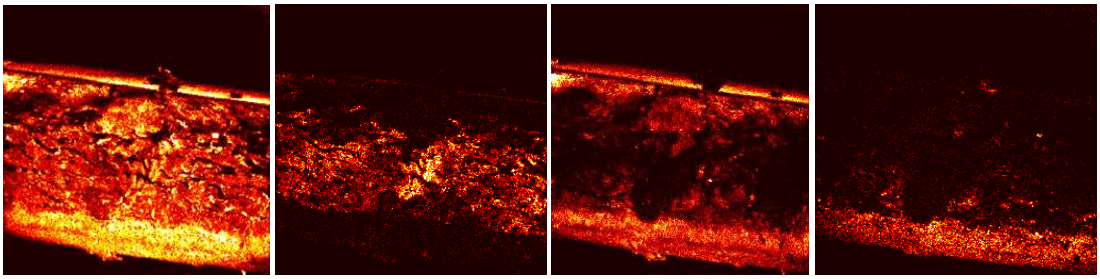

a b c d

Figure10 (300µm X 300µm). (a) Total Ion image of a coated paper cross-section; (b) organic fragment of the $C_3H_7O^+$ (cellulose) peak; (c) Na^+ (sodium) peak from the clay coating; and (d) the Fe^+ (iron) peak from contamination due to the cutting of the paper with a razor blade (PHI, 2009b).

2.8.6 Dynamic SIMS

Dynamic SIMS can be applied via TOF instruments in the application of shallow sputter depth profiling (Wilson and others, 1989). A primary ion accelerator is operated for a known time in order to sputter into the sample a known distance, this same primary accelerator or a second is then used in pulsed mode for the acquisition of spectra at each depth of interest into the sample. Sputter depth profiling via TOF-SIMS allows for extremely high mass resolution and the capability of monitoring all of the species of interest simultaneously. Figure 11 shows a typical TOF-SIMS depth profile, which was

taken of a polycrystalline uranium substrate passivated through carbon implantation (Nelson and others, 2006). The oxide layer, carbon and fluorine can all be seen at the surface whereas the uranium oxides and uranium carbide are deeper.

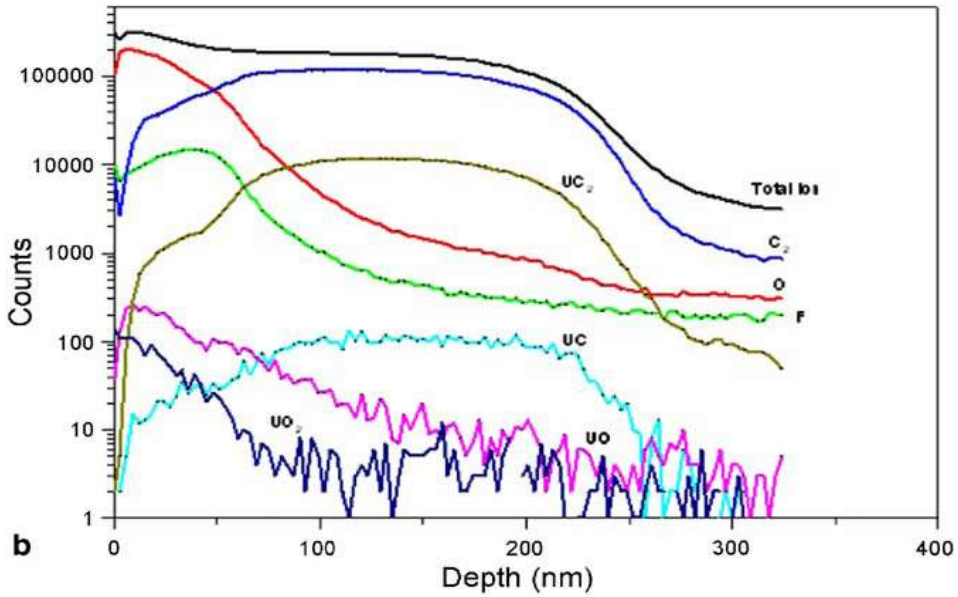

Figure 11. Depth profile of polycrystalline uranium passivated through carbon implantation (Nelson and others, 2006).

2.8.7 Individual Particle Isolation

Another interest in nuclear forensics applications is the ability to analyze a large sample with a complex matrix and have the ability to find the one particle of interest (PHI, 2009a). These complex matrices make quantitation extremely difficult, however accurate data can be obtained if an analytical standard matched to the matrix is analyzed prior to the unknown sample (Hou and Roos, 2008). In the past, much sample preparation would have to take place in order to isolate a particle of interest prior to analysis hence there has been little use of TOF-SIMS for such analyses (Morrall and others, 2007). The innovative stage design of modern TOF-SIMS instruments allows a

user to scan a sample with a 5-axis fully automated stage (PHI, 2009a). Once a particle has been located, an in-depth analysis of that particle can provide isotopic abundance in the parts-per-billion range (Kohli and Mittal, 2008).

III. Methodology

3.1 General Details

The goal of this research was to determine whether TOF-SIMS could be used to provide rapid actionable forensics information from very small samples of uranium. In order to meet this goal, uranium samples were prepared using standard reference uranium oxide materials covering a wide range of isotopic and stoichiometric forms. TOF-SIMS measurements were then performed on all prepared samples and a detailed analysis was conducted on all of the spectra collected.

Powdered uranium oxide samples of isotopically natural UO_3 and U_3O_8, isotopically depleted UO_2 and U_3O_8, and isotopically enriched U_3O_8 were measured. Samples were affixed to a silicon substrate using carbon tape for analysis in the TOF-SIMS instrument. Spectra were obtained in both the positive and negative modes and qualitative and semi-quantitative measurements were performed for the various clusters and fragments of ions collected. Further reduction of the data was performed in order to validate the use of TOF-SIMS measurements for the determination of isotopic and elemental abundances.

3.2 Standard Reference Materials

Pure uranium oxides from the New Brunswick Laboratory's (NBL) certified reference materials (CRM) collection, as well uranium oxide powders from Cerac and NIST were selected as the samples of interest for this study. The standards selected covered a range of isotopic abundances from depleted to highly enriched uranium. In an

effort to characterize the differences in cluster ion formation stemming from stoichiometry, various stoichiometric forms of the uranium oxide CRMs were also selected. Table 5 provides stoichiometric and isotopic information for all of the standards chosen for this research.

Table 5. Stoichiometric and isotopic information for samples chosen for experiment (the isotopic information for the Cerac samples is unknown and had to be estimated).

Sample ID	Supplier	Material	Chemical Purity	234 %	235 %	236 %	238 %
T100	Cerac	UO_2	99.80%	≈ 0.0034	≈ 0.5064	≈ 0.00118	≈ 99.489
T101	Cerac	UO_3	99%	≈ 0.0055	≈ 0.72	≈ 0	≈ 99.2745
T102	Cerac	U_3O_8	99.80%	≈ 0.0034	≈ 0.5064	≈ 0.00118	≈ 99.489
U005	NBL	U_3O_8	100%	0.0034	0.5064	0.00118	99.489
U18	NIST	UO_3	82.10%	0.0055	0.72	0	99.2745
U129	NIST	U_3O_8	99.968%	0.0055	0.72	0	99.2745
U500	NBL	U_3O_8	100%	0.5181	49.696	0.0755	49.711
U900	NBL	U_3O_8	100%	0.7777	90.196	0.3327	8.693

3.3 Sample Preparation

Sample mounting procedures were first conducted using a surrogate material to perfect the technique and allow for precise mass measurements of loaded samples. Cerium oxide was chosen as the surrogate material due to the fact that it has approximately the same density as various uranium oxides (Delegard and others, 2004, Sandia National Laboratories, 1999 and Yang and others, 2002). A total of six samples were prepared according to the detailed instructions provided in Appendix C. The masses of cerium oxide measured for these samples were used in the activity estimations provided in Appendix F. Results of the mass measurements are provided in Table 6. An

SEM image is provided in Figure 12 to verify the monolayer of widely dispersed particles.

Table 6. Results from mass measurements of cerium oxide samples with the mean and standard deviation provided for each measurement.

	Mass 1	Mass 2	Mass 3	Mean	Std Dev
Tare 1	0.252342	0.252347	0.252345	0.252344667	2.52E-06
Tot 1	0.252372	0.252368	0.25237	0.25237	2E-06
Samp 1	3E-05	2.1E-05	2.5E-05	2.53333E-05	4.51E-06
Tare 2	0.281392	0.281393	0.281397	0.281394	2.65E-06
Tot 2	0.281409	0.281412	0.281414	0.281411667	2.52E-06
Samp 2	1.7E-05	1.9E-05	1.7E-05	1.76667E-05	1.15E-06
Tare 3	0.196813	0.196808	0.196811	0.196810667	2.52E-06
Tot 3	0.196823	0.19682	0.196825	0.196822667	2.52E-06
Samp 3	1E-05	1.2E-05	1.4E-05	1.2E-05	2E-06
Tare 4	0.184729	0.184727	0.184725	0.184727	2E-06
Tot 4	0.184747	0.184746	0.184744	0.184745667	1.53E-06
Samp 4	1.8E-05	1.9E-05	1.9E-05	1.86667E-05	5.77E-07
Tare 5	0.196642	0.19664	0.196645	0.196642333	2.52E-06
Tot 5	0.196652	0.19665	0.196657	0.196653	3.61E-06
Samp 5	1E-05	1E-05	1.2E-05	1.06667E-05	1.15E-06
Tare 6	0.17282	0.17282	0.172824	0.172821333	2.31E-06
Tot 6	0.172838	0.172841	0.172843	0.172840667	2.52E-06
Samp 6	1.8E-05	2.1E-05	1.9E-05	1.93333E-05	1.53E-06

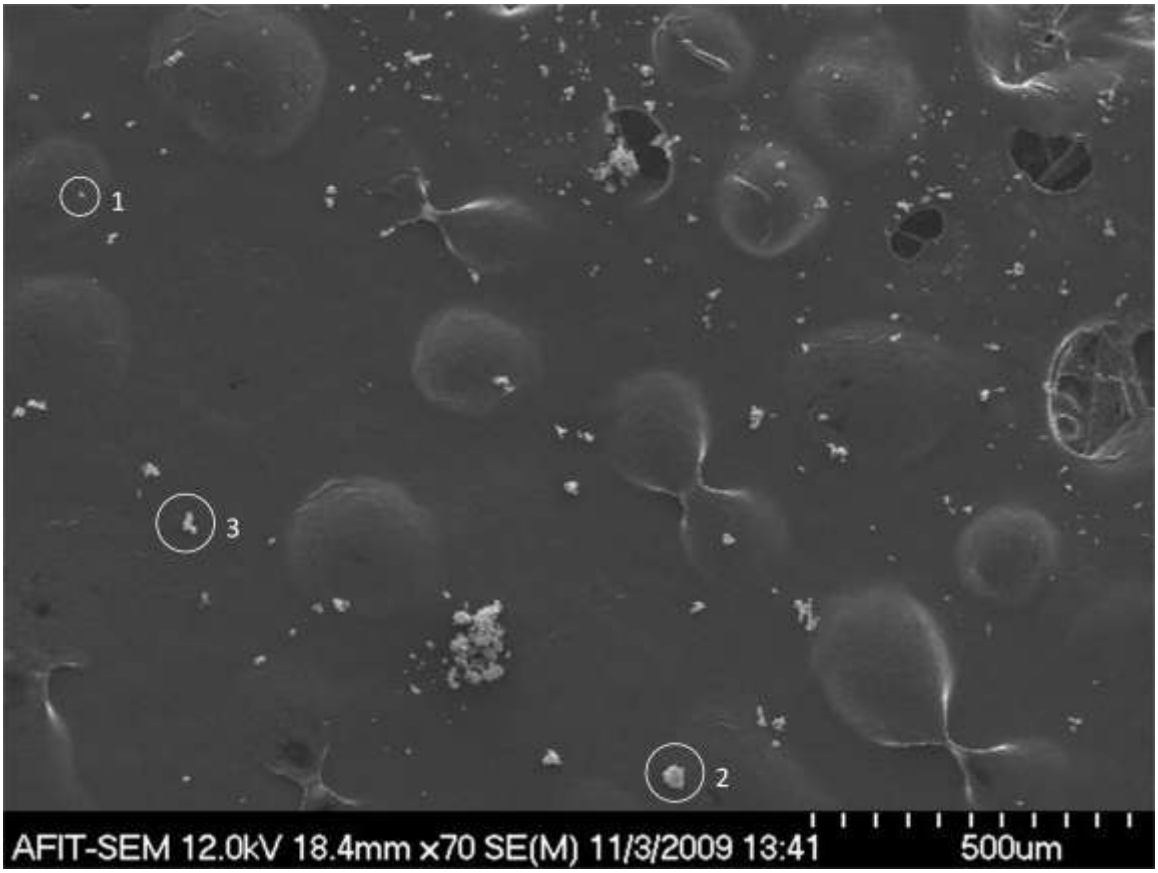

Figure 12. SEM image of dispersed cerium oxide particles verifying individual particles dispersed across the surface of the mounting media (1: completely isolated particle ≈ 10µm in diameter; 2: larger isolated particle ≈ 100µm in diameter; 3: small cluster of particles ≈ 75 X 100µm).

Only one sample for each of the standards was prepared for the TOF-SIMS analysis due to the fact that we have less than 10mg of the U005, U500 and U900 samples. The goal of the sample preparation was to have individually isolated particles well separated from nearest neighbors to ensure individual particles could be analyzed by the TOF-SIMS instrument. Samples were prepared by dispersing the powders onto a large silicon wafer then transferring the particles to a small fragment of silicon wafer with double-sided carbon tape. Detailed instructions for the sample mounting procedures can be found in Appendix C. A photograph of a prepared sample is provided in Figure 13.

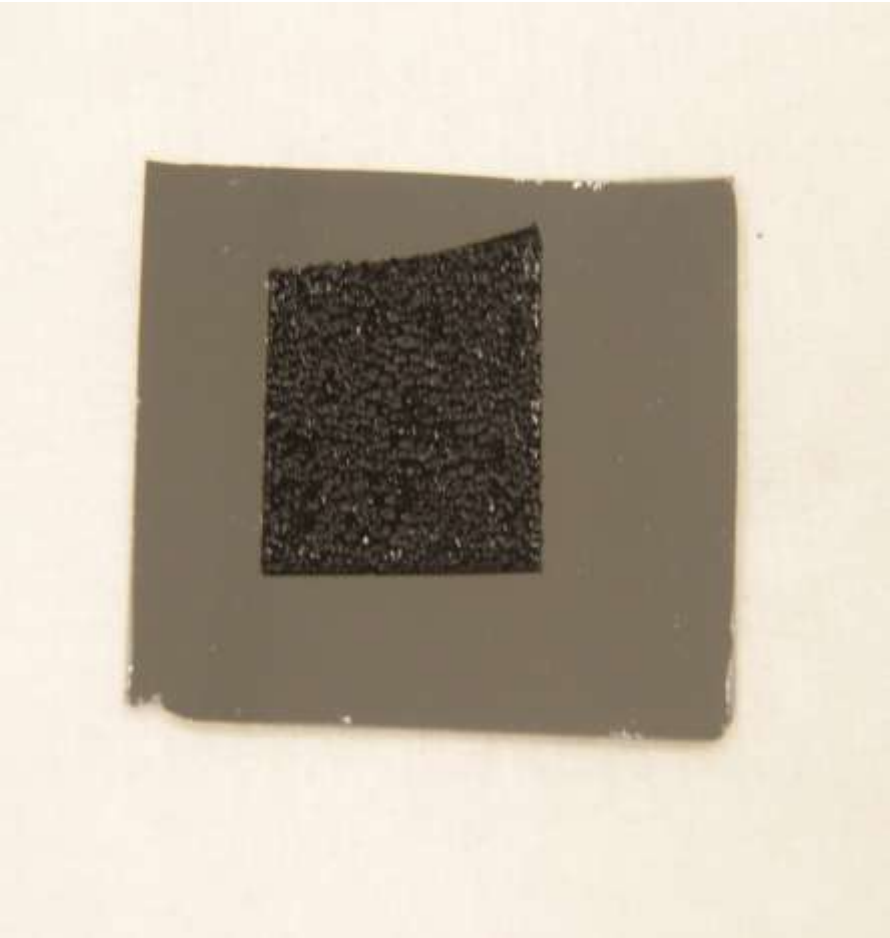

Figure 13. Photograph of mounted sample (in the instrument it is difficult to notice the subtle difference between the carbon tape and silicon wafer and almost impossible to differentiate the actual particles from the carbon tape without magnification).

3.4 TOF-SIMS Analysis

TOF-SIMS measurements were conducted to provide qualitative and semi-quantitative data of the uranium oxide cluster ions detected by the spectrometer.

3.4.1 Equipment

An Ion Tof TOF-SIMS V located at the State University of New York (SUNY) was used to analyze the uranium oxide particles. Appendices I-K to this document

provide detailed instructions for the use of the instrument as well as reprocessing of data. The appendices are provided as a general guide for instrument startup, analysis conditions and reprocessing of spectra and images. A new user should always consult with an expert and make full use of the vendor-supplied technical manuals. Reprocessing of the spectra allows a user to remove only information relevant to current research from the nebulous cloud of raw data. Some of the data was reprocessed on a stand-alone computer located at AFRL/RXB with the help of Ms. Linda Kasten and Dr. Benjamin Phillips.

3.4.2 Data Collection

Spectra were collected on individual particles for the all of the U_3O_8 samples. Spectra were composed on collections of particles for the UO_2 and UO_3samples. An initial scan of the surface of the first sample analyzed revealed most particles were slightly smaller than 100 μm. A spot size of 75 X 75 μm was determined the best for the size of the particles in the samples. The analyses of the collections of particles were performed to keep the spot size of the primary beam at 75 X 75 μm. Three positive ion spectra were collected for each sample and one negative ion spectrum were collected for each sample. The extremely low ion yield in the negative mode spectra led to the collection of only one spectrum for each sample. The majority of the sampling time was then focused on the higher yielding positive scans.

The chosen polarity of the mode of operation for a given measurement determines the polarity of the secondary ions and must be set prior to analysis. The UO_2^+, UO^+ and $U_2O_4^+$ peaks showed the greatest intensities in the positive mode while UO_3^+ and UO_4^+

had the greatest intensities in the negative ion mode. Ion yields were more than order of magnitude greater in the positive mode than in the negative mode. Data were collected up to mass number 1200 as $U_4O_9^+$ was observed, but no higher clusters were detected. The data showed a small abundance of elemental uranium isotopes and a wide array of uranium oxide cluster ions. It was not possible to compare the differences between the positive and negative spectra due to differences in instrument sampling parameters used during the analyses. A sample positive mode spectrum is provided in Appendix L for one of the depleted U_3O_8 scans.

3.4.3 Initial Instrument Parameters

The initial instrument parameters were chosen based upon the parameters used in similar TOF-SIMS studies. Table 7 provides a summary of the instrument parameters used in the prior uranium research. None of the instruments used in the previous studies were equipped with a bismuth primary ion source. The bismuth primary source has several modes of operation and Bi_3^+ was chosen for this research due to its ion yield and effectiveness in generating large cluster species (Nagy and Walker, 2007, Ravanel and others, 2008). The counting time of 2100 seconds was chosen in order to provide an optimal compromise between counting statistics and numbers of samples that could be analyzed. The analysis area was based on a cursory scan of the first sample analyzed, which revealed many particles on the order of 100 μm. The primary ion intensity of 0.4 pA was chosen to optimize the secondary ion yield in the positive mode. Table 8 lists the TOF-SIMS instrument parameters used for this study.

Table 7. Summary of instrument parameters used in similar studies (Img-imaging, Iso-isotopics, DP-depth profiling).

Author	Broczkowski	Erdmann	Francis	Morrall	Zhu
Instrument	Ion Tof IV	Ion Tof III	Ion Tof IV	PHI Trift III	Ion Tof IV
Primary Voltage	3 kV	25 kV	3 kV,15 kV	22 kV	25 kV
Primary Source	Ar^+	Ga	Ar^+, Ga^+	Au	Ga^+
Pulse Width		10-1000 ns	30 ns		
Intensity			150 nA, 2.5 pA	0.6 nA	3 pA
Acquisition Time					3 min
Analysis Area	50 X 50 um	100 X 100 um	200 X 200 um	50 X 50 um	500 X 500 um
Secondary			Pos		Pos/neg
Spot Size			1.5 um		
Primary Fluence					10^{13} ions cm^{-2}
Results	Img	Iso/Img	Iso/Img/DP	Iso/Img	Iso/Img

Table 8. Instrument parameters used for research at SUNY.

Instrument	Ion Tof TOF-SIMS V
Primary Voltage	9 kV
Primary Source	Bi_3^+
Intensity	0.4 pA
Acquisition Time	2100 s
Acquisition Frequency	2163 Hz
Analysis Area	75 X 75 um
Secondary	Pos/neg
Primary Ion Fluence	5 X 10^{13} ions cm^{-2}
Results	Isotopics/Imaging

3.4.4 Sample Ion Images

Ion images were generated for each spectra based upon a peak list constructed from selected peaks from each sample. The peak of any species can easily be added to or removed from the peak list to provide a result tailored to the researcher's interest. Images

can easily be reconstructed from reprocessed data if the peak list is changed for any reason. The image represents ion intensity and includes the integrated total ion count for each species. Color bars are included with each image and can be changed by the user for overlays and comparative image studies. The beauty of the ion image is the absolute speed in which a qualitative assessment of the overall sample can be attained. It is easy to observe in Figure 14 that the UO_2^+ and UO^+ peaks provide the greatest intensity while the $U_3O_3^+$ and $U_4O_5^+$ peaks returned an extremely weak intensity. Appendix M contains sample ion images for each of the samples.

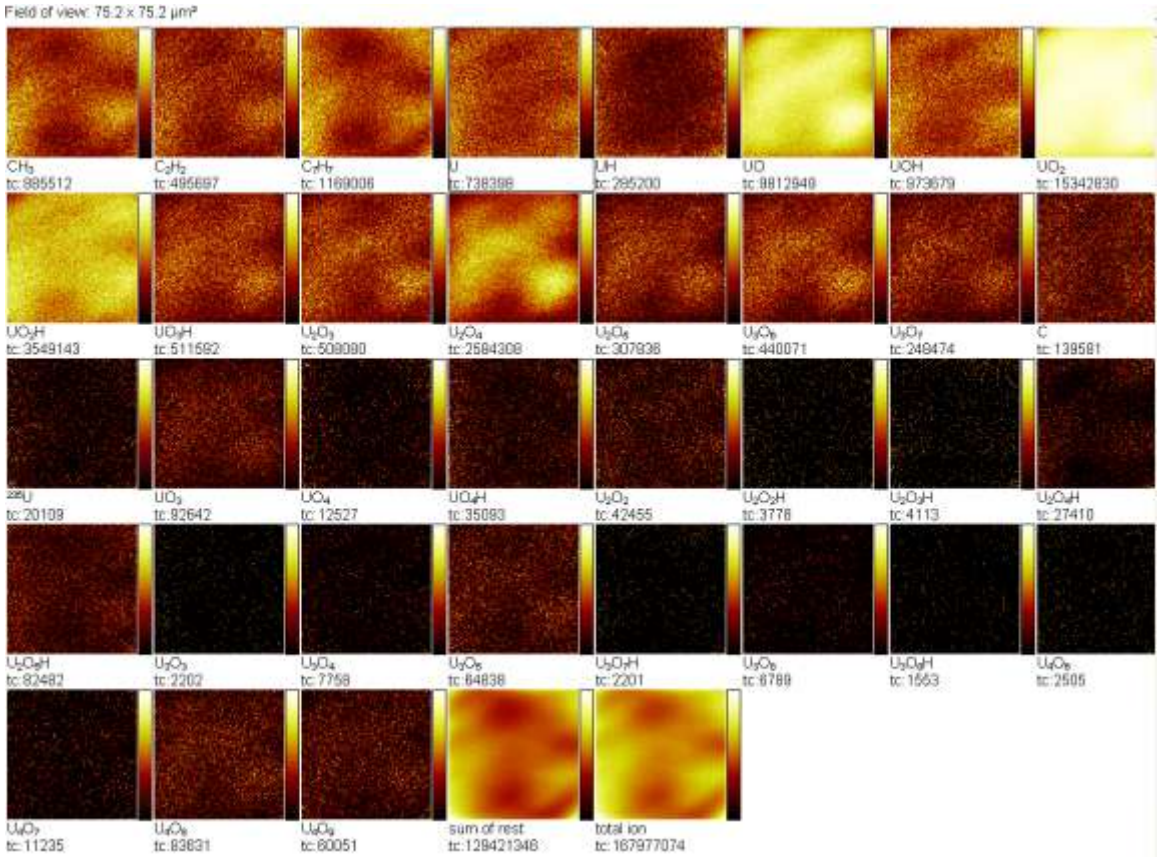

Figure 14. Sample ion image highlighting the ease and speed at which qualitative assessments can be attained.

IV. Data Description and Analysis

Over 10 gigabytes of data were collected during this research effort and much time was spent trying to extract as much useful information as possible from the data set. Appendix L contains a sample mass spectrum for one selected sample. Appendix M contains the images for all samples. This chapter follows the course of actions taken in the effort to reveal as much worthwhile information which can be extracted from the data. The analysis of the data was focused on these subjects:

1. A qualitative assessment of the data.
2. A construction of simulated spectra in an effort to perform spectral stripping.
3. Analysis of simultaneous equations to provide quantitative measurements of protonation, diprotonation and triprotonation of ions.
4. A peak reassessment with hydrocarbon subtraction of $^{235}UO_2$ and $^{238}UO_2$ to provide isotopic measurements of the uranium samples.
5. Calculations of average oxidation states.

4.1 Qualitative Data Assessment

A multitude of uranium oxide peaks were detected using the Bi_3^+ source in the TOF-SIMS instrument. In order to interpret the data, a list of expected peaks was generated for each of the major cluster ions detected using the instrument. Exact masses for each of the peaks were calculated using an Excel spreadsheet. A code was developed corresponding to the number of atoms of each isotope in each peak as follows: ^{16}O – ^{18}O – ^{235}U – ^{238}U. Many of the peaks overlap such as the three possible combinations for the base peak of the $U_4O_8^+$ at mass 1080. These overlapping peaks made it extremely

difficult to resolve each one successfully based upon the observed resolution of the instrument. Results of the calculations are provided according to each cluster in Table 31 and as a consolidated list in Table 32 in Appendix N of this document.

4.1.1 Cluster Ion Comparisons

In all of the samples collected, it was observed that the UO_2^+ peak provided the greatest intensity of any ion observed in the spectra. An analysis was then performed to identify whether or not the same U/O ratio would follow for all of the other higher uranium containing clusters. Based upon the U/O ratios, the highest intensity peaks would be $U_2O_4^+$, $U_3O_6^+$, and $U_4O_8^+$ for the U_2, U_3, and U_4-containing species, respectively. Tables 9 through 12 contain all of the integrated peak counts as well as the counts relative to the amount of UO_2^+ observed for each sample.

Table 9. Comparison of single uranium-containing oxide species, normalized to UO_2^+.

Sample	Depleted UO_2	Natural UO_3	Depleted U_3O_8	Depleted U_3O_8	Natural UO_3	Natural U_30_8	Enriched U_30_8	Enriched U_30_8
UO^+	2845359	583766	3794994	5861275	2921412	1121756	533502	907102
Norm	0.608062	0.44034	0.593906	0.624112	0.402575	0.503067	0.452131	0.343248
UO_2^+	4679387	1325716	6389891	9391390	7256819	2229835	1179971	2642705
Norm	1	1	1	1	1	1	1	1
UO_3^+	10924	2051	25289	34877	18163	7534	4562	27863
Norm	0.002334	0.001547	0.003958	0.003714	0.002503	0.003379	0.003866	0.010543
UO_4^+	14597	1646	3788	3057	3068	12370	1136	3486
Norm	0.003119	0.001242	0.000593	0.000326	0.000423	0.005547	0.000963	0.001319

Table 10. Comparison of dual uranium-containing oxide species, normalized to UO_2^+.

Sample	Depleted UO_2	Natural UO_3	Depleted U_3O_8	Depleted U_3O_8	Natural UO_3	Natural U_30_8	Enriched U_30_8	Enriched U_30_8
$U_2O_2^+$	11020	1889	12265	11659	8267	8819	687	3170
Norm	0.002355	0.001425	0.001919	0.001241	0.001139	0.003955	0.000582	0.0012
$U_2O_3^+$	104329	11910	136344	132885	73792	64420	3619	23304
Norm	0.022295	0.008984	0.021337	0.01415	0.010169	0.02889	0.003067	0.008818

$U_2O_4^+$	382090	40579	791817	703003	363320	173076	16018	87929
Norm	0.081654	0.030609	0.123917	0.074856	0.050066	0.077618	0.013575	0.033272
$U_2O_5^+$	38647	7404	104087	70890	58267	17399	3131	14423
Norm	0.008259	0.005585	0.016289	0.007548	0.008029	0.007803	0.002653	0.005458

Table 11. Comparison of triple uranium-containing oxide species, normalized to UO_2^+.

Sample	Depleted UO_2	Natural UO_3	Depleted U_3O_8	Depleted U_3O_8	Natural UO_3	Natural U_30_8	Enriched U_30_8	Enriched U_30_8
$U_3O_3^+$	698	0	934	439	354	436	0	0
Norm	0.000149	0	0.000146	4.67E-05	4.88E-05	0.000196	0	0
$U_3O_4^+$	2784	332	3953	1463	1225	2060	0	522
Norm	0.000595	0.00025	0.000619	0.000156	0.000169	0.000924	0	0.000198
$U_3O_5^+$	15381	1414	20578	13302	8359	9915	263	2507
Norm	0.003287	0.001067	0.00322	0.001416	0.001152	0.004447	0.000223	0.000949
$U_3O_6^+$	61557	6397	160619	94108	51387	32200	1285	12151
Norm	0.013155	0.004825	0.025136	0.010021	0.007081	0.014441	0.001089	0.004598
$U_3O_7^+$	33269	5381	98391	46540	41593	14788	1086	9035
Norm	0.00711	0.004059	0.015398	0.004956	0.005732	0.006632	0.00092	0.003419

Table 12. Comparison of quadruple uranium-containing oxide species, normalized to UO_2^+.

Sample	Depleted UO_2	Natural UO_3	Depleted U_3O_8	Depleted U_3O_8	Natural UO_3	Natural U_30_8	Enriched U_30_8	Enriched U_30_8
$U_4O_5^+$	294	0	408	155	151	253	0	0
Norm	6.28E-05	0	6.39E-05	1.65E-05	2.08E-05	0.000113	0	0
$U_4O_6^+$	701	0	1044	370	303	565	0	155
Norm	0.00015	0	0.000163	3.94E-05	4.18E-05	0.000253	0	5.87E-05
$U_4O_7^+$	1885	235	4333	1779	1076	1905	0	352
Norm	0.000403	0.000177	0.000678	0.000189	0.000148	0.000854	0	0.000133
$U_4O_8^+$	10252	1088	25626	14478	8302	5940	0	1875
Norm	0.002191	0.000821	0.00401	0.001542	0.001144	0.002664	0	0.00071
$U_4O_9^+$	8125	1219	23436	9644	8940	3682	151	1926
Norm	0.001736	0.00092	0.003668	0.001027	0.001232	0.001651	0.000128	0.000729

From the tables above, the hypotheses relating higher intensities for $U_2O_4^+$, $U_3O_6^+$, and $U_4O_8^+$ hold true with one exception. In samples T101 and U18, both naturally occurring varieties of UO_3, the $U_4O_9^+$ peak is the highest intensity peak for the $U_4O_y^+$

clusters. Also of note with these samples is that they had the lowest ion yield of any of the samples analyzed. Ion yields for all of the U_4 oxide clusters were quite low and some species were below the limit of detection for the instrument. Longer counting times would have improved the ion intensities and could have generated more of the $U_4O_y^+$ cluster ions.

4.1.2 Protonation and Hydroxide Ion Ratios

It was discovered early in the analysis of this data that there was a rather large level of protonation present in our spectra. Fahey and Messenger concluded that the deposition rate of H^+ ions exceeds the erosion rate of the sample's surface leading to this protonation (Fahey and Messenger, 2001). An effort was made to characterize the level of protonation in both a qualitative and quantitative manner. The qualitative characterization is presented here, which led to the further quantization presented later in this chapter. Protonation ratios were calculated for depleted UO_2 and U_3O_8 samples as well as a naturally occurring UO_3 sample and are tabulated in Table 13. A trend was discovered in the UO_2^+ protonation between the different uranium oxide stoichiometries. The trend shows a good linear correlation with a Pearson correlation coefficient of 0.9397 as depicted in Figure 15.

Table 13. Protonation ratios for various uranium oxides.

Sample	UO_2	UO_3	U_3O_8
UO^+	3094919	831166	9812949
UOH^+	488504	94551	973679
Ratio	0.157841	0.113757	0.099224
UO_2^+	7023521	1842164	15342830
UO_2H^+	1781410	293897	3549143
Ratio	0.253635	0.159539	0.231323

UO_3^+	16871	3109	92642
UO_3H^+	143168	24796	511592
Ratio	8.486041	7.975555	5.522247
UO_4^+	16543	2711	12527
UO_4H^+	20570	2968	35093
Ratio	1.243426	1.094799	2.801389

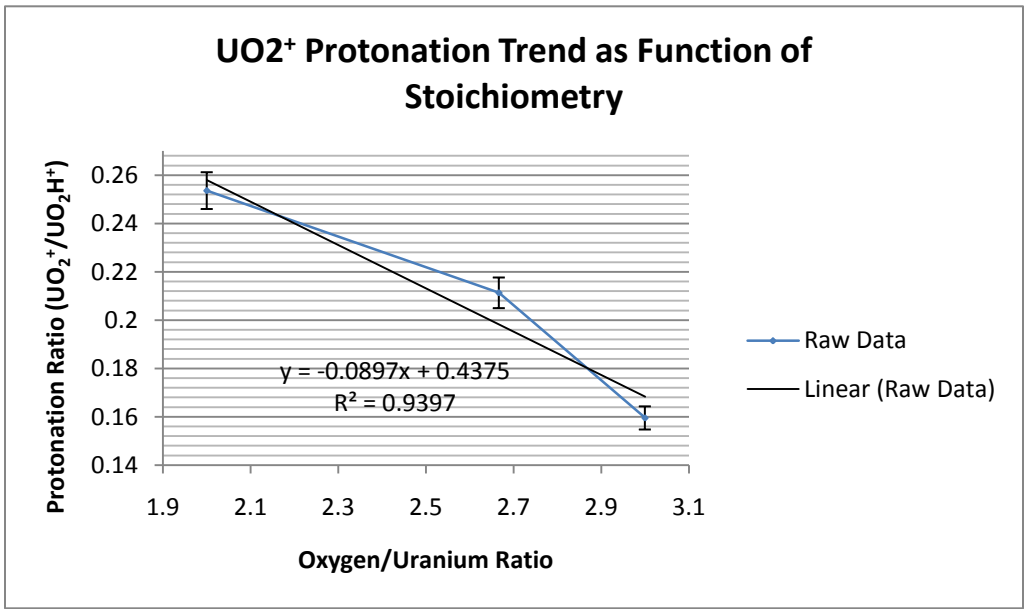

Figure 15. Graphical representation of protonation trend as a function of stoichiometry ranging from UO_2 at the highest level to UO_3 at the lowest.

The correlation of protonation to stoichiometry raised the question as to whether the opposite would hold true for hydroxide ions (OH^+). Data were again tabulated for depleted UO_2 and U_3O_8 samples as well as a naturally occurring UO_3 sample and are provided below in Table 14. The hypothesis was confirmed and the correlation between the ratio of OH^+ ions and UO_2^+ ions for the various stoichiometries was even better than the correlation of protonation between the various stoichiometries. Figure 16 graphically

represents the ratio of OH^+/UO_2^+ and has a Pearson correlation coefficient of 0.9915, which illustrates a high level of correlation.

Table 14. Ratios of hydroxide ions versus UO_2^+ signals for selected samples.

Sample	UO_2	UO_3	U_3O_8
UO_2^+	7023521	1842164	15342830
OH^+	12809	12447	84836
Ratio	0.001824	0.006757	0.005529

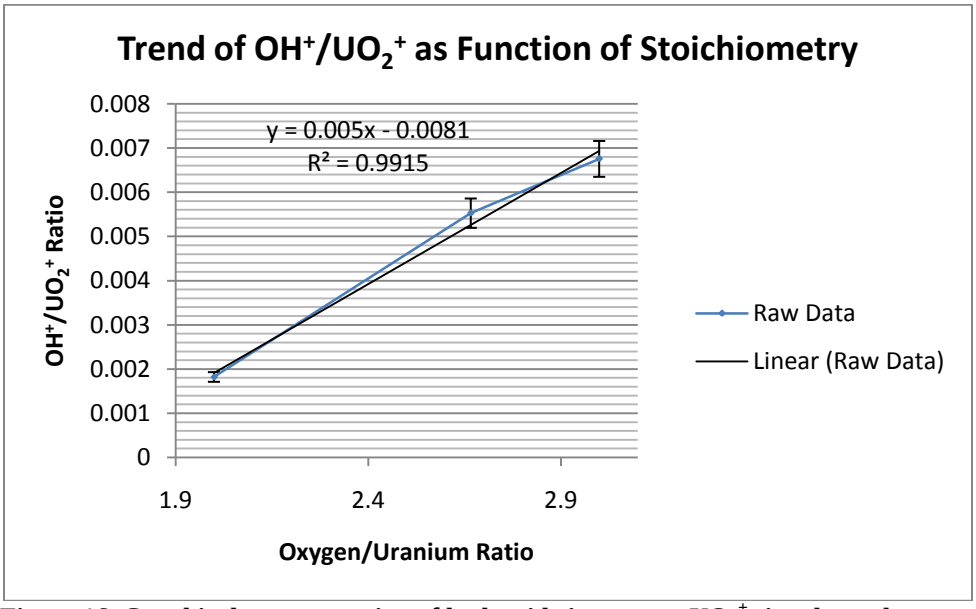

Figure 16. Graphical representation of hydroxide ion versus UO_2^+ signal trend as a function of stoichiometry ranging from UO_2 at the highest level to UO_3 at the lowest.

The correlation of the OH^+ to UO_2^+ suggested that proton transfer could occur from the OH^+ to the sample's surface. Fahey and Messenger assert that this mechanism does occur and has a significant effect on isotope measurements (Fahey and Messenger, 2001). In order to verify that this is the case, data were again tabulated for depleted UO_2 and U_3O_8 samples as well as a naturally occurring UO_3 sample and are provided below in

Table 15. The same upward linear trend as noticed in the in the OH^+/UO_2^+ ratios was observed and is graphically represented in Figure 17. The trend in the ratio of OH^+/UO_2H^+ has a Pearson correlation coefficient of 0.9915, which also illustrates a high level of correlation.

Table 15. Ratios of hydroxide ions versus UO_2H^+ signals for selected samples.

Sample	UO_2	UO_3	U_3O_8
UO_2H^+	1781410	293897	3242293
OH^+	12809	12447	84836
Ratio	0.00719	0.042352	0.026165

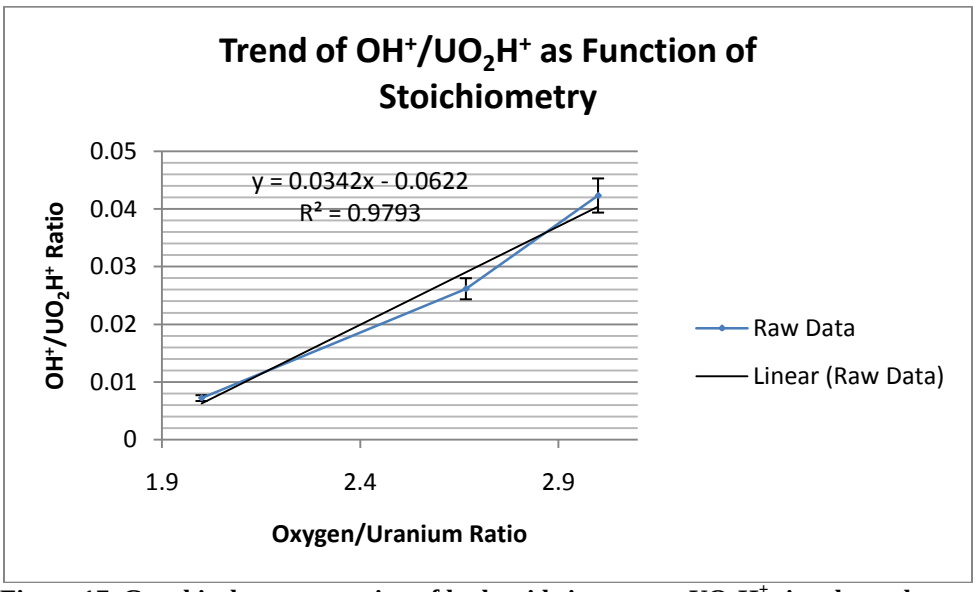

Figure 17. Graphical representation of hydroxide ion versus UO_2H^+ signal trend as a function of stoichiometry ranging from UO_2 at the highest level to UO_3 at the lowest.

4.2 Simulated Spectra and Spectral Stripping

Due to the determination of the protonation in our samples, an effort was made to produce simulated spectra based upon the isotopic and stoichiometric abundances of each of the samples. There are a multitude of isotopic calculators available to aid in the

reproduction and simulation of spectra. Many of these were compared by Massila and others in an effort to provide a better isotope pattern generator than currently exists (Massila, 2007). Some of the isotope calculators provide only the abundance of each ion cluster or isotope while others provide peaks constructed from a Gaussian distribution.

No calculator could be found that provided a Gaussian distribution that allowed the user to alter isotopic abundances from naturally occurring ratios. For this reason, two separate isotope calculators were used to simulate the spectra for the samples in this research. The first isotope calculator is a web-based Java-script which allows a user to alter the isotopic abundances for given species. The web-based isotope calculator is available here: http://www-personal.umich.edu/~junhuay/pattern1.htm (Massila and others, 2007). Isotopic cluster abundances for UO^+, UO_2^+ and UO_3^+ for and isotopic abundances generated by this calculator are provided in Table 16 for enriched and depleted U_3O_8 samples. The second isotope calculator used provides a Gaussian distribution for isotope clusters but does not allow the user to modify isotopic values from naturally occurring. The Gaussian-based calculator can be downloaded here: http://surfacespectra.com/software/isotopes/index.html (Massila and others, 2007). The surface spectra calculator must be downloaded and installed on a computer to use (administrator rights will be needed on the computer).

Table 16. Isotopic cluster abundances for UO^+, UO_2^+, and UO_3^+ for enriched and depleted U_3O_8 samples samples.

Enriched U_3O_8 (90%) UO^+

Exact Mass	%
250.036	0.8622

Enriched U_3O_8 (90%) UO_2^+

Exact Mass	%
266.031	0.8622

Enriched U_3O_8 (90%) UO_3^+

Exact Mass	%
282.026	0.8622

251.039	**100**
251.04	0.0003
252.04	0.0018
252.04	0.3689
252.043	0.0381
253.043	0.2055
253.045	0.0001
254.045	0.0008
254.046	**9.6379**
255.05	0.0037
256.05	0.0198

267.034	**100**
267.035	0.0007
268.035	0.0035
268.035	0.3689
268.038	0.0762
269.038	0.411
269.04	0.0003
270.04	0.0015
270.041	**9.6379**
270.042	0.0002
271.042	0.0004
271.045	0.0073
272.045	0.0396

283.029	**100**
283.03	0.001
284.03	0.0053
284.03	0.3689
284.033	0.1143
285.033	0.6165
285.035	0.0004
286.035	0.0023
286.036	**9.6379**
286.037	0.0005
287.037	0.0013
287.04	0.011
288.04	0.0594
290.044	0.0001

Enriched U_3O_8 (50%) UO^+

Exact Mass	**%**
250.036	1.0422
251.039	99.9698
251.04	0.0004
252.04	0.0021
252.04	0.1519
252.043	0.0381
253.043	0.2054
254.045	0.0003
254.046	**100**
255.05	0.0381
256.05	0.2055

Enriched U_3O_8 (50%) UO_2^+

Exact Mass	**%**
266.031	1.0422
267.034	99.9698
267.035	0.0008
268.035	0.0043
268.035	0.1519
268.038	0.0762
269.038	0.4109
269.04	0.0001
270.04	0.0006
270.041	**100**
270.042	0.0002
271.042	0.0004
271.045	0.0762
272.045	0.411
273.049	0.0002
274.049	0.0004

Enriched U_3O_8 (50%) UO_3^+

Exact Mass	**%**
282.026	1.0422
283.029	99.9698
283.03	0.0012
284.03	0.0064
284.03	0.1519
284.033	0.1142
285.033	0.6163
285.035	0.0002
286.035	0.0009
286.036	**100**
286.037	0.0005
287.037	0.0013
287.04	0.1143
288.04	0.6165
289.044	0.0005
290.044	0.0013

Depleted U_3O_8 (0.5%) UO^+

Exact Mass	**%**
250.036	0.0034
251.039	0.509

Depleted U_3O_8 (0.5%) UO_2^+

Exact Mass	**%**
266.031	0.0034
267.034	0.509

Depleted U_3O_8 (0.5%) UO_3^+

Exact Mass	**%**
282.026	0.0034
283.029	0.509

252.04	0.0012
252.043	0.0002
253.043	0.001
254.046	**100**
255.05	0.0381
256.05	0.2055

268.035	0.0012
268.038	0.0004
269.038	0.0021
270.041	**100**
271.045	0.0762
272.045	0.411
273.049	0.0002
274.049	0.0004

284.03	0.0012
284.033	0.0006
285.033	0.0031
286.036	**100**
287.04	0.1143
288.04	0.6165
289.044	0.0005
290.044	0.0013

The Gaussian-based isotope pattern calculation software allows the user to define the full-width at half-maximum (FWHM) for the peaks generated for the cluster ions. An average value of the FWHM for the peaks appearing in the experimental spectra was found to be 0.06 amu. The 0.06 amu value was then used in the isotope pattern calculator to determine the ion cluster abundances for UO^+, UO_2^+ and UO_3^+ clusters. The standard deviation was then calculated to be 0.02548 amu using equation 5 below (Skoog and others, 2006). The two sets of data were then combined to provide calculators to simulate spectra when normalized to the most abundant species present in each spectrum. Figure18 provides an overlay of a simulated spectrum and a spectrum collected during this research.

$$FWHM = 2\sqrt{2\ln 2}\sigma \qquad 5$$

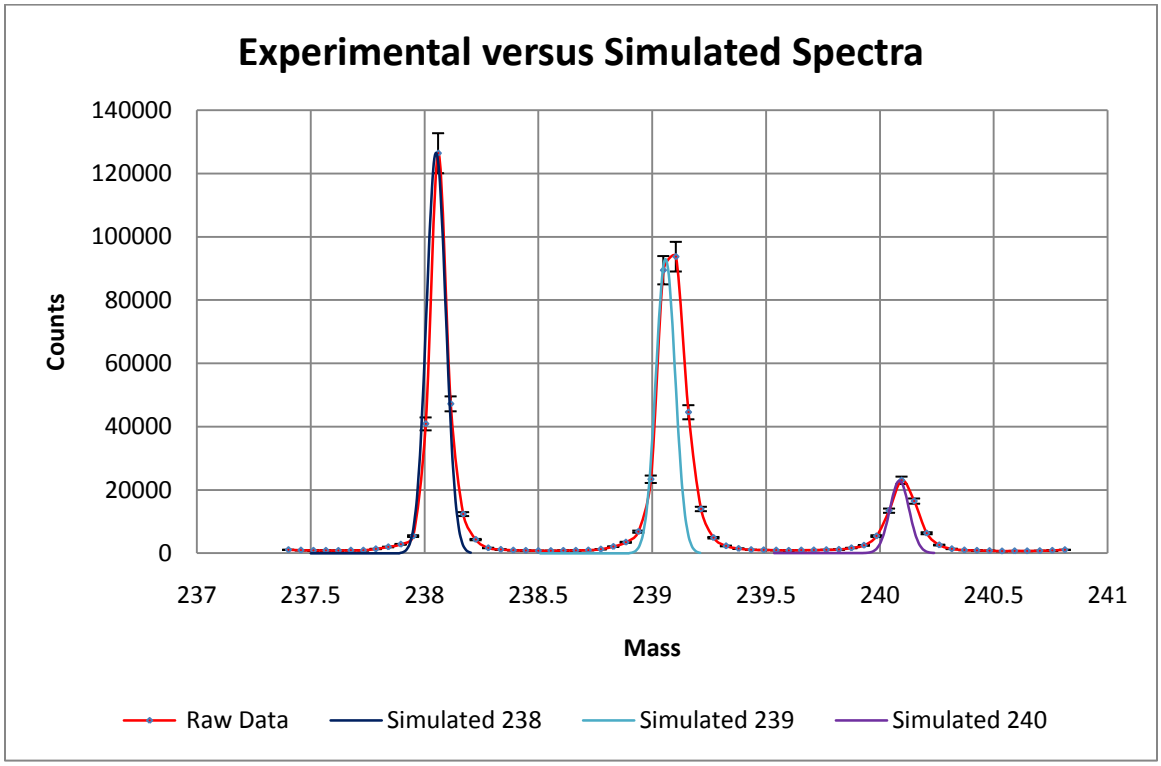

Figure 18. Comparison of experimental and simulated spectra.

The comparison between the experimentally derived spectrum and the simulated spectrum revealed several important features about the data. The calculated value for the FWHM measurement appears to be accurate when correlated to the $^{238}U^{+}$ peak. The data points for each peak are extremely sparse making it difficult, if not impossible to reliably strip any features from these spectra. The problem in the sparse number of data points available could have easily been remedied by selecting a higher sampling data rate. Some of the peaks are composite peaks, as evidenced by the broadening of the 239^{+} and 240^{+} peaks. The 239^{+} and 240^{+} peaks are comprised of protonated $^{238}U^{+}$ as well as other unknown hydrocarbon species. Even the $^{238}U^{+}$ peak shows evidence of a minor contribution from some other species due to the tailing feature at the high end of the

peak. For these reasons it was necessary to attempt to quantify the protonation which is carried out in the next section.

4.3 Quantitation of Protonation

The Beer-Bouguer-Lambert law, often referred to as Beer's law, is commonly used in molecular spectroscopy to quantify the amounts of various analytes within a given sample (Skoog and others, 2006). Beer's law provides a solution for simultaneous quantitative analyses of multiple species with different absorption spectra. Beer's law states that the fraction of radiation absorbed in a solution of an absorbing analyte can be quantitatively related to the concentration of the analyte (Christian, 1986). An analogous multi-component analysis strategy offers a unique solution to our problem of resolving and further quantification of protonation within each of our samples.

In both cases, for a given spectroscopy bin, different species contribute intensity in proportion to their concentration. This allows for either problem to be satisfied through the solution to a series of simultaneous equations. The solution for a multicomponent system is given below in equation 6 where the subscripts refer to analyte 1, 2, …, n, ε is a proportionality constant, and c is the concentration (Skoog and other, 2006). This analysis method can be applied for any number of analytes that overlap to resolve each analyte separately through the solutions of simultaneous equations. Once all known analytes are identified, a system of equations is developed for simultaneous solution. An illustration of such a system of equations is presented in Figure 19.

$$A_{total} = A_1 + A_2 + \ldots + A_n \qquad (6)$$

$$= \varepsilon_1 c_1 + \varepsilon_2 c_2 + \ldots \varepsilon_n c_n$$

$$\left.\begin{aligned} A_1 &= (\varepsilon_{11} c_1 + \varepsilon_{21} c_2 + \ldots) \\ A_2 &= (\varepsilon_{12} c_1 + \varepsilon_{22} c_2 + \ldots) \\ A_3 &= (\varepsilon_{13} c_1 + \varepsilon_{23} c_2 + \ldots) \\ A_4 &= (\varepsilon_{14} c_1 + \varepsilon_{24} c_2 + \ldots) \end{aligned}\right\} \text{Solve Simultaneously}$$

Figure 19. Sample system of equations based upon a multi-component analysis strategy.

Similar systems of equations were developed for the protonated species of UO^+, UO_2^+, and UO_3^+. The protonation factor, α, and diprotonation factor, β, were developed for all three series and a triprotonation factor, γ, was developed for the UO_3^+. Protonation factors were all normalized to the abundance of UO_2^+ present in each sample. For each set of equations "A" denotes the total abundance of a given mass, "I" denotes the intensity of the peak associated with the given mass, and "a" denotes the abundance of the analyte of interest.

The $^{18}O^+/^{16}O^+$ fraction was defined as the term Q and was assigned a value of 0.205 based upon its naturally occurring isotopic abundance. Using an average value for the $^{18}O^+/^{16}O^+$ fraction could potentially lead to the propagation of error in our calculations. The error would arise due to variability in the isotopic values in oxygen noted in prior research (Pajo, 2001 and Betti and others, 1999). Unfortunately, methane was ubiquitous in our samples and created a composite peak in the 16 amu mass channel. The presence of the methane created a major interference in the direct measurement of

the $^{16}O^+$ ions. A system of equations was first developed for the UO^+, the simplest of the calculations and is illustrated in Figure 20.

$$A_1 = A\ UO = I_{254} = \varepsilon_1 a\ U^{16}O$$
$$A_2 = A\ UOH = I_{255} = \varepsilon_2 a\ U^{16}OH \longrightarrow \alpha$$
$$A_3 = A\ UOH_2 = I_{256} = \underbrace{\varepsilon_3 a\ U^{18}O}_{Q} + \underbrace{\varepsilon_4 a\ U^{16}OH_2}_{\beta}$$

Figure 20. System of equations used to determine α and β for UO^+.

Similar systems of equations were then developed for the other stoichiometric clusters and their protonated species. Figure 21 illustrates the system of equations developed for calculating α and β for the UO_2^+ cluster ions. Figure 22 illustrates the system of equations developed for calculating α, β, and γ for the UO_3^+ cluster ions. The solutions to the systems of equations developed were easily calculated by a code developed in Matlab. The calculated values of α, β, and γ were determined by the intensities listed in Appendix Q and results are provided in Table 17.

$$A_1 = A\ UO_2 = I_{270} = \varepsilon_1 a\ U^{16}O_2$$
$$A_2 = A\ UO_2H = I_{271} = \varepsilon_2 a\ U^{16}O_2H \longrightarrow \alpha$$
$$A_3 = A\ UO_2H_2 = I_{272} = \underbrace{\varepsilon_3 a\ U^{16}O^{18}O}_{Q} + \underbrace{\varepsilon_4 a\ U^{16}O_2\ H_2}_{\beta}$$

Figure 21. System of equations used to determine α and β for UO_2^+.

$$A_1 = A\,UO_3 = I_{286} = \varepsilon_1 a\,U^{16}O_3$$
$$A_2 = A\,UO_3H = I_{287} = (\varepsilon_2 a\,U^{16}O_3H) \longrightarrow \alpha$$
$$A_3 = A\,UO_3H_2 = I_{288} = (\varepsilon_3 a\,U^{16}O_3H_2) \longrightarrow \beta + (\varepsilon_4 a\,U^{16}O_2{}^{18}O) \longrightarrow Q$$
$$A_4 = A\,UO_3H_3 = I_{289} = (\varepsilon_5 a\,U^{16}O_3H_3) \longrightarrow \gamma + (\varepsilon_6 a\,U^{16}O_2{}^{18}OH) \longrightarrow \alpha \cdot Q$$
$$A_5 = A\,UO_3H_2 = I_{290} = (\varepsilon_7 a\,U^{16}O_2{}^{18}OH_2) \longrightarrow \beta \cdot Q + (\varepsilon_8 a\,U^{16}O^{18}O_2) \longrightarrow Q^2$$
$$A_6 = A\,UO_3H_3 = I_{291} = (\varepsilon_9 a\,U^{16}O_2{}^{18}OH_3) \longrightarrow \gamma \cdot Q + (\varepsilon_{10} a\,U^{16}O^{18}O_2H) \longrightarrow \alpha \cdot Q^2$$
$$A_7 = A\,UO_3H_2 = I_{292} = (\varepsilon_{11} a\,U^{16}O^{18}O_2) \longrightarrow Q^2 + (\varepsilon_{12} a\,U^{16}O_2{}^{18}OH_2) \longrightarrow \beta \cdot Q$$
$$A_8 = A\,UO_3H = I_{293} = (\varepsilon_{13} a\,U^{16}O^{18}O_2H) \longrightarrow \alpha \cdot Q^2 + (\varepsilon_{14} a\,U^{16}O_2{}^{18}OH_3) \longrightarrow \gamma \cdot Q$$
$$A_9 = A\,UO_3 = I_{294} = (\varepsilon_{15} a\,U^{18}O_3) \longrightarrow Q^3$$

Figure 22. System of equations used to determine α, β, and γ for UO_3^+.

Table 17. Calculated values of α, β, and γ for UO^+, UO_2^+, and UO_3^+ for each sample.

UO^+	Depleted UO_2	Natural UO_3	Depleted U_3O_8	Depleted U_3O_8	Natural UO_3	Natural U_3O_8	Enriched U_3O_8	Enriched U_3O_8
α	0.070910	0.053608	0.041985	0.066405	0.042821	0.026128	0.029718	0.023609
β	0.005936	0.002821	0.001851	0.002503	0.002622	0.006658	0.001453	0.000813

UO_2^+	Depleted UO_2	Natural UO_3	Depleted U_3O_8	Depleted U_3O_8	Natural UO_3	Natural U_3O_8	Enriched U_3O_8	Enriched U_3O_8
α	0.253635	0.156264	0.203193	0.249932	0.221579	0.423279	0.110659	0.094353
β	0.025555	0.012004	0.015610	0.028270	0.016787	0.036577	0.018270	0.016276

UO_3^+	Depleted UO_2	Natural UO_3	Depleted U_3O_8	Depleted U_3O_8	Natural UO_3	Natural U_3O_8	Enriched U_3O_8	Enriched U_3O_8
α	0.025828	0.020032	0.022682	0.033630	0.024807	0.056369	0.014606	0.013000
β	0.009280	0.006187	0.002197	0.002295	0.003639	0.012081	0.002176	0.002223
γ	0.016059	0.009661	0.003872	0.004161	0.004215	0.015173	0.004603	0.003665

These values reveal some useful information regarding the levels of protonation of the surfaces of the samples. The UO_2 sample showed the highest level of protonation which correlates to the fact that the surface chemistry dictates the level of protonation within a given sample (Fahey and Messenger, 2001). Conversely, the UO_3 samples showed the lowest levels of protonation, which is also supported by the work of Fahey

and Messenger (Fahey and Messenger, 2001). Fahey and Messenger also suggest the use of a sputtering beam in addition to the primary ion beam to lessen the effects of protonation (Fahey and Messenger, 2001). We were not able to use the sputtering source on the instrument during our research due to unscheduled maintenance that occurred in conjunction with our measurements.

4.4 Isotopic Determinations

With the protonation factors calculated for each species, the $^{235}UO_2^+$ and $^{238}UO_2$+ peaks were reassessed in order to determine isotopic ratios. An average hydrocarbon count was determined using mass channels 259^+, 260^+, 261^+, 304^+, 308^+, and 318^+. Much care was taken to ensure that no interferences such as ^{235}U cluster species or various UC clusters were indentified in the same mass channels. The hydrocarbon-subtracted isotopic ratios were then compared to the raw isotopic calculations based upon the integrated peak areas from the reconstructed ion images. Results from the depleted UO_2 and one of the depleted U_3O_8 samples were excluded due to the fact that their exact isotopic abundances are unknown.

Ratios of the $^{235}UO_2^+$ and $^{238}UO_2^+$ ions were determined based upon ion intensities reported in the integrated ion intensities from reprocessed ion images. The uncorrected relative ion intensities for each sample are provided in Table 18. The ratios of the $^{235}UO_2^+$ and $^{238}UO_2^+$ ions were then compared to the expected values determined by the values reported in the certificate of analysis for each of the samples and reported as well in Table 18. Figure 23 illustrates that there was a good correlation between the measured values and the expected values with a Pearson correlation coefficient of 0.9985.

Table 18. Uncorrected ion intensities, $^{235}UO_2^+$ and $^{238}UO_2^+$ ratios, and expected isotopic ratios for selected samples.

Sample	Natural UO_3	Depleted U_3O_8	Natural UO_3	Natural U_3O_8	Enriched U_3O_8	Enriched U_3O_8
235 Cts	93701	354482	177491	43942	2259137	9072533
238 Cts	1842164	15342830	9960259	3231374	2241281	1232067
Ratio	0.05086464	0.02310408	0.01781992	0.01359855	1.007967	7.363669
Expected	0.00725262	0.00509001	0.00725262	0.00725262	0.999698	10.3757

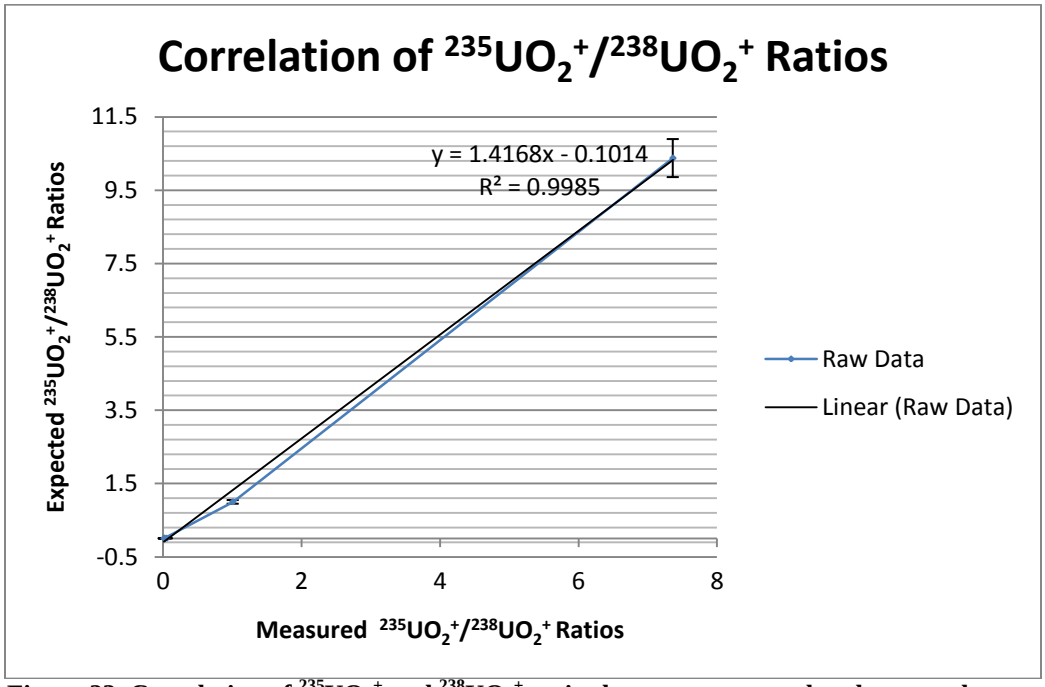

Figure 23. Correlation of $^{235}UO_2^+$ and $^{238}UO_2^+$ ratios between measured and expected values.

Hydrocarbon intensities were then calculated by determining the average intensities for the 259^+, 260^+, 261^+, 304^+, 308^+, and 318^+ peaks. Values for each of these intensities as well as the average and standard deviations are provided in Appendix O. The average values were then subtracted from the raw counts and corrected $^{235}UO_2^+$ / $^{238}UO_2^+$ ratios were calculated with the results provided in Table 19. Reported errors were based on the propagation of error calculated by equation 7 (Christian, 1986) using

the calculated standard deviations for each sample. The corrected values show an even stronger correlation than the uncorrected values as illustrated in Figure 24.

$$(s_a^2)_{rel} = (s_b^2)_{rel} + (s_c^2)_{rel} + (s_d^2)_{rel} \quad (7)$$

$$(s_a)_{rel} = \sqrt{(s_b^2)_{rel} + (s_c^2)_{rel} + (s_d^2)_{rel}}$$

Table 19. Hydrocarbon averages, uncorrected ion intensities, corrected ion intensities, $^{235}UO_2^+/^{238}UO_2^+$ ratios, and expected isotopic ratios for selected samples.

Sample	235 Cts	238 Cts	HC Cts	235 Corr	238 Corr	Ratio	Error	Expected
Natural UO_3	93701	1842164	80645	13055	1761518	0.00741	6.51E-05	0.007253
Depleted U_3O_8	354482	15342830	272984	81498	15069846	0.00540	1.9E-05	0.00509
Natural UO_3	177491	9960259	101015	76476	9859244	0.00775	2.82E-05	0.007253
Natural U_3O_8	43942	3231374	18667	25275	3212707	0.00786	4.97E-05	0.007253
Enriched U_3O_8	2259137	2241281	11376	2247761	2229904	1.00800	0.00095	0.999698
Enriched U_3O_8	9072533	1232067	52711	9019822	1179355	7.64809	0.00748	10.3757

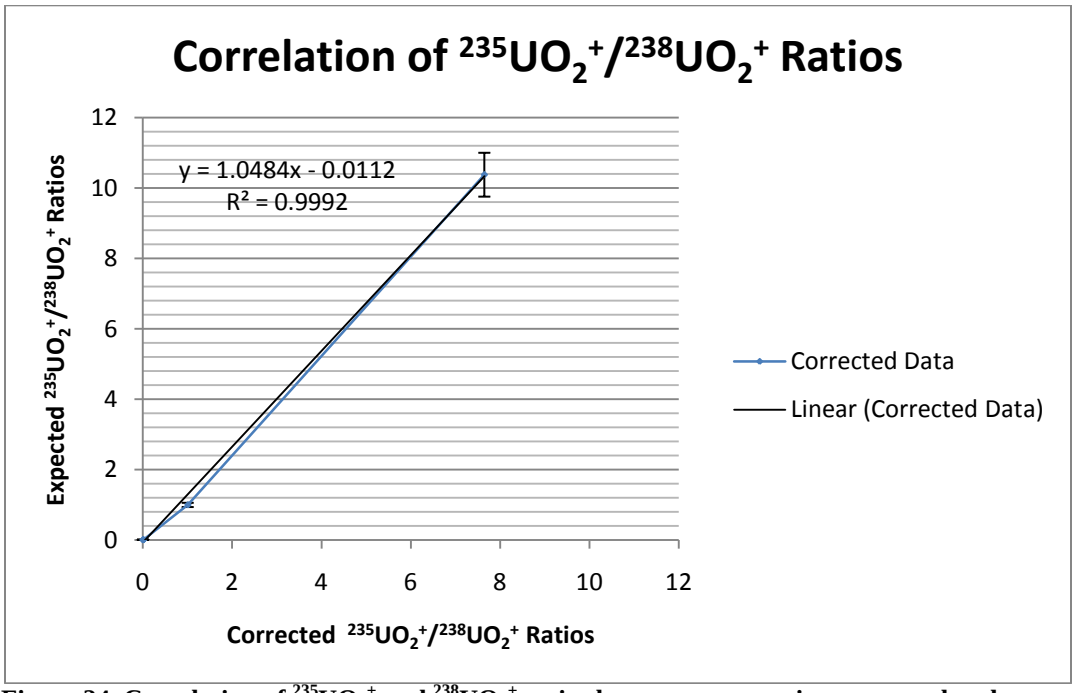

Figure 24. Correlation of $^{235}UO_2^+$ and $^{238}UO_2^+$ ratios between protonation-corrected and NIST-certified values.

Removing the average hydrocarbon intensities from the $^{235}UO_2^+$ and $^{238}UO_2^+$ intensities improved the Pearson correlation coefficient from 0.9985 to 0.9992 for the raw and corrected values, respectively. The corrected values are all within 7.5% of the known values with the exception of the 90% enriched U_3O_8 sample. All of the samples chosen for the data analysis were the highest intensity replicate from within the data sets for each of the samples analyzed. Applying the same methodology to a different 90% enriched U_3O_8 sample, the $^{235}UO_2^+/^{238}UO_2^+$ ratio was adjusted from 9.79 to 10.32, which is within 0.5% of the known value as shown in Table 20. Using this value provided an almost perfect correlation of 0.99998 as shown in Figure 24.

Table 20. Comparison of two U900 samples which highlights the significant differences that can occur between replicates in a given sample.

Sample	235 Cts	238 Cts	Ratio	HC	235 Corr	238 Corr	Ratio	Expected	%Diff
Original	9072533	1232067	7.3637	52711	9019821	1179356	7.64809	10.3757	0.2629
Replicate	3816249	389822	9.7897	22175	3794073	367646.4	10.3199	10.3757	0.0054

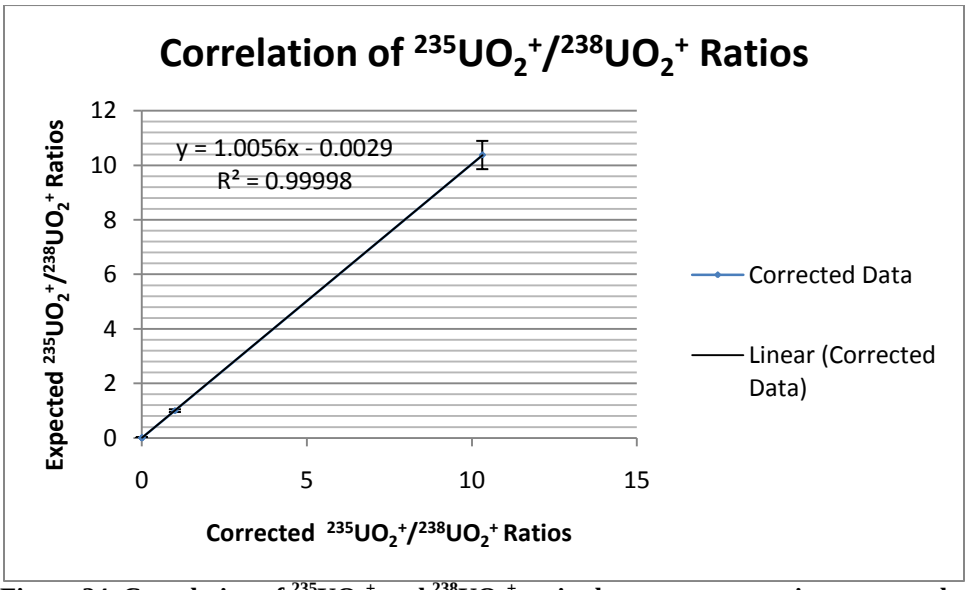

Figure 24. Correlation of $^{235}UO_2^+$ and $^{238}UO_2^+$ ratios between protonation-corrected and NIST-certified values with different replicate of the 90% enriched U_3O_8 sample.

With the protonation and hydrocarbon corrections quantified, a spectrum was simulated using the method developed in section 4.2. This spectrum was compared to the original and is a much better reconstructed spectrum than the original. Both spectra are presented for comparison in Figures 26 and 27.

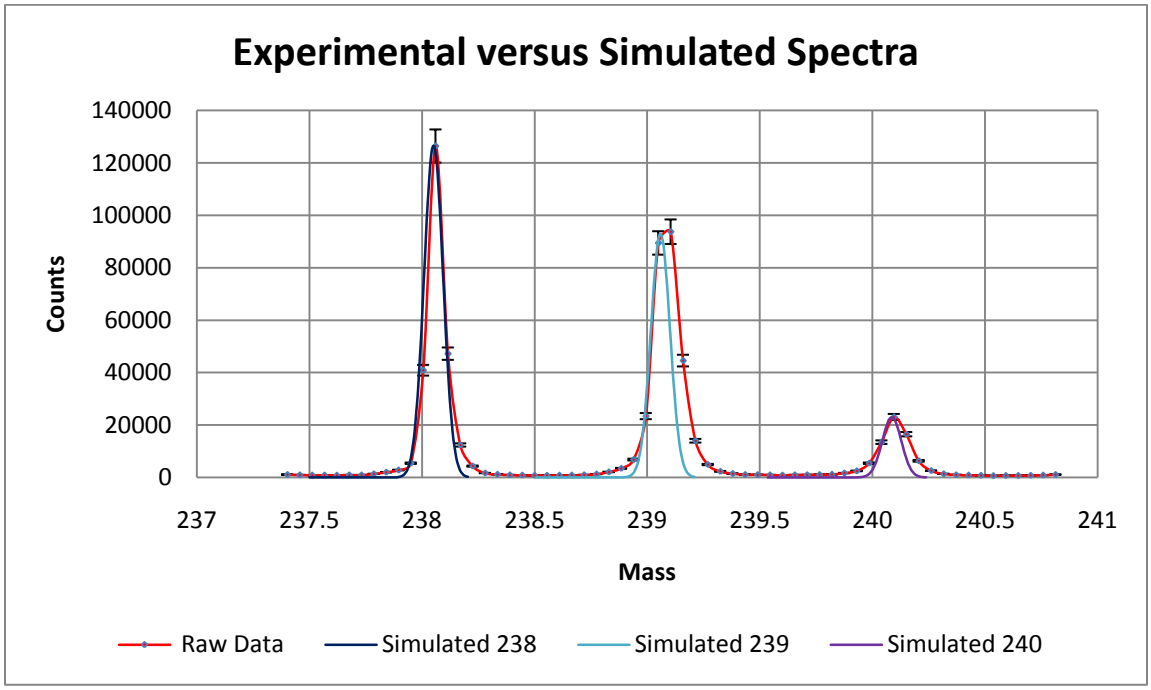

Figure 26. Comparison of experimental and simulated spectra without hydrocarbon and protonation correction.

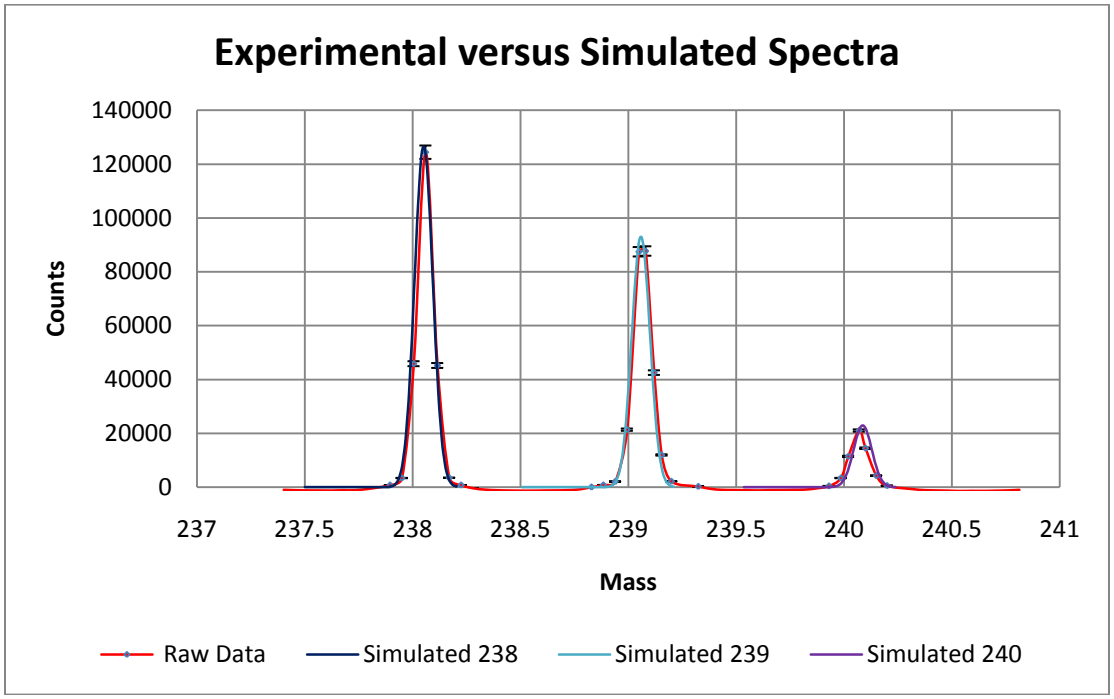

Figure 27. Comparison of experimental and simulated spectra with hydrocarbon and protonation correction.

4.5 Calculation of Average Oxidation State Values

The oxidation state of a metal-oxide as a function of the absolute intensity of the yield of metal-oxygen clusters can be determined by an empirical formula (Gerstmann and others, 2008). Plog and others pioneered the development of the empirical formula based upon the fragment valence *K* (Plog and others, 1977). *K* values can be calculated by assigning a valence of -2 to oxygen then identifying the sum of the valences of all other atoms with the total charge, *q*, of the cluster (Plog and others, 1977). The calculation of *K* values for cluster fragments of $MeO_n^{\pm}$ can be determined by Equation 8 (Plog and others, 1977). Absolute or relative intensities of cluster species are then plotted as a function of *K* values and Gaussian curves are fit to the data (Plog and others, 1977). Values of G^+ and G^- are then determined from the maximum intensities from the

Gaussian curves for the positive and negative clusters (Plog and others, 1977). The average oxidation state can then calculated with Equation 9 (Plog and others, 1977).

$$K = q + 2n \quad (8)$$

$$G^o = \frac{1}{2}(G^+ + G^-) \quad (9)$$

Curves were developed for each of the samples used in this research based on Plog and others' method coupled with modern refinements. Cuynen and others refined the parameters to calculate the average oxidation states in order to establish a spectral library of SIMS data (Cuynen and others, 1999). Aubriet and others furthered Plog and others' research with the inclusion of larger cluster species in the calculation of *K*. Equation 9 describes the calculation of *K* for cluster fragments of $Me_xO_y^{\pm}$ (Aubriet and others, 2001). A list of the calculated oxidation state values is provided in Table 21 and an example of a system of curves is provided in Figure 28. The values used to generate the Gaussian curves as well as each of the system of curves are presented in Appendix R.

$$K = (q + 2y)/x \quad (9)$$

Table 21. Values of G^o calculated for each of the samples used in this research.

Sample	Depleted UO_2	Natural UO_3	Depleted U_3O_8	Depleted U_3O_8	Natural UO_3	Natural U_30_8	Enriched U_30_8	Enriched U_30_8
K (UO_y^-)	5.01	5.68	5.21	5.11	5.49	4.97	5.58	5.49
K ($U_2O_y^-$)	5.25	5.22	5.28	5.31	5.34	5.19	5.31	5.45
G-	5.13	5.45	5.245	5.21	5.415	5.08	5.445	5.47
K ($U_3O_y^+$)	3.82	3.85	3.83	3.94	3.93	3.83	3.95	3.91
K Avg	4.47	4.65	4.58	4.58	4.67	4.46	4.69	4.69

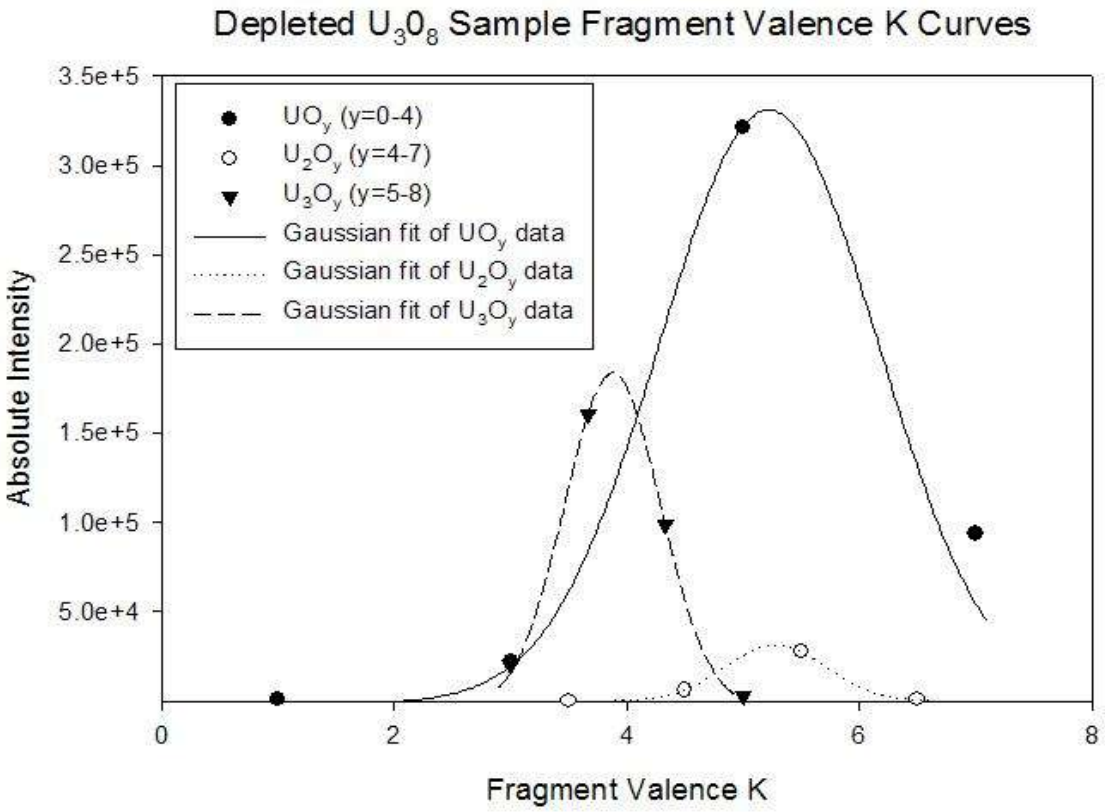

Figure 27. Example of system of Gaussian curves used to calculate average oxidation state for a depleted U_3O_8 sample.

Mean oxidation states vary between each of the samples allowing correlations to be made regarding the stoichiometry and enrichment level of the sample. The natural U_3O_8 sample had the lowest value of 4.46 while the depleted UO_2 sample had a value of 4.47. Both of the depleted U_3O_8 samples had values of 4.58. The natural UO_3 samples had values of 4.65 and 4.67; therefore an average value of 4.66 could be assigned to these samples. The enriched U_3O_8 samples had the highest values, both of which were calculated to be 4.69. All of these numbers are reasonable based upon previous calculations of 4.6 reported in the literature (Gerstmann and others, 2008).

V. Conclusions and Recommendations

5.1 Conclusions

This research provided several useful screening tools that could be used to triage samples and determine which samples require further analysis. Samples with elevated levels of $U_4O_9^+$ in reference to $U_4O_8^+$ were shown to be naturally occurring. Even if a sample has natural $^{235}U^+$ to $^{238}U^+$ ratios, the elevated levels of $U_4O_9^+$ show that some chemical processing has occurred. The research also showed that protonation levels could give some indication as to the stoichiometry of the sample given the trend in the ratios of protonation to O/U ratios. The removal of hydrocarbon information from the raw data also proved to provide much more accurate $^{235}U^+/\ ^{238}U^+$ ratios than the raw data.

This research proved to be a very promising first step into uncovering the usefulness of TOF-SIMS as a forensics tool in the analysis of uranium. Actionable isotopic and cluster ion species information can be obtained extremely quickly with very little sample preparation. If information is necessary in an instant, then TOF-SIMS has been proven to provide data at a moment's notice. Limitations to the technique were also uncovered such as the amount of data points per peak, which could have been improved by using a higher sampling rate. Contamination was also a problem in the analysis of the data and steps should be taken in the future to avoid as much contamination as possible.

5.2 Recommendations

Follow-on research to this experiment should focus obtaining the highest quality data possible. It was evident from this research that much care needs to be taken in order

to prevent any possible contamination to the samples. Sputtering of the samples could have removed much of the contamination and should be employed if at all possible in future studies. A higher scanning rate is a must to ensure more data points are collected for each peak of interest and to aid in data reduction and analysis. Longer scan times could provide information on larger cluster ions in concert with different primary ion species. Time should be taken in order to determine the instrument parameters that will provide optimal results for uranium oxides.

5.2.1 Additional Research

Future work could compare the information that can be achieved from particulate samples using field forward techniques. One field forward technique that could be employed to obtain atomic composition is micro-tube x-ray fluorescence (micro-XRF). It has been proven from past experimentation that the results of a similar technique, XPS have been confirmed with the results of TOF-SIMS (Bonino and others, 2001 and Broczkowski and others, 2006). Further experimentation also used TOF-SIMS to confirm the results of both XPS and scanning electron microscopy results (Nelson and others, 2006) as well as XPS and FTIR spectroscopy (Zhu and others, 2001).

Other techniques such as Raman microprobe, micro-fluorescence, micro-photoluminescence, cathodoluminescence, scanning electron microscopy and micro-FTIR spectrometry could be employed to obtain surface molecular information for a variety of uranium metal, uranium oxides and other uranium-containing materials. While none of these techniques, save TOF-SIMS, are suited to obtain isotopic information, they

are potentially useful as screening tools to identify particulate materials important to further characterize.

5.2.1.1 Elemental Mapping

Complex particle matrices can also be evaluated through the analysis of NIST standard soil samples as well as mixtures of NBL CRM and standard soils. Spatial resolution versus limits of detection can determined for each of the various concentrations of the uranium in the soil samples. A further investigation of the soil samples could determine the applicability of TOF-SIMS for the identification of individual particles of interest in the doped samples via elemental mapping. Elemental maps can be generated using a rastered step-scan technique over the surface of the sample. An example elemental map is provided in Figure 29 of the trace elemental compositions of garnet. The time required for such a scanning technique could then be used to determine the viability of its application for future studies.

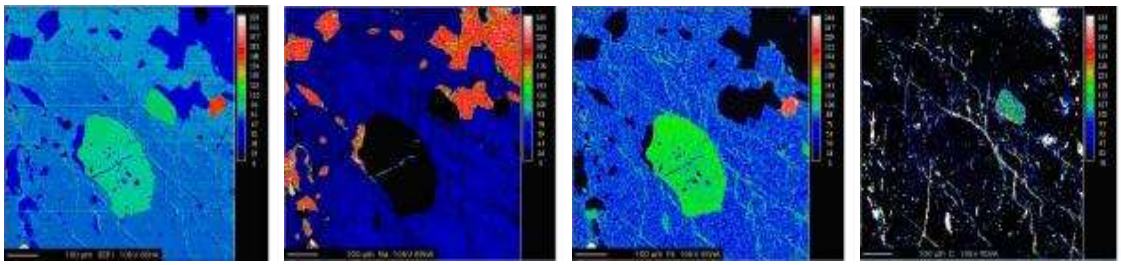

a b c d

Figure 29. (a) Elemental map of garnet amphibolites showing garnet in green and hornblende in light blue; (b) Na map with the Na in the crack in the garnet; (c) Fe enrichment in cleavages in the hornblende; and (d) interconnecting network of carbon along hornblende cleavages (MSU, 2009b).

5.2.1.2 Depth Profiling

Depth profiling can be applied to determine the relative homogeneity of a selected sample. It has been noted in past research that the surface of uranium oxides is rather inhomogeneous, which lead to spurious results when comparing random spectra collected over the surface of a given particle (Schueneman, 2001). Uranium and oxygen ratios could be determined as a function of depth into the particles. Isotopic ratios of uranium and oxygen can also be determined as a function of depth into the particles. The relative abundances of the uranium and oxygen could then be used to estimate the average oxidation states for the selected samples. The application of depth profiling to particles found through step-scans could also be investigated to account for matrix effects.

5.2.2 Sample Preparation

The sample preparation technique employed for this research proved to have good dispersion of particles over the surface of the carbon tape. Particle packing density could be improved by using a smaller section of carbon tape for the loading of the particles. The overwhelming presence of hydrocarbons on the samples' surface could be attributed to the use of the film to cover the samples after preparation. A new method needs to be developed to protect the samples without the use of additional materials to cover the samples. If the fragments of silicon were uniform, plastic tubes could be cut to fit inside the Freund cans to isolate the sample and avoid contamination. A small section of Scotch tape could also be used to affix the silicon fragment to the inside of the Freund can.

Locating particles on the carbon tape proved to be quite difficult with the exception of the UO_3 samples. Finding particles on the carbon tape with the camera on

the TOF-SIMS instrument was virtually impossible. In an effort to locate particles, the instrument operator and I relied on driving over the surface of the sample with the primary ion beam rastering to locate individual particles. The use of copper or aluminum tape would provide a contrast to the dark UO_2 and U_3O_8 particles making them much easier to locate both visually and during analysis in the instrument. The high contrast between the UO_3 samples and the double sided carbon tape make carbon tape the perfect choice when preparing UO_3 samples.

5.2.3 Samples

New sources of standards should be sought for future research. The samples ordered from NBL were quite expensive for the quantities of material received. A new supplier of samples should be referenced in an effort to obtain larger sample sizes. Isotopically pure samples of ^{238}U or ^{235}U would be ideal if at all possible to obtain. It would also help to know the mean particle size of the samples prior to ordering to ensure that individual particles could be located for analysis. Samples with a mean particle size on the order of 100 μm would be ideal. Different enrichment levels for the various uranium oxides could provide much useful information regarding differences between the various stoichiometries. Pure uranium metal samples could also be explored to determine the possible oxides formed during analysis.

Appendix A. Equipment

This appendix contains a comprehensive listing and description of all the equipment that was used in the nuclear forensics of uranium research. Procedural guidance for the use of equipment is provided in the subsequent appendices. Additional information and instructions can be found in the individual equipment operating manuals. Most of the equipment operates with high voltages, high temperatures, or high vacuum and may contain radioactive materials so use caution and follow all safety procedures. These appendices outline the basic procedures to follow when working with loose uranium oxide powders and the prepared uranium oxide samples.

A.1 Glove Box

A Plas-Labs™ model 818-GB glove box was utilized to provide the controlled atmospheric environment that will be required when working with loose uranium oxide powders in preparing samples for measurements. An image is presented in Figure 30.

Figure 30. Plas-Labs™ model 818-GB glove box.

The glove box consists of a working volume and an airlock system. The side airlock system is used to introduce and remove items from the working volume of the glove box while providing a means of controlling the introduction of ambient air and the release of the controlled atmosphere of the working volume as well as any loose particulates of uranium oxide. The airlock has two doors. The outer door opens to the laboratory environment and the inner door opens to the working volume of the glove box. The airlock has a volume of 0.19-cubic meters and is equipped for the introduction of nitrogen and connection to a vacuum system. The glove box is also equipped with a pair of Hypalon™ gloves that are used to manipulate items and equipment located in the working volume of the glove box. The glove box has a grounded electrical power strip in the working volume to provide 110-volt power to requisite electronic equipment. It also has one vacuum valve and three gas valves that allow for control of the atmospheric conditions within the airlock and working volume of the glove box. The following appendix contains the procedures that are to be followed to add and remove items from the glove box.

WARNING: Failure to operate the glove box in strict adherence with applicable safety precautions could result in contamination of the laboratory with loose uranium oxide powders and the working volume of the glove box with ambient air.

A.2 Alpha/Beta Counter

A Gamma Products, Inc. model G5000 alpha/beta counter was used to take measurements of swipes of samples, radioactive waste, and any material taken out of the glove box. Detailed instructions for the use of the alpha/beta counter are provided in appendix D and an image of the counting system is provided in Figure 31.

Figure 31. Gamma Products, Inc. model G5000 alpha/beta counting system.

A.3 TOF-SIMS

The TOF-SIMS measurements were conducted by a graduate student and MSgt Schuler at the State University of New York (SUNY) on their Ion Tof TOF-SIMS V. The University also owns an older PHI model 7200 TOF-SIMS instrument. The PHI instrument uses a pulsed primary ion source of Cesium ions and the Ion Tof instrument has multiple sources of Cesium, Bismuth, or Buckminsterfullerenes (C_{60}) as primary ions. Both instruments offer a large enough working volume to load multiple samples using a standard sample holder with double-sided carbon tape. Figures 32 and 33 contain an image of the Ion Tof TOF-SIMS V and an image of the sample holder from the Ion Tof instrument, respectively.

Figure 32. Image of the Ion Tof TOF-SIMS V.

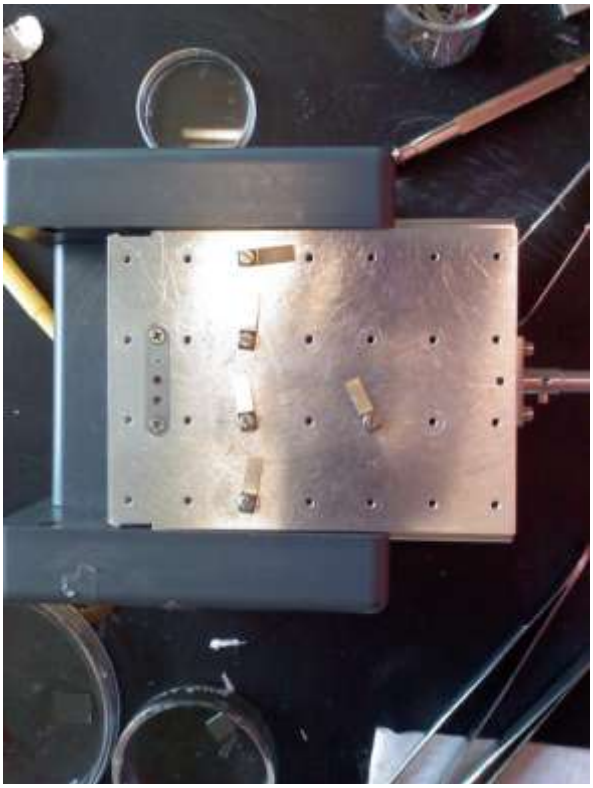

Figure 33. Image of the Ion Tof TOF-SIMS V sample holder.

A.4 Microbalance

A Mettler-Toledo XP-26 microbalance was employed to acquire precision masses of prepared ceric oxide samples. The balance is equipped with a Haug & Co. EN8SLC-type ionizer to ebb the flow of turbulent drafts inside the measurement shield. The balance was certified accurate to within 1.0 μg for a 1.0 mg stainless steel standard. Images of the balance and the ionizer are provided in Figures 34 and 35, respectively.

Figure 34. Mettler-Toledo XP-26 Microbalance.

Figure 35. Haug & Co. EN8SLC-Type Ionizer.

Appendix B. Glove Box Operation

The following section outlines the procedures used to operate the glove box. Adherence to the steps and procedures in this section is essential to prevent contamination of the laboratory with loose uranium oxide powders.

The interior of the glove box will be purged for two weeks prior to use with pure nitrogen and maintained throughout the duration of this research in order to minimize any contamination of the bulk uranium oxide powders and prepared samples prior to measurement. The flow of nitrogen into the glove box will be controlled with a pressure regulator and needle valve assembly and the flow out of the glove box was controlled with a flow meter. The outlet flow of nitrogen from the glove box passes through a HEPA filter prior to exhausting into the laboratory area.

The glove box is composed of a working volume and an airlock system that facilitates moving items in and out of the working volume while providing a means of controlling the introduction of ambient air into the glove box and radiological contaminants out of the glove box. The airlock has an outer door, which opens to the laboratory environment, and an inner door, which opens into the glove box environment.

The air lock has a working volume of 0.19 cubic meters and is equipped for the introduction of N_2 and connection to a vacuum system. The glove box is equipped with Hypalon™ gloves (referred to as gloves from this point forward) so that sample preparation could occur in an N_2 environment.

Prior to working with the uranium oxide powders, the glove box will be cleaned to remove all materials from the previous oxidation experiments. All other equipment

and materials used in this experiment will be passed through the air lock. Table 22 contains a listing of the materials necessary to operate the glove box.

Table 22. Equipment and materials used in operation of glove box.

Equipment	Purpose
α/β Counter	Counter Used to detect contamination on items removed
0 to 1.5 SCFM flow	Used to control flow rate of N_2 through glove box
0 to 50 psi regulator	Used to control pressure and flow rate of N_2 into glove box
Disposable gloves	Worn to keep hands from sticking to Hypalon™ gloves
Filter papers	Used to conduct swipes on all items leaving the glove box
Glove box	Maintains the N_2 environment and contains radioactive
HEPA face mask	Used to prevent inhalation of uranium oxide powders
HEPA filter	Used to filter N_2 flowing out of the glove box
N_2 cylinder	Source of N_2 gas inside glove box
Methanol	Used to wash surface of items before removal from glove
Parafilm®	Used to cover waste uranium oxide powder containers
Portable gamma rate	Used to check for uranium contamination on hands
Tweezers	Used to place filter papers on planchets
Utility wipes	Used to wipe contamination from items removed from glove
Vacuum pump	Used to purge air lock after opening to atmosphere
White cotton lab coat	Used to prevent contamination of clothing with loose
Zip lock bags	Used to dispose of contaminated materials inside glove box

The following steps were developed for operating the glove box with minimal sample contamination and safety of the operator foremost in mind.

Step 1: Verify that nitrogen is flowing through the glove box by examining the flow meter installed on the working volume exhaust valve. During normal operations, the flow rate should be approximately 0.2 SCFM.

Step 2: Put on disposable latex gloves. This will make getting your hands in and out of the gloves much easier and will prevent direct skin contact with any uranium oxide particles.

Step 3: Put on a lab coat, TLD, and HEPA Facemask. Close the laboratory door and restrict access to only those personnel involved in preparing the uranium oxide samples. Ensure that the radiation warning sign on the door indicates that radioactive materials are present in the room and a TLD is required for entry.

Step 4: Close the inner door on the airlock. Open the outer door and place any materials and equipment in the airlock that will be needed in the working volume of the glove box. Limit the amount of time the outer door is open by organizing the items ahead of time. Close the outer door when finished.

Step 5: The airlock must now be purged of all ambient air before the inner door can be opened. Close the nitrogen valve and open the vacuum valve on the airlock. Turn on the vacuum pump and draw a minimum of 20-psi vacuum in the airlock (refer to the pressure gauge on the airlock itself). Turn off the vacuum pump, close the vacuum valve, open the nitrogen valve on the airlock, and fully open the needle valve on the nitrogen regulator. Allow the pressure to return to atmospheric normal in the airlock (vacuum gauge will read 0-psi). Repeat this process two more times. Return the needle valve to the initial position, slightly open, after the airlock is purged.

Step 6: Open the inner airlock door and bring materials into the glove box working area. Leave the inner airlock door open about one-quarter of an inch except when working with loose uranium oxide powders to permit a continuous flow of nitrogen through the glove box. When working with loose uranium

oxide powders, close the inner door to prevent the possible distribution of loose powder into the airlock and lab.

Step 7: When ready to remove items from the glove box, close all loose powder containers (to include the waste container). Wash the surface of each item to be removed with methanol soaked wipes to remove any powder contamination. Place the used wipes in a Ziploc waste bag. Place the items in the airlock and close the inner door.

Step 8: Open the outer airlock door and prepare swipes on all items in the airlock, the disposable gloves, and the inside of the airlock. If an item has more than 10-square centimeters of surface area, use multiple filter papers for the swipe. Place the swipes and items to be removed in the airlock and close the inner door. Using tweezers, place the swipes in empty planchets in the Gamma Products, Inc. model G5000 Alpha/Beta Counter and conduct a radiological survey of all swipes.

Step 9: Confirm the absence of radiological contamination on your hands with a handheld gamma rate meter.

Step 10: If the items in the airlock do not exceed the maximum allowable contamination levels (set at 20 dpm), remove the items from the airlock and close the outer door.

Step 11: Purge the airlock as described in Step 5 above. Leave the inner door open approximately one-quarter of an inch to permit continuous nitrogen gas flow through the glove box.

Appendix C. Sample Mounting Procedures

This appendix lists the procedures to mount powdered uranium samples for measurements. Table 23 lists all of the materials needed in order to mount the samples. Refer to Appendix B for operation of the glove box.

Table 23: Equipment needed for sample mounting.

Equipment	Purpose
Methanol	Used to wash surface of 3" silicon wafer between uses
3" silicon wafer	Used as the surface to disperse uranium powders
Silicon wafer fragments	Used as the mounting medium for the carbon tape
Straight forceps	Used to manipulate substrates and protective film
Curved forceps	Used to manipulate substrates and protective film
Microspatula	Used to remove uranium particles from shipping container
Carbon tape	Used to adhere particles to silicon substrate
Protective film	Used to cover sample to prevent contamination
Razor blade	Used to cut carbon tape and protective film
Freund cans	Used to store samples for shipment

Step 1: Cut pieces of the larger carbon tape into squares and remove the protective film for use as covers for prepared samples.

Step 2: Don laboratory coat, disposable gloves, TLD, finger ring, and HEPA mask.

Step 3: Ensure that all equipment to be used is clean, free of contamination and placed into the glove box. Refer to Appendix B for glove box operations.

Step 4: Apply double-sided carbon tape to small piece of silicon wafer.

Step 5: Use spatula to place small amount of powder onto 3” silicon wafer.

Step 6: Gently tap the wafer to disperse the particles over the surface of the wafer.

Step 7: Remove the protective film from the carbon tape adhered to small piece of silicon wafer.

Step 8: Using tweezers, gently bring the tacky surface of the carbon tape covered silicon wafer into contact with the powder on the 3” wafer.

Step 9: Holding the carbon-tape-coated, uranium particulate containing silicon wafer at a 90° angle, gently tap with spatula to ensure any excess particles not completely adhered to the carbon tape are removed.

Step 10: Using the spatula, gently press the adhered particles into the carbon tape to ensure good adhesion.

Step 11: Place larger piece of protective film over sample.

Step 12: Package sample for shipment and measurements per procedures in Appendix E.

Appendix D. Operation of Gamma Products, Inc. Alpha/Beta Counter

This appendix provides the procedures used to setup and operate the model G5000 Gamma Products, Inc. alpha/beta/gamma counting system located in building 470. These procedures cover the basic operation of the system and the operator's manual should be reviewed for additional information and operational procedures not directly covered in this appendix.

D.1 Setting the Operational Parameters

Prior to using the counting system, the operational parameters must be calculated and entered through the user interface screen. The counting system had been setup for uranium oxidation research and was used on a regular basis for other experiments involving radioactive materials. The counting system was never turned off (recommendation from Gamma Products, Inc.) so the start-up and system initialization procedures were not performed. Table 24 lists the counting system parameters used in this research. Refer to the operator's manual if you must compute new operating parameters for the system or use of the system after powering down.

Table 24. Accepted counting system parameters.

Parameter	Value	Description
Preset Count	999999	Maximum number of counts to record
High Voltage	1550 V	Operating voltage of the detector
Disc Window	550 V	Voltage for α/β channel separation
α Efficiency	22.98%	% of all possible α decays detected
α Cross-Talk	17.72%	% of counts recorded in the β channel that are α decays
β Efficiency	30.89%	% of all possible β decays detected

D.2 Measuring the Alpha and Beta Background Activity

The alpha and beta background information was more than two years old at the start of this research and was recalculated using the procedures listed below.

Step1: Turn on the P-10 gas supply and increase the display intensity on the counting system. Follow the screen instructions and perform a short purge. Allow 30 minutes for the purge to finish before performing step number 2. This will ensure that the proportional tube in the counting system is full of P-10 gas before high voltage is applied.

Step2: Clean an empty planchet with methanol and a tech wipe. Load the planchets into the detector system.

Step 3: Run a manual count (program 0) with the settings from Table 9. Set the alpha and beta background values to zero and set the counting time for 100 minutes.

Step 4: Repeat the manual background count 10 times. This process may take several days due to the time required per count.

Step 5: Turn off the P-10 gas when finished (either finished for the day of finished with all 10 counts).

Step 6: Determine the alpha and beta backgrounds based on the average of the 10 different 100 minute counts. See the next section for the results of the 10 separate 100 minute counts and calculation of the alpha and beta backgrounds used in this research.

D.3 Calculation of the Average Alpha and Beta Background Activity

Table 25 contains the results of the 100 minute background counts for the model G5000 Gamma Products, Inc. alpha/beta counting system. In addition to the gross number of counts, the counting system also reported the net number of counts (based on the detector parameters) and the decays per minute (also based on detector parameters). Only the gross number of counts was meaningful in the background calculations. All calculations were performed according to the statistical methods provided by Dr. Richard Gilbert (Gilbert, 1987). Equations 10 and 11 were used to compute the average (avg) number of α and β counts in the background. The standard deviations (σ) for the α and β background counts were computed with equations 12 and 13.

The critical levels (L_c) and minimum detectable amounts (*MDA*) were not required as a parameter for the counting system but did provide information on the accuracy of the instrument at very low levels of contamination. Equations 14 through 17 were used to compute the L_c and *MDA* based on the α and β backgrounds.

All equations provide results with units of counts. To provide values in units of decays per minute (dpm) divide the result by 100 minutes in order to obtain a value that can be entered directly into the counting system.

Table 25. Results of the 100 minute background counts.

Count	Gross α	Gross β
1	25	528
2	33	489
3	19	581
4	22	517
5	29	492
6	18	567
7	32	506
8	21	521
9	28	493
10	23	518
Average	25	521.2

$$\text{avg } \alpha = \frac{\sum_{i=1}^{10} \alpha_i}{10} \quad (10)$$

$$\text{avg } \beta = \frac{\sum_{i=1}^{10} \beta_i}{10} \quad (11)$$

$$\sigma_\alpha = \sqrt{\frac{\text{avg } \alpha}{10}} \quad (12)$$

$$\sigma_\beta = \sqrt{\frac{\text{avg } \beta}{10}} \quad (13)$$

$$L_{c\alpha} = (2.326 * \sigma_\alpha) \quad (14)$$

$$L_{c\beta} = (2.326 * \sigma_\beta) \quad (15)$$

$$MDA_\alpha = (4.653 * \sigma_\alpha) + 2.706 \quad (16)$$

$$MDA_\beta = (4.653 * \sigma_\beta) + 2.706 \quad (17)$$

The results of equations 8 through 15 are provided in table 26.

Table 26. Results of statistical analysis on background data.

Result	α	β
Average Background	25 counts or 0.25 dpm	521.2 counts or 5.212 dpm
Background σ	1.58 counts or 0.0158 dpm	7.22 counts or 0.0722 dpm
L_c	3.68 counts or 0.0368 dpm	16.79 counts or 0.1679 dpm
MDA	10.06 counts or 0.106 dpm	36.29 counts or 0.3629 dpm

D.4 Measuring the Activity on a Swipe

Swipes are taken on all items that leave the glove box and on any item that may have been contaminated with radioactivity. Swipes will be taken on the following items at a minimum:

1. Sample storage containers.
2. Sample handling materials.
3. Filled radioactive waste bags.
4. Any item being removed from the glove box.

Use the following procedures to obtain and analyze a swipe:

Step 1: Don laboratory coat, disposable gloves, TLD, finger ring, and HEPA mask. If the item you will swipe is in the glove box, close the door to the room to limit the spread of any potential spills.

Step 2: Determine how many swipes you will take and arrange the necessary number of planchets on a flat surface near the item. Place a clean filter paper in each planchet.

Step 3: Starting with the lowest numbered planchet, take the filter paper from the planchet and rub it over the area of the suspected contamination. If the

surface area of the item is larger than 10 cm^2, use more than one filter paper and planchet.

Step 4: Place the filter paper back in the planchet with the contaminated side facing up.

Step 5: Load the planchets into the counting system and measure the activity according to the procedures in the next section of this appendix.

Step 6: If the swipe activity is below the alarm level of 20 dpm, the item is acceptable for use however, as part of the ALARA concept you should attempt to keep the activity as low as possible. If the item has a measured activity level above background try to clean the item again and remove any possible contamination.

Step 7: Dispose of all swipes appropriately. If the activity on the swipe is 20 dpm or higher, treat it as radioactive waste and put it in the waste bag in the glove box.

D.5 Operating the Gamma Products, Inc. Alpha/Beta Counting System

The counting system has several stored programs for counting the activity of a swipe. Program zero is used for manual counting and programs one through five are automatic programs. In the automatic programs, the planchets containing swipes are advanced automatically with a bar code reader inside the counting system. For this research, program one was used to count the activity of all swipes.

Use the following procedures to analyze a swipe:

Step 1: Turn on the P-10 gas and increase the intensity for the counting system display terminal.

Step2: Follow the screen instructions and purge the detector. Select the short purge and wait 30 minutes before using the detector.

Step 3: Load the planchets into the counting system by placing the planchets from the lowest bar code number to the highest bar code number into the input cylinder. Place a metal planchet on top of the planchets containing swipes.

Step 4: Edit the counting program by pressing the EDIT button and then the "1" button. Press the ENTER button to start editing the program. Pres the ENTER button to move to each parameter and change the values as necessary. Table 27 contains a list of the parameters used in this research for swipe analyses.

Table 27. Parameters used for swipe analyses.

Parameter	Value
Preset Count	999999
Time	100 min
HV	1550 V
Disc Window	550
Start Sample	Bar code number from first planchet
Stop Sample	Bar code number from last planchet
Error	1.96 σ
Repeat	0
α Efficiency	22.98%
α Cross Talk	17.72&
α Background	0.28 dpm
β Efficiency	30.89%
β Background	5.34 dpm
Background Time	100 min
Volume Units	0
Volume Units	1

Activity Units	1 (dpm)
Alarm	20 dpm

Step 5: Run the automatic programs by pressing the RUN button followed by the "1" button then the ENTER button.

Step 6: After the program has finished counting the activity on each swipe, press the RESTACK button to return the planchets to the input cylinder.

Step 7: If the display screen indicates that any sample was above the alarm limit, press the DATA button to see a list of the results and which swipe exceeded the maximum activity level.

Step 8: Clean any items that exceed the alarm limit (only those items in the glove box or air lock) and repeat the swipe procedure testing. If the contaminated item is an instrument or fixture in the building, report the contamination to the permit radiation safety officer (PRSO) or alternate PRSO.

Step 9: Turn off the P-10 gas supply and turn down the intensity of the counting system display screen.

Appendix E. Sample Transportation Procedures

This appendix provides an overview of the procedures used to transport the uranium samples to the SUNY. Ensure that the SUNY radiation safety office (RSO) is contacted prior to the arrival of samples to ensure no surprises. Information regarding the SUNY RSO can be obtained at the following web site: http://www.facilities-buffalo.org/Home/Departments/ehs/SafetyPrograms/RadiationSafety or by phone at: (716) 829-3281.

The Wright Patterson Air Force Base (WPAFB) Radiation Safety Office (RSO) inspected and packaged all prepared samples that required transportation to the SUNY. It is recommended that you coordinate a time with the Base RSO in advance by calling them at 257-2221 to discuss requirements with Chris Anthony, Ben Wilmoth, or Brian Harcek.

The steps below provide a summary of the procedures used to prepare the samples for shipment in order to obtain TOF-SIMS measurements.

Step 1: After confirming a date for the TOF-SIMS analysis with the SUNY, contact the Base RSO to coordinate a time to package the samples the day before the analyses will take place. Ensure that the AFIT PRSO is notified as well.

Step 2: Remove the samples in the storage jars from the glove box as described in Appendix B.

Step 3: Attach a radioactive information label to one side of the jar and annotate the isotope, activity (in units of μCi) and the date of the activity calculation or measurement. Attach a radioactive warning label to the other side of the jar.

The lid of each jar must reflect the identification number of the sample and the approximate mass of the sample.

Step 4: Assist the representative from the Base RSO with the placement of the samples in the transport box.

Step 5: After the box has been checked for activity with a handheld rate meter and swiped for external contamination, it is ready for transportation.

Step 6: The Base RSO will fill out the RSO Shipment Checklist (Figure 36).

Step 7: You will need to repackage the sample for the return trip to AFIT. Once the samples are inside the box and the lid is secured with tape, check the outside surface with a handheld rate meter for any activity. The maximum acceptable activity for an excepted package is 0.5mR/hr. If the box exceeds this level, contact the university radiation safety office for assistance and inform the AFIT PRSO of the situation and what steps you are taking to resolve the problem.

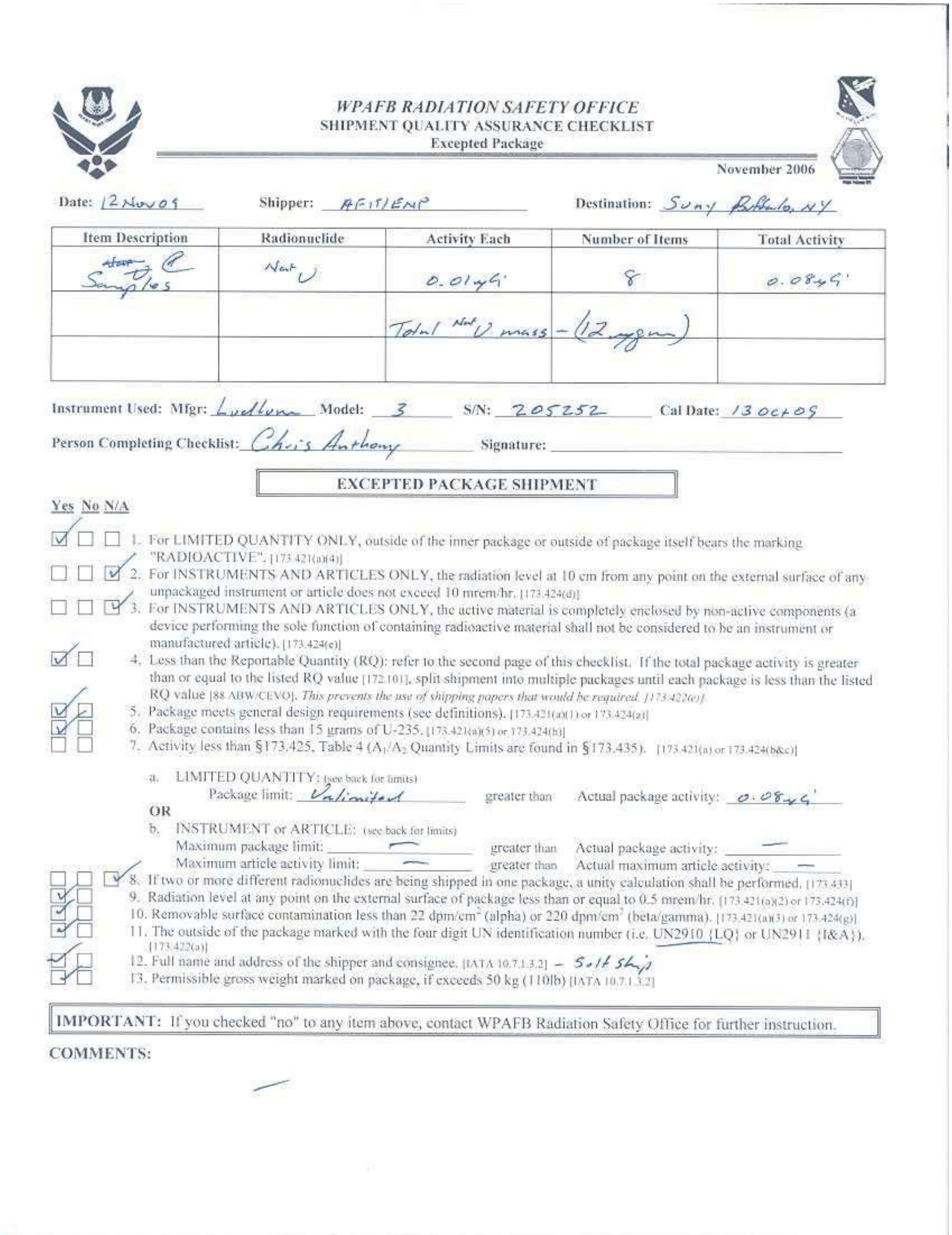

WPAFB RADIATION SAFETY OFFICE
SHIPMENT QUALITY ASSURANCE CHECKLIST
Excepted Package

November 2006

Date: 12 Nov 09 Shipper: AFIT/ENP Destination: SUNY Buffalo, NY

Item Description	Radionuclide	Activity Each	Number of Items	Total Activity
~~Nat~~ U Samples	Nat U	0.01µCi	8	0.08µCi
		Total Nat U mass	− (12 µgm)	

Instrument Used: Mfgr: Ludlum Model: 3 S/N: 205252 Cal Date: 13 Oct 09

Person Completing Checklist: Chris Anthony Signature:

EXCEPTED PACKAGE SHIPMENT

Yes No N/A

☑ ☐ ☐ 1. For LIMITED QUANTITY ONLY, outside of the inner package or outside of package itself bears the marking "RADIOACTIVE". [173.421(a)(4)]

☐ ☐ ☑ 2. For INSTRUMENTS AND ARTICLES ONLY, the radiation level at 10 cm from any point on the external surface of any unpackaged instrument or article does not exceed 10 mrem/hr. [173.424(d)]

☐ ☐ ☑ 3. For INSTRUMENTS AND ARTICLES ONLY, the active material is completely enclosed by non-active components (a device performing the sole function of containing radioactive material shall not be considered to be an instrument or manufactured article). [173.424(e)]

☑ ☐ 4. Less than the Reportable Quantity (RQ): refer to the second page of this checklist. If the total package activity is greater than or equal to the listed RQ value [172.101], split shipment into multiple packages until each package is less than the listed RQ value [88 ABW/CEVO]. *This prevents the use of shipping papers that would be required. [173.422(e)]*

☑ ☐ 5. Package meets general design requirements (see definitions). [173.421(a)(1) or 173.424(a)]

☑ ☐ 6. Package contains less than 15 grams of U-235. [173.421(a)(5) or 173.424(h)]

☐ ☐ 7. Activity less than §173.425, Table 4 (A_1/A_2 Quantity Limits are found in §173.435). [173.421(a) or 173.424(b&c)]

a. LIMITED QUANTITY: (see back for limits)
Package limit: Unlimited greater than Actual package activity: 0.08µCi

OR

b. INSTRUMENT or ARTICLE: (see back for limits)
Maximum package limit: — greater than Actual package activity: —
Maximum article activity limit: — greater than Actual maximum article activity: —

☐ ☐ ☑ 8. If two or more different radionuclides are being shipped in one package, a unity calculation shall be performed. [173.433]

☑ ☐ 9. Radiation level at any point on the external surface of package less than or equal to 0.5 mrem/hr. [173.421(a)(2) or 173.424(f)]

☑ ☐ 10. Removable surface contamination less than 22 dpm/cm^2 (alpha) or 220 dpm/cm^2 (beta/gamma). [173.421(a)(3) or 173.424(g)]

☑ ☐ 11. The outside of the package marked with the four digit UN identification number (i.e. UN2910 {LQ} or UN2911 {I&A}). [173.422(a)]

☑ ☐ 12. Full name and address of the shipper and consignee. [IATA 10.7.1.3.2] − Self Ship

☑ ☐ 13. Permissible gross weight marked on package, if exceeds 50 kg (110lb) [IATA 10.7.1.3.2]

IMPORTANT: If you checked "no" to any item above, contact WPAFB Radiation Safety Office for further instruction.

COMMENTS:

—

Figure 36. Sample WPAFB RSO Shipping Checklist.

Appendix F. Estimation of Sample Mass and Activity

An estimation of the mass and activity of each sample needs to be determined prior to shipment of any samples for inclusion in the WPAFB RSO shipment checklist (an example checklist is provided in the previous appendix). The mass and activity will be estimated based on several factors: the balance inside the glovebox does not have the accuracy or precision to measure the extremely small amounts of uranium in our samples; purchasing a balance of this precision is approximately $20,000.00; a balance with the precision does exist in building 644; and radioactive samples are not allowed in 644. The instructions below outline the procedures and regulations required to operate the high precision microbalance in building 644.

Step 1: Ensure the following rules are followed: never place anything on balance by hand; never place anything directly on pan, always use weighing boat or filter paper; allow display to settle for at least five seconds after darkening; always take measurements in triplicate.

Step 2: Tare balance with weighing boat/filter/foil/weighing paper.

Step 3: Place item to be massed on balance.

Step 4: Repeat steps two and three in triplicate for all items to be massed.

Step 5: Compute the average of the three measurements and standard deviation of the measurements.

Step 6: Ensure measurements are statistically sound and take new measurements as necessary.

In order to estimate the amount of uranium loaded onto the carbon tape for this experiment, a suitable surrogate needed to be obtained. Cerium oxide (CeO_2) was chosen as a surrogate based on studies performed in the past, which proves that CeO_2 behaves very similarly to various uranium oxides and has approximately the same density (Delegard and others, 2004, Yang and others, 2002, and Sandia, 1999). Table 28 lists all of the equipment necessary to acquire mass measurements. The steps be low outline the procedures for obtaining estimations of mass and activity for all of our samples using the CeO_2 as a surrogate for the uranium.

Table 28: Equipment needed for sample mass and activity estimation.

Equipment	Purpose
Methanol	Used to wash surface of 3" silicon wafer between uses
3" silicon wafer	Used as the surface to disperse cerium oxide powder
Silicon wafer fragments	Used as the mounting medium for the carbon tape
Straight forceps	Used to manipulate substrates and protective film
Curved forceps	Used to manipulate substrates and protective film
Microspatula	Used to remove particles from shipping container
Carbon tape	Used to adhere particles to silicon substrate
Razor blade	Used to cut carbon tape
Freund cans	Used to store samples for shipment

Step 1: Ensure that all materials to be used for this procedure are clean and placed inside a fume hood.

Step 2: Prepare substrates by applying double-sided carbon tape to small piece of silicon wafer and cut off excess with razor blade.

Step 3: Remove the protective film from the carbon tape.

Step 4: Perform three mass measurements on each of the prepared substrates and record in lab notebook.

Step 5: Use a microspatula to place a small amount of CeO_2 powder onto the 3" silicon wafer.

Step 6: Gently tap the wafer to disperse the particles over the surface of the wafer.

Step 7: Using tweezers, gently bring the tacky surface of the carbon tape covered silicon wafer into contact with the powder on the 3" wafer.

Step 8: Holding the carbon tape coated, cerium oxide particulate containing silicon wafer at a 90° angle, gently tap with spatula to ensure any excess particles not completely adhered to the carbon tape are removed.

Step 9: Using the spatula, gently press the adhered particles into the carbon tape to ensure good adhesion.

Step 10: Perform three mass measurements on the loaded substrates and subtract from the tare obtained step 4 to obtain the estimated mass for each sample and results are provided in Table 29.

Table 29. Masses recorded for empty substrates, loaded substrates, and the differences with the mean and standard deviation recorded for each sample.

	Mass 1	Mass 2	Mass 3	Mean	Std Dev
Tare 1	0.252342	0.252347	0.252345	0.252344667	2.52E-06
Tot 1	0.252372	0.252368	0.25237	0.25237	2E-06
Samp 1	3E-05	2.1E-05	2.5E-05	2.53333E-05	4.51E-06
Tare 2	0.281392	0.281393	0.281397	0.281394	2.65E-06
Tot 2	0.281409	0.281412	0.281414	0.281411667	2.52E-06
Samp 2	1.7E-05	1.9E-05	1.7E-05	1.76667E-05	1.15E-06
Tare 3	0.196813	0.196808	0.196811	0.196810667	2.52E-06
Tot 3	0.196823	0.19682	0.196825	0.196822667	2.52E-06
Samp 3	1E-05	1.2E-05	1.4E-05	1.2E-05	2E-06
Tare 4	0.184729	0.184727	0.184725	0.184727	2E-06
Tot 4	0.184747	0.184746	0.184744	0.184745667	1.53E-06
Samp 4	1.8E-05	1.9E-05	1.9E-05	1.86667E-05	5.77E-07
Tare 5	0.196642	0.19664	0.196645	0.196642333	2.52E-06

Tot 5	0.196652	0.19665	0.196657	0.196653	3.61E-06
Samp 5	1E-05	1E-05	1.2E-05	1.06667E-05	1.15E-06
Tare 6	0.17282	0.17282	0.172824	0.172821333	2.31E-06
Tot 6	0.172838	0.172841	0.172843	0.172840667	2.52E-06
Samp 6	1.8E-05	2.1E-05	1.9E-05	1.93333E-05	1.53E-06

The Q-test can be used to identify outliers from our data set and whether the outliers should be rejected from our statistical analysis and can be determined from Figure 37 and applying equation18:

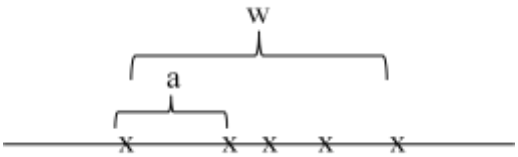

Figure 37. Illustration of the calculation of Q-values (adapted from Christian, 1986).

$$Q = \frac{a}{w} \qquad 18$$

We then compare this test statistic to the tabular value of Q for the given number of samples. If the test statistic is less than or equal to the tabular value of Q, then we can reasonably reject the data point from our statistical analysis. If the measured Q-values are lower than tabulated values then none of the values will be rejected (Christian, 1984). Table 30 illustrates the calculated Q-values for our data set and shows that all none are above the prescribed value of 0.56 for rejection (Christian, 1984).

Table 30. Q-test results for cerium oxide measurements (Christian, 1984, table 3.3 states to reject at 0.56 therefore all data points valid with no outliers).

Mass 1	Mass 2	Mass 3	Mass 4	Mass 5	Mass 6
1.06667E-05	1.2E-05	1.76667E-05	1.87E-05	1.93333E-05	2.53E-05
Dif:	1.33333E-06	5.66667E-06	1E-06	6.66667E-07	6E-06
Q:	0.090909091	0.386363636	0.068182	0.045454545	0.409091

Confidence intervals and a Student's t-test were conducted on the samples to determine if the samples are statistically valid. Results from Statistical Analysis System's JMP software are provided in Figure 38 and show that the results of the mass measurements are statistically valid.

Figure 38. Statistical analysis of cerium oxide mass measurements (all values are within the confidence level and mean within Student's t-test statistic).

Using the estimated average mass, densities of CeO_2 and uranium oxides, percentages of each uranium isotope, and activity levels of each isotope, an estimation of the activity in each sample was constructed. Isotopic abundances were provided in certificates of analysis for the NIST and NBL standards, which are provided in Appendix G. Specific activity levels for each isotope were taken from the tables provided in section nine of the MSDS, copies of which are provided in Appendix H. Results of all calculations are provided in the Table 31.

Table 31. Calculations of estimations of mass and activity for all samples.

U-233	U-234	U-235	U-236	U-238	U005-A
0.0097	0.0062	0.0000021	0.000063	0.00000033	Ci/g
0	0.0000334	0.005	0.0000117	0.994955	Weight%
0	2.071E-07	1.05E-08	7.371E-10	3.28335E-07	Ci/g
			Specific Activity:	5.46652E-07	Ci/g
			Mass:	0.00001498	grams
			Total Activity:	8.18885E-12	Ci
				8.18885E-06	uCi

U-233	U-234	U-235	U-236	U-238	U500
0.0097	0.0062	0.0000021	0.000063	0.00000033	Ci/g
0	0.005126	0.49383	0.000754	0.50029	Weight%
0	3.178E-05	1.037E-06	4.7502E-08	1.65096E-07	Ci/g
			Specific Activity:	3.30308E-05	Ci/g
			Mass:	0.00001408	grams
			Total Activity:	4.65074E-10	Ci
				0.000465074	uCi

U-233	U-234	U-235	U-236	U-238	U900
0.0097	0.0062	0.0000021	0.000063	0.00000033	Ci/g
0	0.007735	0.90098	0.003337	0.08795	Weight%
0	4.796E-05	1.892E-06	2.10231E-07	2.90235E-08	Ci/g
			Specific Activity:	5.00883E-05	Ci/g
			Mass:	0.00001345	grams
			Total Activity:	6.73688E-10	Ci
				0.000673688	uCi

U-233	U-234	U-235	U-236	U-238	U-129
0.0097	0.0062	0.0000021	0.000063	0.00000033	Ci/g
0	0.000055	0.0072	0	0.992745	Weight%
0	3.41E-07	1.512E-08	0	3.27606E-07	Ci/g
			Specific Activity:	6.83726E-07	Ci/g
			Mass:	0.00001705	grams
			Total Activity:	1.16575E-11	Ci
				1.16575E-05	uCi

U-233	U-234	U-235	U-236	U-238	U-18
0.0097	0.0062	0.0000021	0.000063	0.00000033	Ci/g
0	0.000055	0.0072	0	0.992745	Weight%
0	3.41E-07	1.512E-08	0	3.27606E-07	Ci/g
			Specific Activity:	6.83726E-07	Ci/g
			Mass:	0.00001207	grams
			Total Activity:	8.25257E-12	Ci
				8.25257E-06	uCi

U-233	U-234	U-235	U-236	U-238	T-100
0.0097	0.0062	0.0000021	0.000063	0.00000033	Ci/g
0	0.0000334	0.005	0.0000117	0.994955	Weight%
0	2.071E-07	1.05E-08	7.371E-10	3.28335E-07	Ci/g
			Specific Activity:	5.46652E-07	Ci/g
			Mass:	0.00002349	grams
			Total Activity:	1.28409E-11	Ci
				1.28409E-05	uCi

U-233	U-234	U-235	U-236	U-238	T-101
0.0097	0.0062	0.0000021	0.000063	0.00000033	Ci/g
0	0.000055	0.0072	0	0.992745	Weight%
0	3.41E-07	1.512E-08	0	3.27606E-07	Ci/g
			Specific Activity:	6.83726E-07	Ci/g
			Mass:	0.00001469	grams
			Total Activity:	1.00439E-11	Ci
				1.00439E-05	uCi

U-233	U-234	U-235	U-236	U-238	T-102
0.0097	0.0062	0.0000021	0.000063	0.00000033	Ci/g
0	0.0000334	0.005	0.0000117	0.994955	Weight%
0	2.071E-07	1.05E-08	7.371E-10	3.28335E-07	Ci/g
			Specific Activity:	5.46652E-07	Ci/g
			Mass:	0.00001498	grams
			Total Activity:	8.18885E-12	Ci
				8.18885E-06	uCi

Appendix G. Certificates of Analysis

This appendix provides copies of the certificates of analysis provided by the certifying laboratories.

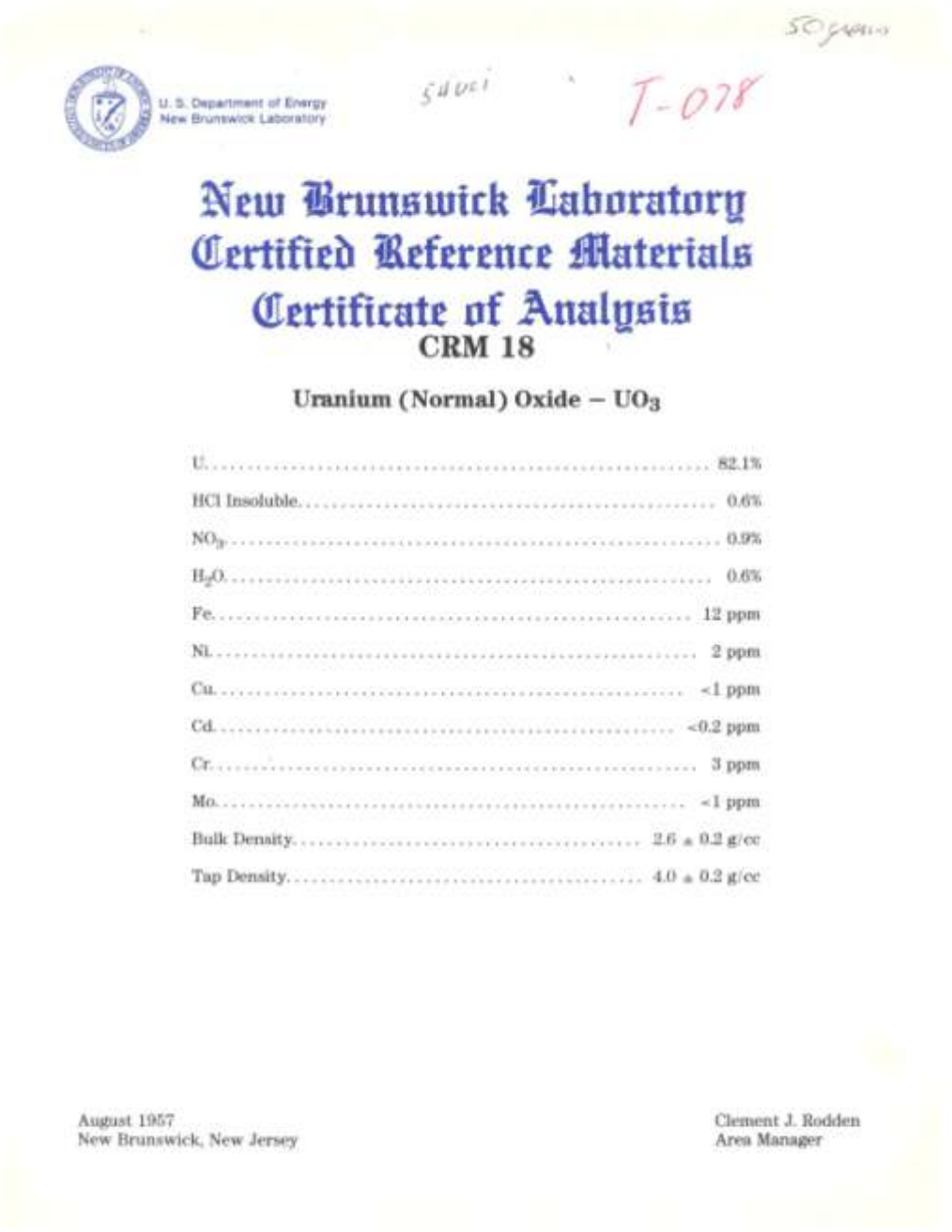

U. S. Department of Energy
New Brunswick Laboratory

T-078

New Brunswick Laboratory
Certified Reference Materials
Certificate of Analysis

CRM 18

Uranium (Normal) Oxide – UO_3

U	82.1%
HCl Insoluble	0.6%
NO_3	0.9%
H_2O	0.6%
Fe	12 ppm
Ni	2 ppm
Cu	<1 ppm
Cd	<0.2 ppm
Cr	3 ppm
Mo	<1 ppm
Bulk Density	2.6 ± 0.2 g/cc
Tap Density	4.0 ± 0.2 g/cc

August 1957
New Brunswick, New Jersey

Clement J. Rodden
Area Manager

Figure 39. Certificate of analysis for CRM 18.

25 grams

27 uci

T-077

U. S. Department of Energy
New Brunswick Laboratory

New Brunswick Laboratory
Certified Reference Materials
Certificate of Analysis

CRM 129

Uranium Oxide (U_3O_8) Assay Standard

Uranium Oxide (U_3O_8) ..... 99.968 ± 0.018 Wt. %

This Certified Reference Material (CRM) is an assay standard for use in uranium determinations. Each unit of CRM 129 contains approximately 22 grams of uranium, in the form of a highly-purified U_3O_8, contained in a glass bottle.

The uncertainty ascribed to the certified assay value is the 95% confidence limit for the mean. This limit consists of components for random analytical error and an estimated upper limit of possible systematic errors which includes material variability.

This CRM was originally issued in 1978 by the National Bureau of Standards (NBS) as Standard Reference Material (SRM) 950b. The assay measurements were made by N. M. Trahey, NBL, and J. R. Moody and W. Koch, NBS. Selected impurities measurements were made by B. I. Diamondstone and S. A. Wicks, NBS. All work was performed under the direction of I. L. Barnes, NBS. In 1987, the technical and administrative transfer of NBS Special Nuclear SRMs into the NBL CRM Program was coordinated by the NBS Office of Standard Reference Materials and N. M. Trahey, NBL.

The uranium assay was determined using the NBL titrimetric method for the precise assay of uranium metal[1,2]. NBS Potassium Dichromate (SRM 136c) was used as the oxidizing agent. The assay values obtained are compatible with those obtained from the assay of NBS Uranium Metal (SRM 960) and NBS Uranium Oxide (SRM 950a). A coulometric assay procedure on this lot of uranium oxide was used to confirm the certified value.

The total impurities in CRM 129 were determined by spectrochemical analysis and are estimated to be less than 50 μg/g. Iron and vanadium content, which are titratable impurities which can cause interferences, were determined to be approximately 3 μg/g and 1 μg/g, respectively. These impurities values are not certified.

October 1, 1987
Argonne, Illinois
(Revision of NBS Certificate dated March 1, 1978)

Carleton D. Bingham
Director

(Over)

Figure 39. Certificate of analysis for CRM 129.

New Brunswick Laboratory
U.S. Department of Energy

Certificate of Analysis

CRM U005-A

Uranium Isotopic Standard

10 mg Uranium as U_3O_8

	^{234}U	^{235}U	^{236}U	^{238}U
Atom Percent:	0.00340	0.5064	0.00118	99.4890
Uncertainty:	±0.00007	±0.0003	±0.00001	±0.0003
Weight Percent:	0.00334	0.5000	0.00117	99.4955

This Certified Reference Material (CRM) is primarily intended for the calibration of mass spectrometers used to perform uranium isotopic measurements. The specific purpose of this isotopic standard is for the determination of mass discrimination effects for uranium isotopes being measured under similar analytical conditions. Each unit of CRM U005-A consists of approximately 10 milligrams of uranium, in the form of highly purified U_3O_8, contained in a glass bottle.

The indicated uncertainties for the isotopic composition of the CRM are 95% confidence intervals for the mean. For the minor isotopes (^{234}U and ^{236}U), these uncertainties take into account the uncertainties associated with separated and spike isotopes used in this certification work.

This CRM was originally issued in 1984 by the National Bureau of Standards (NBS) as Standard Reference Material (SRM) U-005a. The measurements made at NBS leading to the certification were performed by J.W. Gramlich, L. A. Machlan, and J.R. Moody, under the direction of E.L. Garner. The statistical analyses were performed by W. S. Liggett, NBS. In 1987, the technical and administrative transfer of NBS Special Nuclear SRMs into the NBL CRM Program was coordinated by the NBS Office of Standard Reference Materials and N. M. Trahey, NBL.

The certified isotopic abundance values were determined using a solid-sample thermal ionization mass spectrometer equipped with a Faraday cup detection system. The measured $^{235}U/^{238}U$ values were corrected for mass discrimination effects by intercomparison with synthetic calibration mixtures of similar ^{235}U levels, prepared from high-purity ^{235}U and ^{238}U separated isotopes. The $^{235}U/^{238}U$ value for this standard, 0.005090, is known to at least 0.03%.

The ^{234}U and ^{236}U abundances were determined by isotope dilution mass spectrometry using high-purity ^{233}U as the spike.

March 30, 2008
Argonne, Illinois

www.nbl.doe.gov
Page 1 of 1

Jon Neuhoff, Director
New Brunswick Laboratory

(Editorial revision of Certificate dated October 1, 1987)

Figure 40. Certificate of analysis for CRM U005.

New Brunswick Laboratory
U.S. Department of Energy

Certificate of Analysis

CRM U500

Uranium Isotopic Standard

10 mg Uranium as U_3O_8

	^{234}U	^{235}U	^{236}U	^{238}U
Atom Percent:	0.5181	49.696	0.0755	49.711
Uncertainty:	±0.0008	±0.050	±0.0003	±0.050
Weight Percent:	0.5126	49.383	0.0754	50.029

This Certified Reference Material (CRM) is primarily intended for the calibration of mass spectrometers used to perform uranium isotopic measurements. The specific purpose of this isotopic standard is for the determination of mass discrimination effects for uranium isotopes being measured under similar analytical conditions. Each unit of CRM U500 consists of approximately 10 milligrams of uranium, in the form of highly purified U_3O_8, contained in a glass bottle.

The indicated uncertainties for the isotopic composition of the CRM are 95% confidence intervals for a single determination. This term can be defined as an approximate two-sigma limit, where sigma is the standard deviation of the measurements data obtained from the material. The uncertainties include allowances for inhomogeneity of the material as well as analytical error.

This CRM was originally issued in 1970 by the National Bureau of Standards (NBS) as Standard Reference Material (SRM) U-500. The measurements made at NBS leading to the certification were performed by E. L. Garner, L. A. Machlan, M.S. Richmond and W.R. Shields. In 1987, the technical and administrative transfer of NBS Special Nuclear SRMs into the NBL CRM Program was coordinated by the NBS Office of Standard Reference Materials and N. M. Trahey, NBL.

The certified isotopic abundance values were determined using a solid-sample thermal ionization mass spectrometer equipped with a Faraday cup detection system. The measured $^{235}U/^{238}U$ values were corrected for mass discrimination effects by intercomparison with synthetic calibration mixtures of similar ^{235}U levels, prepared from high-purity ^{235}U and ^{238}U separated isotopes. The $^{235}U/^{238}U$ value for this standard, 0.9997, is known to at least 0.1%.

The ^{234}U and ^{236}U abundances were determined at NBS by isotope dilution mass spectrometry using high-purity ^{233}U as the spike.

NOTE: NBS Special Publication 260-27 presents further details of the measurements made at NBS which provided the basis for the certification, and is available from the NBS Office of Standard Reference Materials

March 30, 2008
Argonne, Illinois

www.nbl.doe.gov
Page 1 of 1

Jon Neuhoff, Director
New Brunswick Laboratory

(Editorial revision of Certificate dated October 1, 1987)

Figure 41. Certificate of analysis for CRM U500.

New Brunswick Laboratory
U.S. Department of Energy

Certificate of Analysis

CRM U900

Uranium Isotopic Standard

10 mg Uranium as U_3O_8

	^{234}U	^{235}U	^{236}U	^{238}U
Atom Percent:	0.7777	90.196	0.3327	8.693
Uncertainty:	±0.0015	±0.011	±0.0010	±0.008
Weight Percent:	0.7735	90.098	0.3337	8.795

This Certified Reference Material (CRM) is primarily intended for the calibration of mass spectrometers used to perform uranium isotopic measurements. The specific purpose of this isotopic standard is for the determination of mass discrimination effects for uranium isotopes being measured under similar analytical conditions. Each unit of CRM U900 consists of approximately 10 milligrams of uranium, in the form of highly purified U_3O_8, contained in a glass bottle.

The indicated uncertainties for the isotopic composition of the CRM are 95% confidence intervals for a single determination. This term can be defined as an approximate two-sigma limit, where sigma is the standard deviation of the measurements data obtained from the material. The uncertainties include allowances for inhomogeneity of the material as well as analytical error.

This CRM was originally issued in 1970 by the National Bureau of Standards (NBS) as Standard Reference Material (SRM) U-900. The measurements made at NBS leading to the certification were performed by E. L. Garner, L. A. Machlan, M.S. Richmond and W. R, Shields. In 1987, the technical and administrative transfer of NBS Special Nuclear SRMs into the NBL CRM Program was coordinated by the NBS Office of Standard Reference Materials and N. M. Trahey, NBL.

The certified isotopic abundance values were determined using a solid-sample thermal ionization mass spectrometer equipped with a Faraday cup detection system. The measured ^{238}U values were calculated from the $^{235}U/^{238}U$ values, which were corrected for mass discrimination effects by intercomparison with synthetic calibration mixtures of similar ^{235}U levels, prepared from high-purity ^{235}U and ^{238}U separated isotopes. The $^{235}U/^{238}U$ value for this standard, 10.375, is known to at least 0.1%.

The ^{234}U and ^{236}U abundances were determined by isotope dilution mass spectrometry using high-purity ^{233}U as the spike.

NOTE: NBS Special Publication 260-27 presents further details of the measurements made at NBS which provided the basis for the certification, and is available from the NBS Office of Standard Reference Materials upon request.

March 30, 2008
Argonne, Illinois

www.nbl.doe.gov
Page 1 of 1

Jon Neuhoff, Director
New Brunswick Laboratory

(Editorial revision of Certificate dated October 1, 1987)

Figure 42. Certificate of analysis for CRM U900.

Appendix H. Material Safety Data Sheet

This appendix includes a copy of the MSDS for the radioactive samples used in this research.

MATERIAL SAFETY DATA SHEET

URANIUM OXIDE

(U_3O_8)

SECTION 1: CHEMICAL PRODUCTS & COMPANY IDENTIFICATION

New Brunswick Laboratory
U. S. Department of Energy
9800 South Cass Avenue
Argonne, IL 60439
1-630-252-CRMS

Off Hours Emergency Numbers:
1-630-252-6131 or 1-630-252-5731

CAS Number: 1344-59-8

Substance: Uranium oxide (U_3O_8)

Trade Names/Synonyms:

URANOUS OXIDE, TRIURANIUM OCTAOXIDE, PITCHBLENDE, URANITE NASTURAN, CRM 149, CRM 969, CRM U970, CRM U900, CRM U850, CRM U800; CRM U750, CRM U630, CRM U500, CRM U350, CRM U200, CRM U150, CRM U100, CRM U030-A, CRM U020-A, CRM U015, CRM U010, CRM U005-A, CRM U0002, CRM 129-A, CRM 124 (1-7), CRM 123 (1-7), U_30_8 FOR SAFEGUARDS MEASUREMENT EVALUATION (SME) PROGRAM.

Chemical Family:
Metal oxide

Radioactive

Creation Date: December 6, 1993 Revision Date: June 25, 2008

SECTION 2: COMPOSITION/INFORMATION ON INGREDIENTS

Component: Uranium oxide (U_3O_8)
CAS Number: 1344-59-8
Percentage: 100
Other Contaminants: None

SECTION 3: HAZARDS IDENTIFICATION

CERCLA Ratings (SCALE 0-3): HEALTH=U FIRE=0 REACTIVITY=0 PERSISTENCE = 3
NFPA RATINGS (SCALE 0-4): HEALTH=U FIRE=0 REACTIVITY=0

EMERGENCY OVERVIEW: Uranium oxide is an odorless, dark green to black powder or crystal. Avoid breathing dust. Avoid contact with skin, eyes and clothing. May damage kidneys. Wash thoroughly after handling. Use only with adequate ventilation.

POTENTIAL HEALTH EFFECTS:

INHALATION:
Short Term Exposure: May cause irritation. May cause kidney damage, yellowing of the skin and eyes, lack of appetite, nausea, vomiting, diarrhea, dehydration, blood in the urine, weakness, drowsiness, incoordination, twitching, sterility, blood disorders, convulsions and shock.

Long Term Effects: In addition to effects from short-term exposure, anemia, cataracts, lung damage, liver damage and bone effects may occur.

SKIN CONTACT:
Short Term Exposure: May cause irritation.

Long Term Effects: May cause irritation.

EYE CONTACT:
Short Term Exposure: May cause irritation, redness and swelling. Additional effects may include sores and eye damage.

Long Term Effects: In addition to effects from short-term exposure, cataracts may occur.

INGESTION:

Short Term Exposure: May cause kidney damage.

Long Term Effects: Same effects as short-term exposure.

CARCINOGEN STATUS:

OSHA:N
NTP: N
IARC: N

SECTION 4: FIRST AID MEASURES

INHALATION: Remove from exposure area to a restricted area with fresh air as quickly as possible. If breathing has stopped, perform artificial respiration by administering oxygen; mouth-to-mouth resuscitation should be avoided to prevent exposure to the person rendering first aid. Any evidence of serious contamination indicates that treatment must be instituted. (Inhalation of radioactive particles may indicate that other parts of the body were also contaminated, such as the digestive tract, skin and eyes.) If time permits, wipe the face with wet filter paper, force coughing and blowing of the nose. Get medical attention immediately. The victim may be contaminated with radioactive particles. Thorough decontamination should be started before the victim is moved to the medical area. Any personnel involved in rendering first aid must be monitored for radioactivity and thoroughly decontaminated if necessary (IAEA #3, Pg. 65).

SKIN CONTACT: Remove victim to a suitable area for decontamination as quickly as possible. Remove clothing and shoes immediately. Thoroughly wash the victim with soap and water, paying particular attention to the head, fingernails and palms of the hands. Upon completion of washing, monitor the victim for radioactivity. It is imperative that the skin should be decontaminated as quickly as possible. Minute skin injuries greatly increase the danger of isotope penetration into the victim; shaving should not be attempted. If water and soap have been inadequate in removing the radioactive compound, decontaminating compounds consisting of surfactants and absorbent substances may be effective. Complexing reagents may also be of use. The use of organic solvents is to be avoided, as they may increase the solubility and absorption of the radioactive substance. Skin contamination with radiation may be an indication that other parts of the body have been exposed. Contaminated clothing must be stored in a metal container for later decontamination or disposal. The water used to wash the victim must be stored in metal containers for later disposal. Any personnel involved in rendering first aid to the victim must be monitored for radioactivity and decontaminated if necessary (IAEA #47, Pg. 9; IAEA #3, Pg. 62).

EYE CONTACT: Remove victim to a restricted area for decontamination. Thoroughly wash eyes with large amounts of water, occasionally lifting the upper and lower lids (approximately 15 minutes). Following the water treatment, provide an isotonic solution. Do not use eyebaths, rather provide a continuous and copious supply of fluid. Monitor the victim for radioactivity. If activity is present, rewash the eyes, and remonitor until little or no radioactivity is present. Get medical attention immediately. Any water used to wash the victim's eyes must be stored in a metal container for later disposal. Any other articles that are used to decontaminate the victim must also be stored in metal containers for later decontamination or disposal. Any personnel involved in rendering first aid to the victim must be monitored for radioactivity and decontaminated if necessary (IAEA #3, Pg. 65; IAEA #47, Pg. 35).

INGESTION: In the case of ingestion of radioactive substances, the mouth should be rinsed out immediately after the accident, care being taken not to swallow the water used for this purpose. Vomiting should be induced either mechanically, or with syrup of ipecac. Do not induce vomiting in an unconscious person. Lavage may be useful. Care should be taken to avoid aspiration. The vomitus and lavage fluids should be saved for examination and monitoring. Further action depends on the nature of the radioactive substance. Get medical attention immediately. The gastric fluids and fluids used for lavage must be stored in metal containers for later disposal. The victim must be monitored for radioactivity and decontaminated, if necessary, before being transported to a medical facility. Any personnel involved in rendering first aid to the victim must be monitored for radioactivity and decontaminated if necessary (IAEA #47, Pg. 9; IAEA #3, Pp. 59, 66)

NOTE TO PHYSICIAN:

ANTIDOTE: The following antidote has been recommended. However, the decision as to whether the severity of poisoning requires administration of any antidote and actual dose required should be made by qualified medical personnel.

There is no antidote for radiation sickness. Treatment should be symptomatic and supportative, regardless of the dose received. In all cases, medical attention should be obtained immediately.

SECTION 5: FIRE FIGHTING MEASURES

FIRE AND EXPLOSION HAZARD: Negligible when exposed to flame or heat.

EXTINGUISHING MEDIA: Dry chemical, carbon dioxide, water spray or regular foam (2000 *Emergency Response Guidebook*, (ERG 2000), developed jointly by Transport Canada (TC), the U. S. Department of Transportation (DOT) and the Secretariat of Transportation and Communications of Mexico (SCT).)
For Larger Fires, use water spray or fog (flooding amounts) (2000 *Emergency Response Guidebook*, ERG 2000.)

FIREFIGHTING: Move container from fire area if you can do it without risk. Apply cooling water to sides of containers exposed to flames until well after fire is out (2000 *Emergency Response Guidebook*, ERG 2000).

Do not move damaged containers; move undamaged containers out of fire zone. For massive fire in cargo area, use unmanned hose holder or monitor nozzles (2000 *Emergency Response Guidebook*, ERG 2000).

Contact the local, State, or Department of Energy radiological response team. Use suitable agent for surrounding fire. Cool containers with flooding amounts of water, apply from as far a distance as possible. Avoid breathing dusts or vapors, keep upwind. Keep unnecessary people out of area until declared safe by radiological response team.

FLASH POINT: Non-flammable solid.

HAZARDOUS COMBUSTION PRODUCTS: Thermal decomposition may release toxic/hazardous gases.

SECTION 6: ACCIDENTAL RELEASE MEASURES

OCCUPATIONAL SPILL: Do not touch damaged containers or spilled material. Damage to outer container may not affect primary inner container. For small liquid spills, take up with sand, earth or other absorbent material. For large spills, dike far ahead of spill for later disposal. Keep unnecessary people at least 150 feet upwind; greater distances may be necessary if advised by qualified radiation authority. Isolate hazard area and deny entry. Enter spill area only to save life; limit entry to shortest possible time. Detain uninjured persons and equipment exposed to radioactive material until arrival or instruction of qualified radiation authority. Delay cleanup until arrival or instruction of qualified radiation authority.

SECTION 7: HANDLING AND STORAGE

Observe all Federal, State, and local regulations when storing this substance.

SECTION 8: EXPOSURE CONTROLS/PERSONAL PROTECTION

EXPOSURE LIMITS:

Uranium, insoluble compounds (As U):

0.05 mg/m^3 OSHA PEL-TWA
0.2 mg/m^3 ACGIH TWA; 0.6 mg/m^3 ACGIH STEL
0.2 mg/m^3 NIOSH Recommended TWA; 0.6 mg/m^3 NIOSH Recommended STEL

Occupational exposure to radioactive substances must adhere to standards established by the Occupational Safety and Health Administration. 29 CFR 1910.96, and/or the Nuclear Regulatory Commission, 10 CFR Part 20.

VENTILATION: At a minimum, provide local exhaust or process enclosure ventilation. Depending upon the specific workplace activity and the radioactivity of the isotope, a more stringent ventilation system may be necessary to comply with exposure limits set forth by law (10 CFR 20.103)

One method of controlling external radiation exposure is to provide adequate shielding. The absorbing material used and the thickness required to attenuate the radiation to acceptable levels depends on the type of radiation, its energy, the flux and the dimensions of the source.

ALPHA PARTICLES: For the energy range of alpha particles usually encountered, a fraction of a millimeter of any ordinary material is sufficient for absorbance. Thin rubber, acrylic, stout paper, or cardboard will suffice.

BETA PARTICLES: Beta particles are more penetrating than alpha, and require more shielding. Materials composed mostly of elements of low atomic number such as acrylic, aluminum and thick rubber are most appropriate for the absorption of beta particles. For example, 1/4 inch of acrylic will absorb all beta particles up to 1 MeV. With high-energy beta radiation from large sources, Bremsstrahlung (X-ray production) contribution may become significant and it may be necessary to provide additional shielding of high atomic weight material, such as lead, to attenuate the Bremsstrahlung radiation.

GAMMA RAYS: The most suitable materials shielding gamma radiation are lead and iron. The thickness required would depend on whether the source is producing narrow or broad beam radiation. Primary and secondary protective barriers may be required to block all radiation.

EYE PROTECTION: Employee must wear appropriate eye protection that will not allow the introduction of particles into the eyes. Contact lenses should not be worn.

Clothing, glove and eye protection equipment will provide protection against alpha particles, and some protection against beta particles, depending on thickness, but will not shield gamma radiation.
CLOTHING: Disposable overgarments, including head coverings and foot covering, should be worn by any employee engaged in handling any radioactive substance. These garments are also recommended even if the employee is working with a "glovebox" containment system. Certain clothing fibers may be useful in dosimetry so clothing should be kept.

In the event of an accident, large-scale release or a large-scale clean-up full protective clothing will be necessary.

GLOVES: Employee must wear appropriate protective gloves to prevent contact with this substance. Used gloves may present a radiation hazard and should be disposed of as radioactive waste.

RESPIRATOR: The following respirators and maximum use concentrations are recommendations by the U.S. Department of Health and Human Services, NIOSH pocket guide to chemical hazards; NIOSH criteria documents or by the U.S. Department of Labor, 29 CFR 1910 Subpart Z.

The specific respirator selected must be based on contamination levels found in the work place, must not exceed the working limits of the respirator and be jointly approved by the National Institute for Occupational Safety and Health and the Mine Safety and Health Administration (NIOSH-MSHA).

URANIUM, Insoluble compounds (As U):

AT ANY DETECTABLE CONCENTRATION:
Any self-contained breathing apparatus that has a full facepiece and is operated in a pressure-demand or other positive-pressure mode.

Any supplied air respirator that has a full facepiece and is operated in a pressure-demand or other positive-pressure mode in combination with an auxiliary self-contained breathing apparatus operated in pressure-demand or other positive-pressure mode.

Escape - any air-purifying, full-facepiece respirator with a high-efficiency particulate filer.

Any appropriate escape-type, self-contained breathing apparatus.

FOR FIREFIGHTING AND OTHER IMMEDIATELY DANGEROUS TO LIFE OR HEALTH CONDITIONS: Any self-contained breathing apparatus that has a full facepiece respirator with a high-efficiency particulate filter.

Any supplied-air respirator that has a full facepiece and is operated in a pressure-demand or other positive-pressure mode in combination with an auxiliary self-contained breathing apparatus operated in pressure-demand or other positive-pressure mode.

SECTION 9: PHYSICAL AND CHEMICAL PROPERTIES

DESCRIPTION: Dark green or black, dense, radioactive powder or crystals.

Molecular weight: Approximately 833 to 842 (depending on enrichment)
Molecular formula: U_3O_8
Boiling point: Decomposes
Melting point: 1300°C (2372°F) decomposes
Specific Gravity: 8.30
Water Solubility: Insoluble
Solvent Solubility: Nitric acid, sulfuric acid

The half-lives of the various uranium isotopes are as follows:

$^{233}U = 1.59 \times 10^5$ y
$^{234}U = 2.47 \times 10^5$ y
$^{235}U = 7.04 \times 10^8$ y
$^{236}U = 2.39 \times 10^7$
$^{238}U = 4.51 \times 10^9$ y

The specific activities of the various uranium isotopes are as follows:

$^{233}U = 3.6 \times 10^2$ MBq/g (9.7×10^{-3} Ci/g)
$^{234}U = 2.3 \times 10^2$ MBq/g (6.2×10^{-3} Ci/g)
$^{235}U = 7.8 \times 10^{-2}$ MBq/g (2.1×10^{-6} Ci/g)
$^{236}U = 2.3$ MBq/g (6.3×10^{-5} Ci/g)
$^{238}U = 1.2 \times 10^{-2}$ MBq/g (3.3×10^{-7} Ci/g)

See 10 CFR Chapter 1, Pt. 71, Appendix A.

SECTION 10: STABILITY AND REACTIVITY

REACTIVITY:

URANIUM OXIDE: Stable under normal temperatures and pressures.

CONDITIONS TO AVOID: No potentially hazardous conditions could be found in the literature, nor could any accidents be recalled in which uranium oxide reacted in a hazardous manner.

INCOMPATIBILITIES:
Bromine Trifluoride: Reaction is rapid below the boiling point of the trifluoride.

HAZARDOUS DECOMPOSITION: Thermal decomposition may release hazardous and toxic gases.

POLYMERIZATION:
Hazardous polymerization has not been reported to occur under normal temperature and pressure.

SECTION 11: TOXICOLOGY INFORMATION

URANIUM OXIDE:

CARCINOGEN STATUS: None

Uranium oxide is a skin, eye, and mucous membrane irritant, as well as a nephrotoxin. Chronic inhalation may affect the lungs and lymph nodes. Pneumoconiosis may occur. If uranium is deposited in the bone, there is a potential for blood disorders such as anemia and leukopenia. In humans, cancer of the lung, lymphatic and hemopoietic systems, and osteosarcoma have been reported. Uranium compounds usually do not constitute an external radiation exposure hazard since uranium emits mainly alpha-radiation at a low energy level. It may constitute an internal radiation hazard if it is absorbed into the body, thus delivering alpha emission onto tissues in which it is stored. Significant quantities of highly enriched material may also pose a gamma radiation hazard.

HEALTH EFFECTS
INHALATION
URANIUM OXIDE

RADIOACTIVE/NEPHROTOXIN. 30 mg/m^3 immediately dangerous to life and health.
ACUTE EXPOSURE: May cause irritation.

CHRONIC EXPOSURE - In animals, repeated inhalation of insoluble uranium compounds resulted in fibrotic changes indicative of radiation damage in the lungs and tracheobronchial lymph nodes. Pneumoconiosis may occur. If uranium is deposited in the bone, there is a potential for blood disorders such as anemia and leukopenia. In humans, cancer of the lung, lymphatic and hemopoietic systems, and osteosarcoma have been reported. Uranium is a nephrotoxin and exposure may lead to kidney failure. Kidney failure may result in liver damage. See the following section on effects of alpha radiation and radiation sickness.

ALPHA RADIATION:

ACUTE EXPOSURE - Alpha radiation is densely ionizing with very high energy and will kill cells immediately adjacent to the source of contact. Damaged cells may not recover or be repaired. Alpha emitters may or may not be absorbed, depending on the solubility and particle size. Insoluble compounds may remain at or near the site of deposition, and soluble compounds may rapidly enter the bloodstream. Heavier particles will be brought up to the throat by ciliary action, and may then be swallowed. The lighter particles may be lodged deep in the alveolar air sacs and remain. The damage depends on how quickly they are eliminated, and the susceptibility of the tissue in which they are stored. A single large dose of radiation may lead to radiation sickness.

CHRONIC EXPOSURE - The effects of chronic exposure by internally deposited alpha radiation is dependent upon the dose and target organ(s). If the total dose is sufficient, radiation sickness may occur. Possible disorders include lung cancer, sterility, anemia, leukemia, or bone cancer.

RADIATION SICKNESS:

ACTIVE EXPOSURE - Whole body doses of 200-1000 Rads may cause anorexia, apathy, nausea and vomiting and may become maximal within 6-12 hours. An asymptomatic period of 24-36 hours may be followed by lymphopenia and slowly developing neutropenia. Thrombocytopenia may become prominent within 3-4 weeks. The lymph nodes, spleen and bone marrow may begin to atrophy. If bone marrow depression reaches a critical level, death may occur from overwhelming infection. Whole body doses of 400 or more rads may cause intractable nausea, vomiting and diarrhea that may lead to severe dehydration, vascular collapse and death. Regeneration of the intestinal epithelium may occur, but may be followed

by hematopoietic failure within 2-3 weeks. Whole body doses of 600 or more rads may be fatal due to gastrointestinal or hematopoietic malfunction, with doses fatal <600 Rads, the possibility of survival is inversely related to the dose. Whole body doses >3000 Rads generally cause nausea, vomiting, listlessness, and drowsiness ranging from apathy to prostration, tremors, convulsions, ataxia and death within a few hours. The gonads are also particularly radiosensitive among men. In women, loss of fertility may be indicated by loss of menstruation.

CHRONIC EXPOSURE - The delayed effects of radiation may be due either to a single large overexposure or continuing low-level overexposure and may include cancer, genetic effects, shortening of life span and cataracts. Cancer is observed most frequently in the hematopoietic system, thyroid, bone and skin. Leukemia is among the most likely forms of malignancy. Lung cancer may also occur due to radioactive materials residing in the lungs. Genetic effects may range from point mutations to severe chromosome damage such as strand breakage, translocations, and deletions. If the germ cells have been affected, the effects of the mutation may not become apparent until the next generation, or even later.

SKIN CONTACT:
URANIUM OXIDE
RADIOACTIVE:

ACUTE EXPOSURE - There is no evidence that insoluble uranium compounds can be absorbed through the skin; insoluble salts produced no signs of poisoning after skin contact. Animal tests on a variety of uranium compounds caused varying degrees of eye damage, with the oxides causing the mildest. Uranium oxide may irritate the skin.

CHRONIC EXPOSURE - Prolonged skin contact with insoluble uranium compounds should be avoided because of potential radiation damage to basal cells. Dermatitis has occurred as a result of handling some insoluble uranium compounds. Repeated or prolonged contact may cause conjunctivitis. Cataract formation as in acute exposure may occur with significant exposure. See the following sections regarding alpha radiation and radiation sickness.

ALPHA RADIATION:
ACUTE EXPOSURE - Alpha radiation is not usually an external hazard. However, local damage may occur at the site of a wound. Absorption or penetration through damaged skin may result in radiation sickness.

CHRONIC EXPOSURE - Prolonged or repeated contact my result in radiation sickness.

RADIATION SICKNESS: The clinical course of radiation sickness depends upon the dose, dose rate, area of the body affected and time after exposure. External and internal radioactivity of any type may cause radiation sickness.

Radiation sickness has three (3) clearly defined syndromes, which are described in detail in the inhalation section.

EYE CONTACT:
URANIUM OXIDE:
RADIOACTIVE:

ACUTE EXPOSURE - Dust may be irritating to the eyes. A variety of soluble and insoluble compounds or uranium were tested on the eyes of rabbits. The insoluble compounds caused the mildest degree of injury. The effects of eye contact with any uranium compound tend to be necrosis of the conjunctivae and eyelids, and ulceration of the cornea.

CHRONIC EXPOSURE: Prolonged exposure to uranium may produce conjunctivitis, or the symptoms of radiation injury, such as cataracts. See the following sections regarding the effects of alpha radiation on the eyes, and radiation sickness.

ALPHA RADIATION:
ACUTE EXPOSURE - Radiation affects the eye by inducing acute inflammation of the conjunctiva and the cornea. The most sensitive part of the eye is the crystalline lens. A late effect of eye irradiation is cataract formation. It may begin anywhere from 6 months to several years after a single exposure. Cataract formation begins at the posterior pole of the lens, and continues until the entire lens has been affected. Growth of the opacity may stop at any point. The rate of growth and the degree of opacity are dependent upon the dose of radiation.

CHRONIC EXPOSURE - Repeated or prolonged exposure to alpha radiation may result in cataract formation, as described above. Of the well-documented late effects of radiation on man, leukemia and cataracts have been observed at doses lower than those producing skin scarring and cancer or bone tumors. The lens of the eye should be considered to be a critical organ.

RADIATION SICKNESS: The eyes are very radiosensitive; a single dose of 100 rads may cause conjunctivitis and keratitis. It is unlikely that a dose sufficient to cause radiation sickness would occur if only the eyes were irradiated. However, if eye damage by ionizing radiation occurs. It may be best to assume that other parts

of the body have also been contaminated. Symptoms of radiation sickness are described in the inhalation section.

INGESTION:
URANIUM OXIDE:
RADIOACTIVE/NEPHROTOXIN

ACUTE EXPOSURE - Feeding studies on animals indicate that insoluble uranium is much less toxic than soluble uranium compounds. Uranium entering the bloodstream will become stored in the bone marrow, but the majority will become lodged in the kidney, which is the major site of toxicity. More than a year and a half are required to rid the body of an accidental high dose of uranium, after which time measurable uranium is present in the bone and kidney.

CHRONIC EXPOSURE - The toxic action of uranium resides more in its chemical action on the renal tubules, rather than radiation effects. Rats injected with uranium metal in the femoral marrow developed sarcomas, whether this was due to metallocarcinogenic or radiocarcinogenic ingestion of alpha emitters, and radiation sickness. Also see the first aid section for uranium compounds.

ALPHA RADIATION:

ACUTE EXPOSURE - The fate of ingested alpha emitters depends on their solubility and valence. High doses may lead to radiation sickness as described in inhalation exposure.

CHRONIC EXPOSURE - Repeated ingestion of alpha emitters may lead to radiation sickness as described in inhalation exposure.

RADIATION SICKNESS: The symptoms of radiation sickness depends upon the dose received. It may result from acute or chronic exposure to any form of radiation. The symptoms are described in the inhalation section.

FIRST AID FOR URANIUM COMPOUNDS: Although chelating agents act on uranium, they should not be used because the increased migrant fraction leads through renal precipitation to a greater kidney burden than would be received if there were no treatment at all; there is thus the risk of serious toxic nephritis. The basic treatment should be administration of a bicarbonate solution given locally and in intravenous perfusion (one bottle of 250 mL at 1.4%). From IAEA safety series #47 - Manual on early medical treatment of possible radiation injury - 1978. Pg 28.

SECTION 12: ECOLOGICAL INFORMATION

Environmental Impact Rating (0-4): No data available

Acute Aquatic Toxicity: No data available

Degradability: No data available

Log Bioconcentration Factor (BCF): No data available

Log Octanol/water partition coefficient: No data available

SECTION 13: DISPOSAL INFORMATION

Observe all Federal, State and local Regulations when disposing of this substance.

SECTION 14: TRANSPORTATION INFORMATION

U.S. Department of Transportation Hazard Classification, 49 CFR 173 Subpart I - Class 7 - (Radioactive) Materials

U.S. Department of Transportation Labeling Requirements 49 CFR 172.101 and 49CFR 172
Subpart E - Labeling and 172.402 ; Additional Labeling requirements for subsidary hazards.

U.S. Department of Transportation Shipping Name-ID Number, Hazard Class or Division, 49 CFR 172.101

U.S. Department of Transportation Packaging Authorizations:
Exceptions: 49 CFR 173.421, and 173.453
Specific requirements: 49 CFR 173.455
Non-Bulk Packaging: 49 CFR 173.415, or 173.417
Bulk Packaging: None

SECTION 15: REGULATORY INFORMATION

TSCA STATUS: Y

CERCLA SECTION 103 (40 CFR 302.4):	N
SARA SECTION 302 (40 CFR 355.30):	N
SARA SECTION 304 (40 CFR 355.40):	N

SARA SECTION 313 (40 CFR 372.65):	N
OSHA PROCESS SAFETY (29 CFR 1910.119):	N
CALIFORNIA PREPOSITION 65:	N

SARA HAZARD CATEGORIES, SARA SECTIONS 311/312 (40 CFR 370.21)

ACUTE HAZARD:	Y
CHRONIC HAZARD:	Y
FIRE HAZARD:	N
REACTIVITY HAZARD:	N
SUDDEN RELEASE HAZARD:	N

SECTION 16: OTHER INFORMATION

This material is prepared for use as a standard or in interlaboratory comparison programs at analytical laboratories, which routinely handle uranium and/or plutonium. The New Brunswick Laboratory (NBL) assumes that recipients of this material have developed internal safety procedures, which guard against accidental exposure to radioactive and toxic materials, contamination of the laboratory environment, or criticality. NBL further expects that personnel who handle radioactive materials have been thoroughly trained in the safety procedures developed by and for their Laboratory.

The information and recommendations set forth herein are presented in good faith and believed to be correct as of the revision date. However, recipients of this material should use this information only as a supplement to other information gathered by them, and should make independent judgement of the suitability and accuracy of this information. This statement is not intended to provide comprehensive instruction in developing an appropriate safety program and does not include all regulatory guidelines.

This information is furnished without warranty, and any use of the product not in conformance with this Material Safety Data Sheet, or in combination with any other product or process, is the responsibility of the user.

Appendix I. TOF-SIMS Measurements Procedures

All TOF-SIMS measurements were performed by a technician at the State University of New York and MSgt Schuler on an Ion Tof TOF-SIMS V instrument. The samples were placed on the sample holder and loaded into the initial vacuum chamber by MSgt Schuler. All mass spectra collected were downloaded from the instrument and transferred to a computer at AFIT for further data analysis.

The steps below provide a summary of the procedures used to load the samples into the TOF-SIMS instrument.

Step 1: Don HEPA mask, TLD, and disposable gloves. Place a clean tech wipe on the sample preparation table (this will prevent the spread of any material that may leave the carbon tape). Open a zip-lock bag and place it near the tech wipe (this will be used to collect potentially radioactive contaminated waste).

Step 2: Open the sample transport box and place the uranium samples on the sample preparation table (see Appendix E for the procedure used to transport samples).

Step 3: Remove the samples from the storage jar and remove the protective film with tweezers. Place the protective film back into the storage jar with tweezers.

Step 4: Mount the samples on the holder using the screws and pressure clips at various locations across the surface of the holder. Try to ensure that each

sample is sufficiently distant from its nearest neighbor to avoid any cross-contamination.

Step 5: When all samples have been mounted, place the sample holder on the manipulator rod and close the door to the secondary vacuum chamber. Check hands for contamination using a handheld rate meter. Remove the disposable gloves and place into the plastic radioactive waste bag.

Step 6: The TOF-SIMS operator will monitor the vacuum in the secondary chamber and transfer the sample holder to the primary vacuum chamber when a proper vacuum has been established.

Step 7: It can take up to 60 minutes to reach the required vacuum level in the primary chamber. The TOF-SIMS technician will then perform surface scans on each sample. The TOF-SIMS instrument will be calibrated using known peaks from those found during sample analyses.

Step 8: When the analysis is complete, the TOF-SIMS technician will transfer the sample holder to the secondary vacuum chamber and vent the secondary chamber in order to remove the sample holder.

Step 9: Don HEPA mask and new disposable gloves (your TLD should still be on). Remove the sample holder from the manipulator rod and remove each sample with tweezers. Replace the protective film on each sample then place each sample back into its storage jar. Mount additional samples if necessary by repeating steps three through eight.

Step 10: When all of the TOF-SIMS measurements are complete, return the sample jars to the transport box and close it with tape. Carefully fold up the tech wipe from the preparation table and place it in the plastic radioactive waste bag. Police the preparation area with a moistened tech wipe (any cleaner should suffice) and place the tech wipe into the plastic radioactive waste bag. Close the radioactive waste bag and place into a secondary containment vessel.

Step 11: Scan the preparation table, TOF-SIMS sample holder, transport box, and waste bag for any possible contamination with the handheld rate meter (levels should be below normal background of 0.5mR/hr).

Step 12: Return the samples to building 470 for storage upon return to AFIT.

Appendix J. TOF-SIMS Instrument Startup Procedures

The steps below describe the procedures used for initial startup of the TOF-SIMS instrument.

Step 1: Vent the load lock chamber by pressing the "vent" button on the linear actuator. Load samples onto the sample holder, place sample holder onto linear actuator, and close the load lock door. Pump down the load lock by pressing the "pump" button on the linear actuator and wait for a vacuum of at least 5 X 10^{-7} mbar to be achieved.

Step 2: Once a stable vacuum has been achieved, open the gate valve by pressing the "open" button on the linear actuator. Move the sample holder into the analysis chamber with the linear actuator and close the gate valve by pressing the "close" button on the linear actuator.

Step3: Ensure that the check boxes for "Power Analyzer, Power LMIG, LMIG, and Illumination" are all checked.

Step 4: Open two instrument windows by pressing the "instrument" button twice and then select "LMIG" in one of them.

Step 5: Click the wrench in the toolbox, then select "file," then "open," then "Bi gun start 9000V.job." Once the batch has been selected, click the play button to start up the Liquid Metal Ion Gun (LMIG).

Step 6: Click the "settings" button the select "load," then "Analyzer NM.tmt" to start the analyzer in normal mode.

Step 7: Select a primary species by clicking in the "primary species" window (Bi_3^+ was used for all of our analyses).

Step 8: Open the stage control window by pressing the "stage control" button.

Step 9: Open the SE/SI/Video window by pressing the "SE/SI/Video" button.

Step 10: Open the pressure window by pressing the "P" button.

Step 11: Open the spectrum window by pressing the "spectrum" button.

Step 12: Move the sample holder to the Faraday cup position by selecting the "cup top mount" position in the stage control window. Once the stage has moved to the appropriate position, click the "micro" button in the SE/SI/Video window. Ensure that field of view is centered on the Faraday cup then uncheck the "beam blanking" check box in order to obtain the ion current. Annotate the ion current on the data parameter sheet then uncheck the "beam blanking" check box.

Step13: Position stage to an appropriate sample and adjust the z-axis to within several mm of the extraction cone. Click the "start raster" button on the stage control window then check the "adjust SI" check box to optimize the z-axis position then uncheck the "adjust SI" checkbox.

Step 14: Right click in the image and select "adjust CC" to optimize the Charge Compensation (CC) by dropping the voltage until the image starts to go fuzzy then returning 20V.

Step 15: Open a peak list from the “tools” menu in the spectrum window or create a new one for use with current sample. Screen shots are provided In Figures 44 and 45 to illustrate the proper instrument setup.

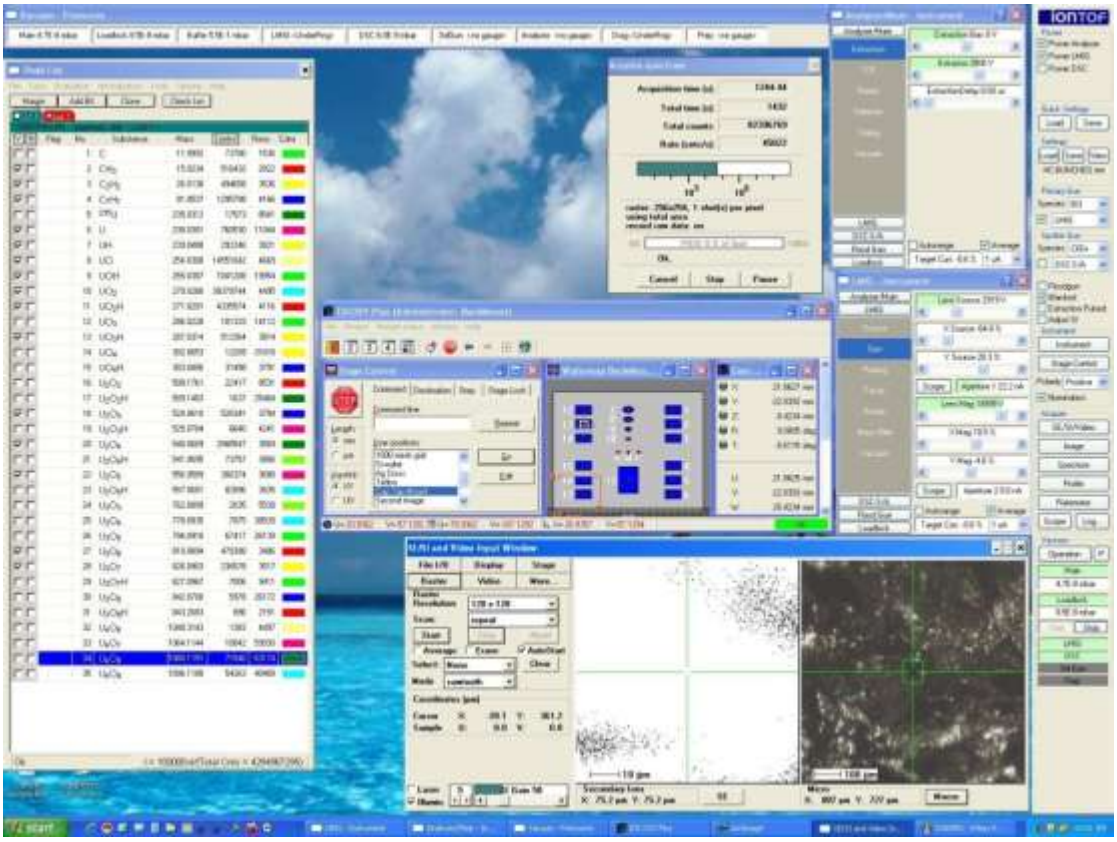

Figure 44. Screen capture depicting all windows opened for sample analyses.

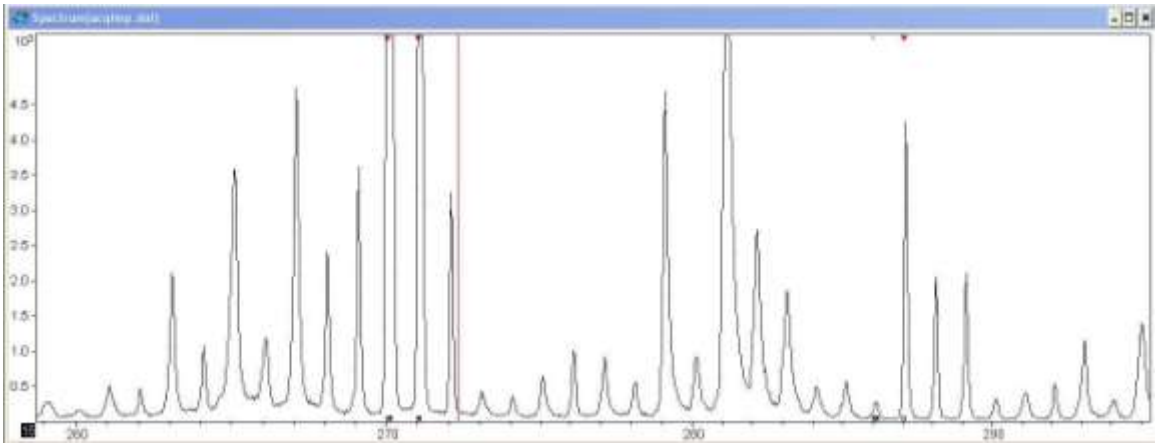

Figure 45. Screen capture depicting mass spectrum collection window.

Appendix K. TOF-SIMS Analysis Instructions

The steps below describe the procedures used for sample analysis with the TOF-SIMS instrument.

Step 1: Indentify a particle/area of interest and adjust the analysis area to an appropriate size by right clicking in the image then selecting "specify area" and entering an appropriate analysis area size (75X75μm, for our scans).

Step 2: Start the raster by clicking the "start raster" button in the stage control window and ensure you are receiving counts from the species of interest in the spectrum window.

Step 3: Stop the raster by clicking the "stop raster" button in the stage control window and adjust the CC as in step 14 of the preceding appendix.

Step 4: Restart the raster and ensure a stable secondary ion yield (a complete field of white is perfect).

Step 5: Stop the raster then select the "acquisition" tab in the spectrum window then select the "spectrum" option to start data acquisition.

Step 6: Press the "F3" button to start a mass calibration. H, H_2, H_3, CH_3, C_2H_2, C_7H_7, ^{238}U, UO, UO_2, U_2O_3, U_2O_4, U_3O_6, and U_4O_8 were used for positive secondary ions and H, C, O, OH, C_2H, SiO_2, UO_3, U_2O_6, and U_3O_8 were used for negative secondary ions. Press "P" to select each mass/molecule, right click on center of peak, click "Select ion" then press the "Do" button and repeat for each ion in the mass calibration list.

Step 7: Construct a new peak list, if necessary, by selecting the "tools" menu from the spectrum window and clicking on the "peak list" option. Select "evaluation" then "peak evaluation" to select of peak of interest, ensure the proper ion is identified then select "add to peak list" and continue until all peaks of interest have been identified.

Step 8: Once analysis is completed the spectrum can be reconstructed by selecting the "acquisition" tab in the spectrum window and selecting the "spectrum" option. Ensure the "reconstruct from raw data" and "use mass calibration from raw data" check boxes are both checked. Adjust peak margins by selecting the "adjust margins" button in the peak list window. Once a spectrum has been reconstructed, save the spectrum as a dat file as well as exporting the spectrum to ASCII.

Step 9: Images can reconstructed by selecting the "acquisition" tab in the image window then selecting "image acquisition." Ensure the "reconstruct from raw data" check box is checked to start the image reconstruction. Save the image as an imw file and cut and paste images of interest into an appropriate software application for future analysis.

Appendix L. Sample Mass Spectrum

This appendix contains a sample mass spectrum that was extracted from the raw data using Microsoft Excel. Only one positive-mode spectrum of a U-500 sample is presented in order to limit the length of this document. The U-500 sample is the most relevant spectrum due to the fact that it contains all of the predicted peaks of interest.

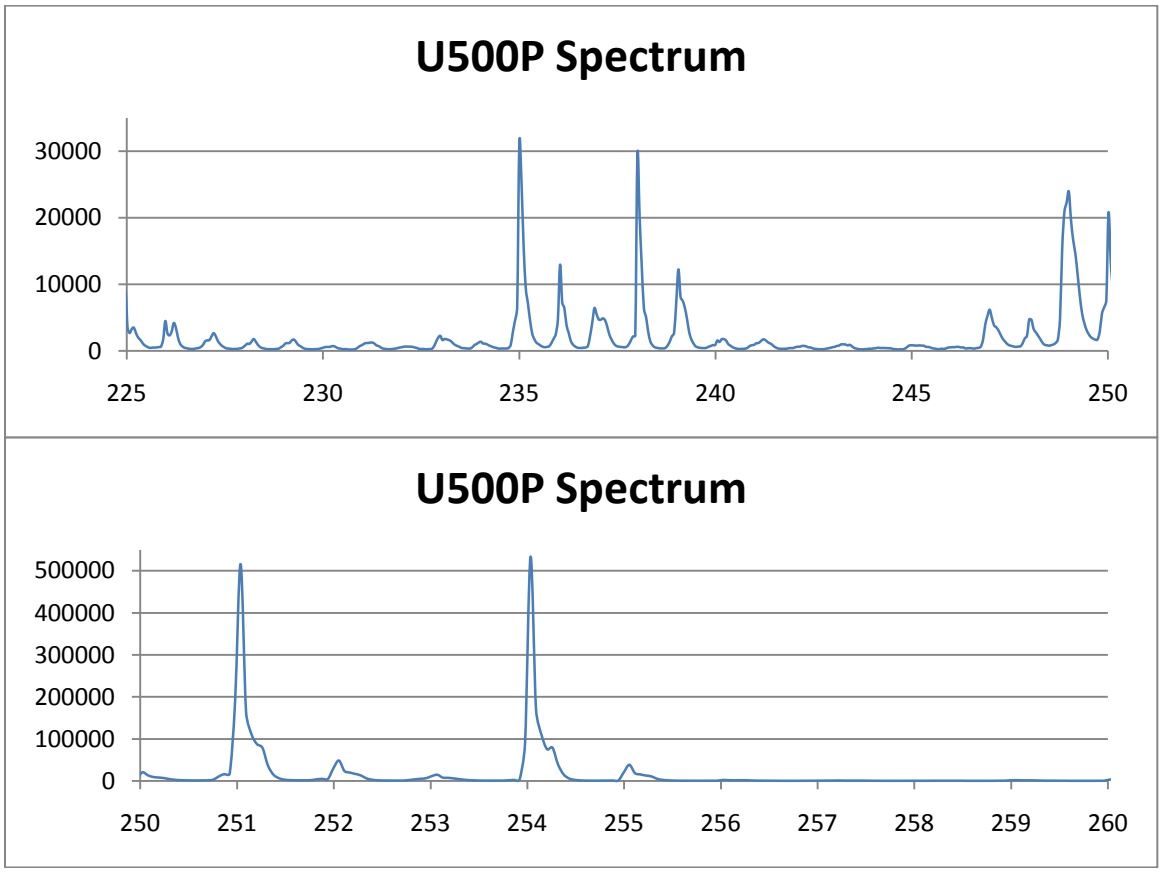

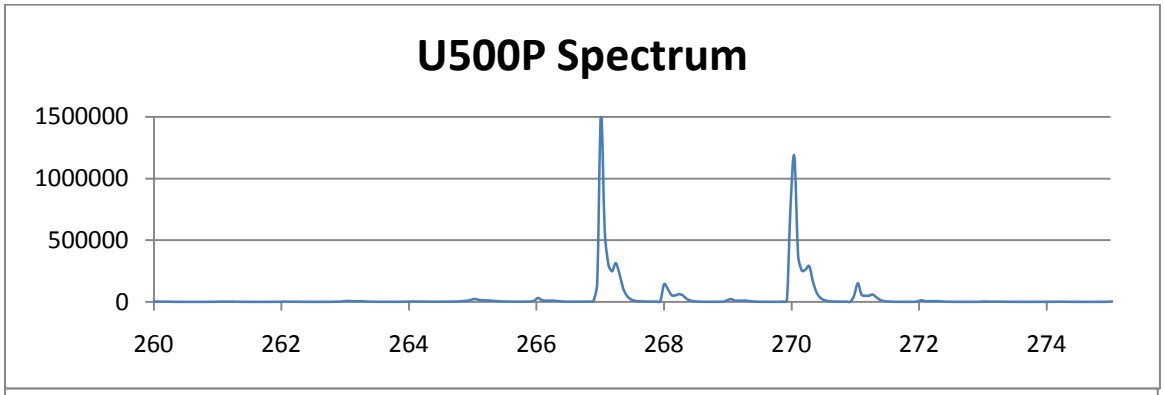

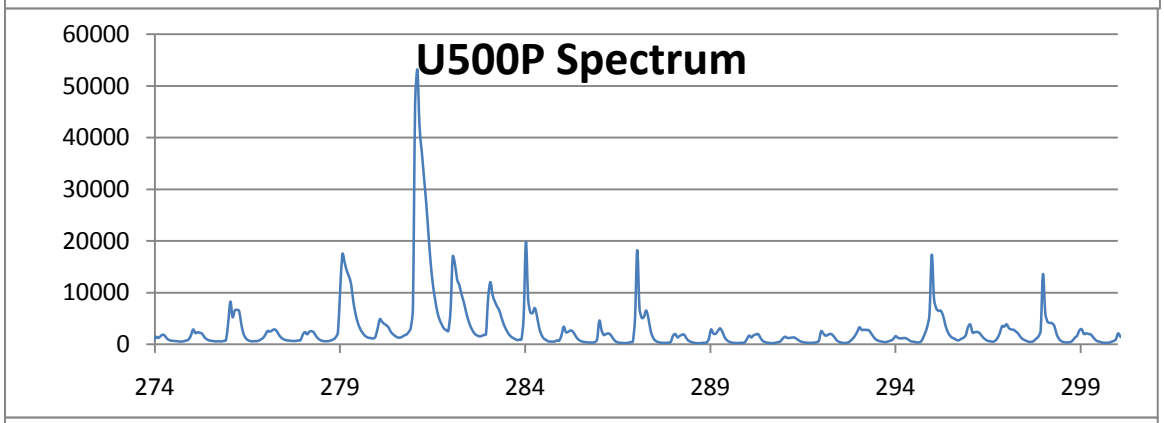

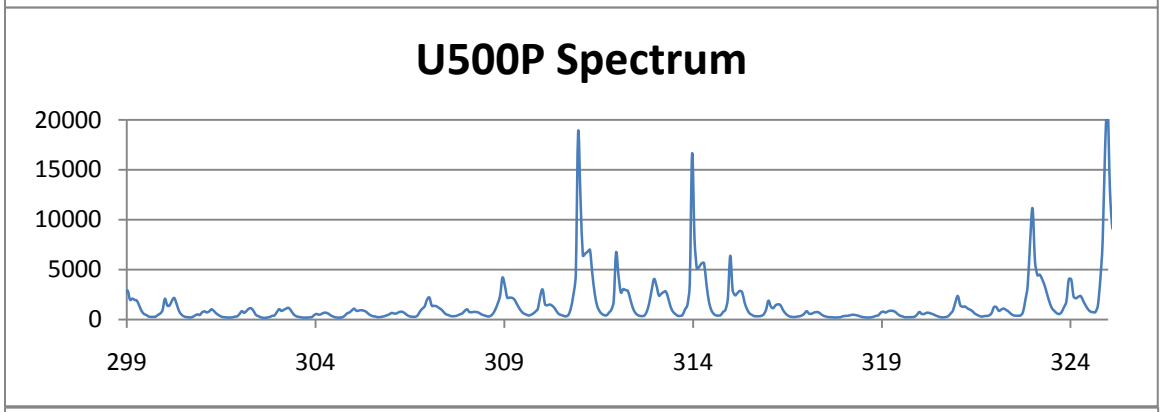

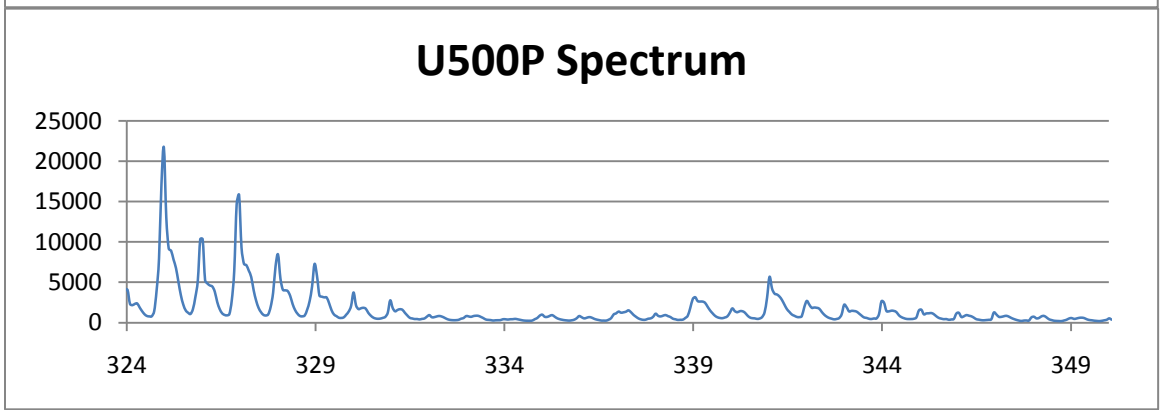

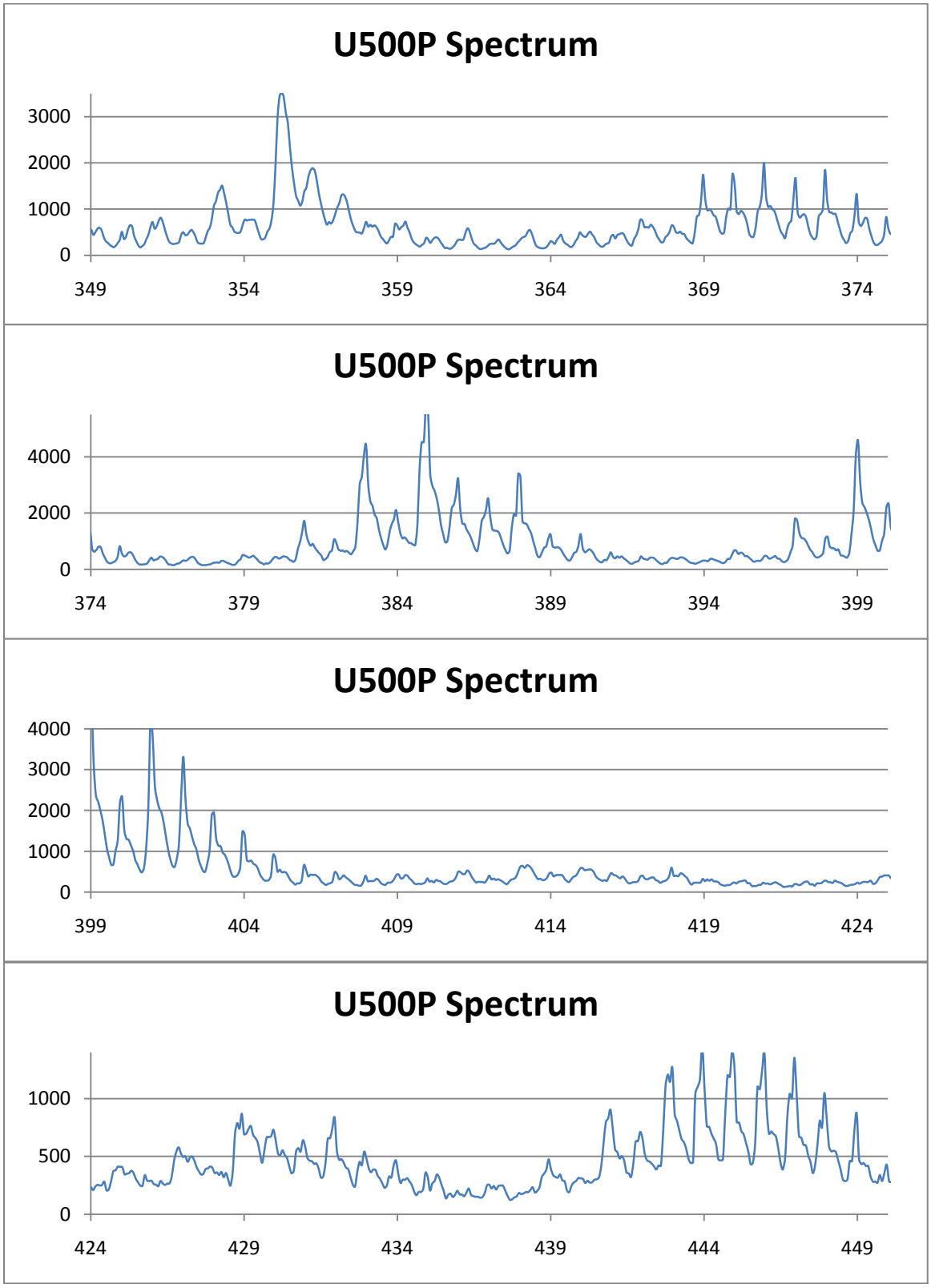

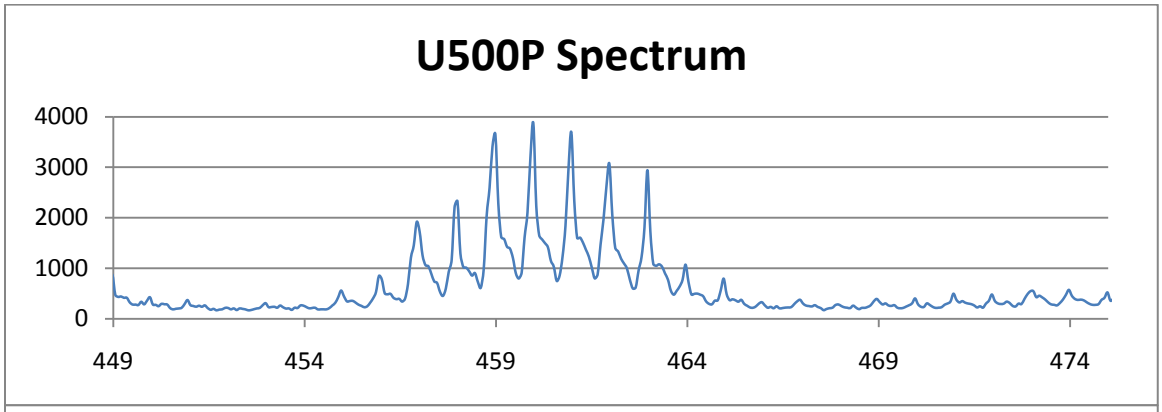

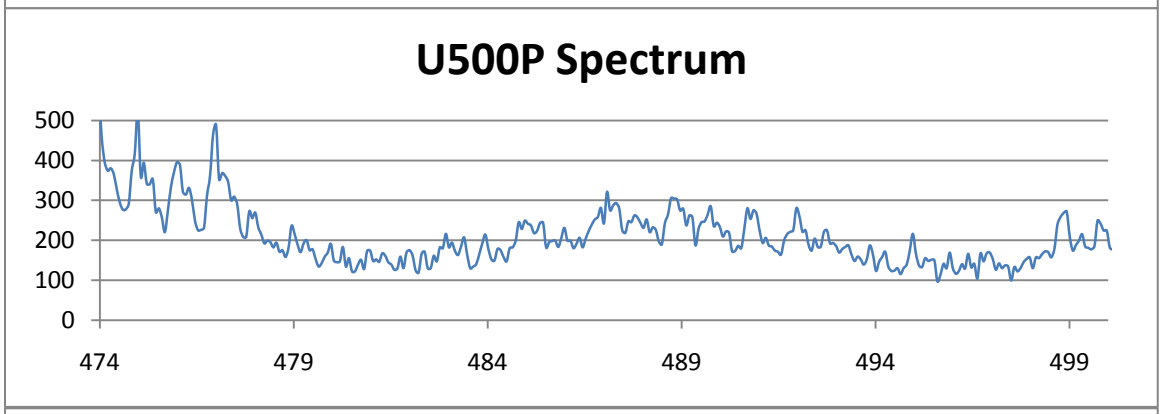

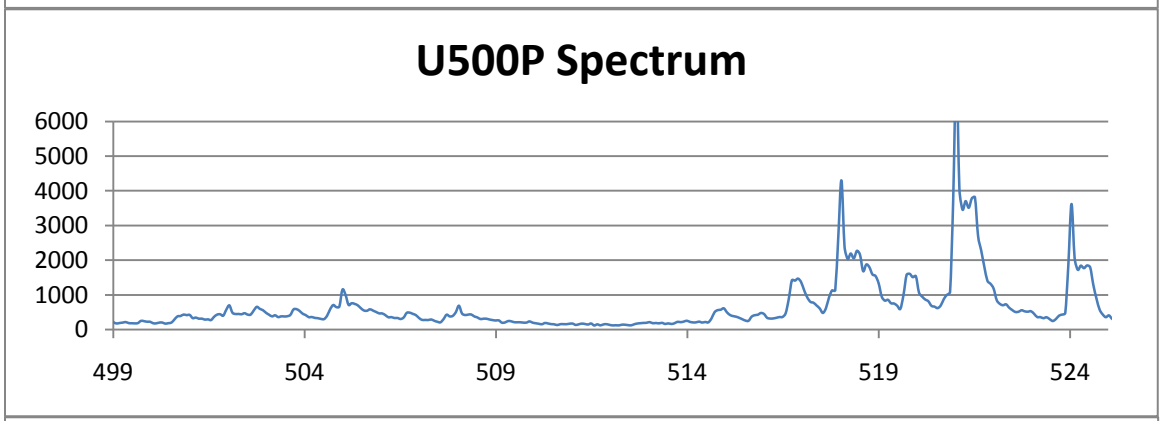

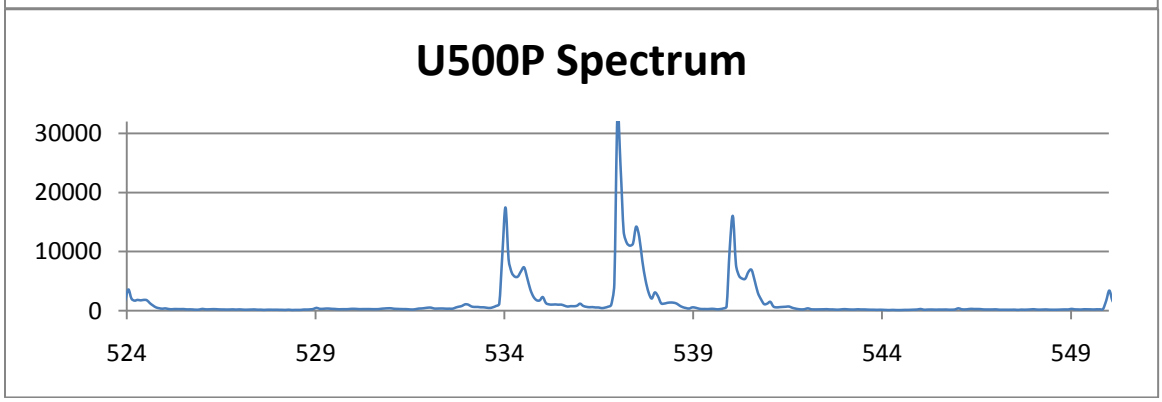

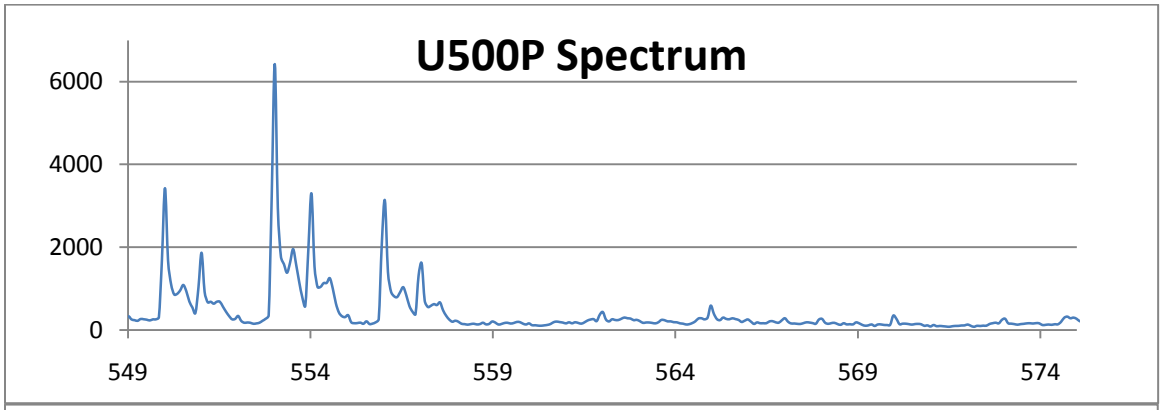

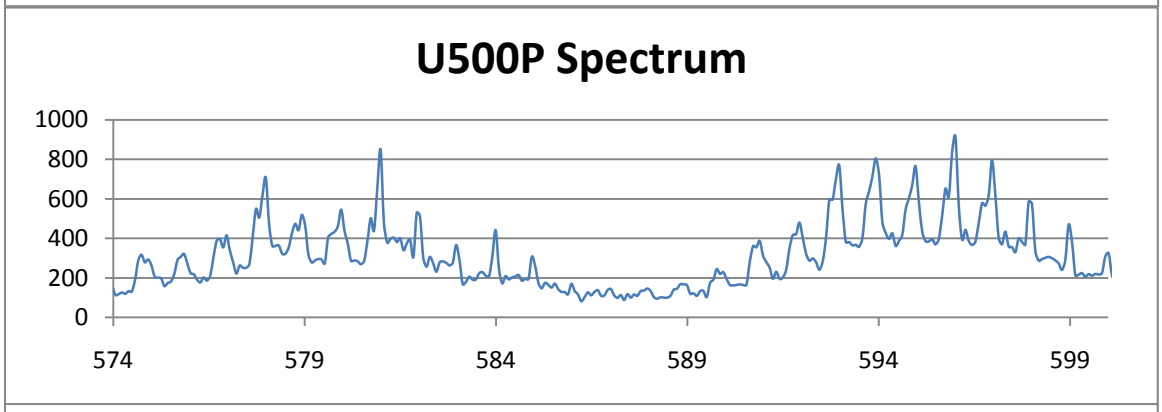

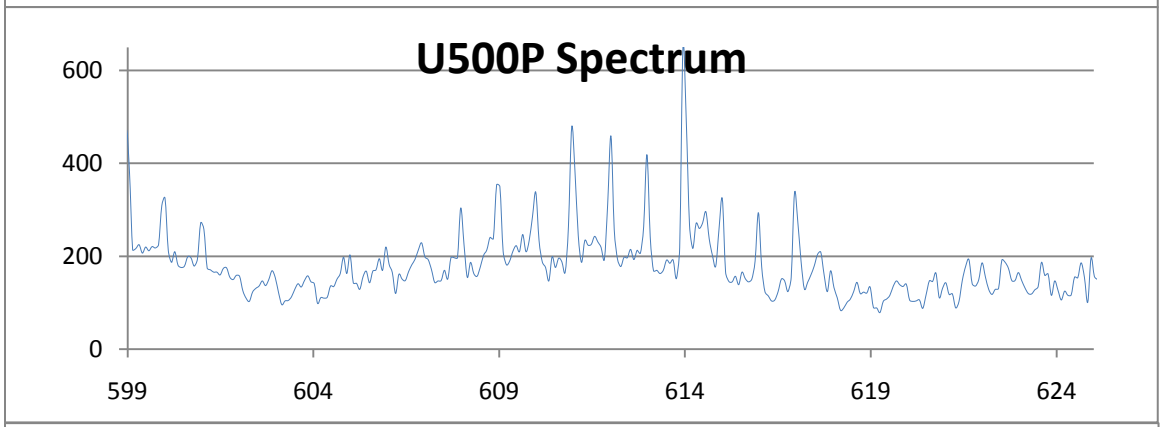

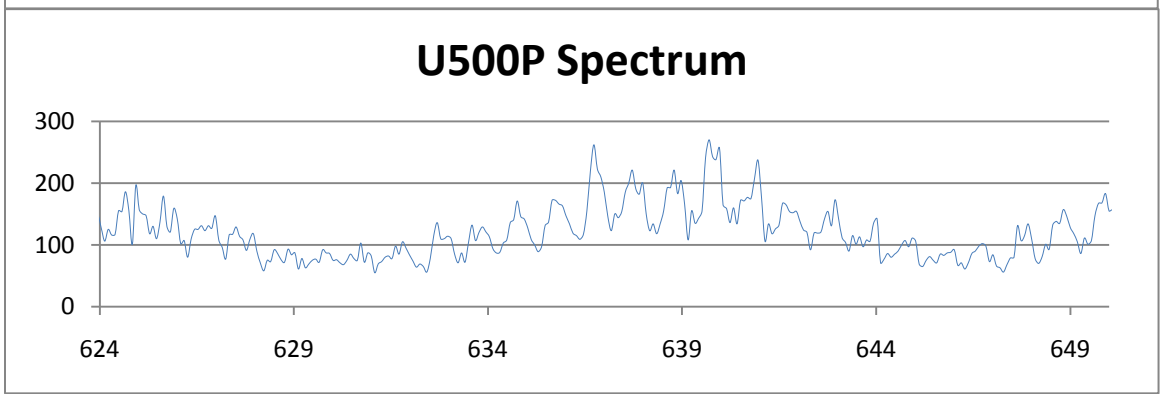

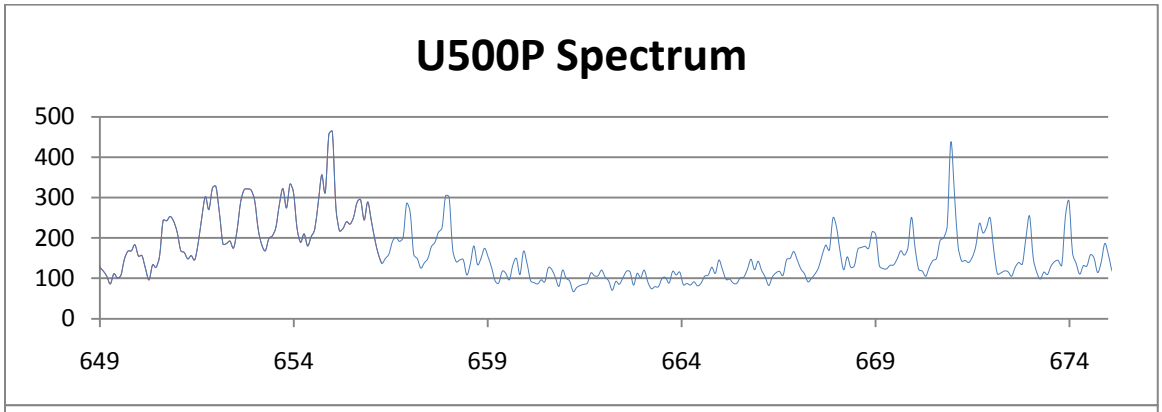

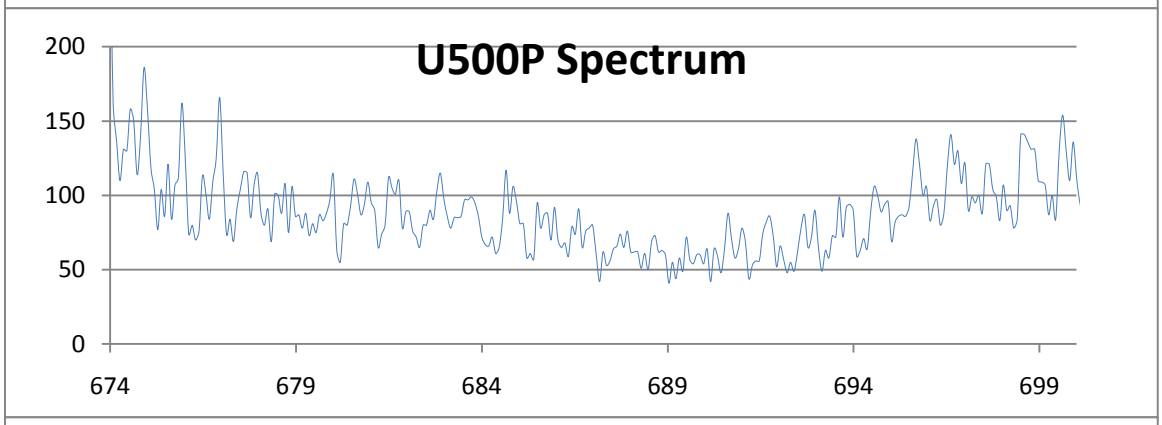

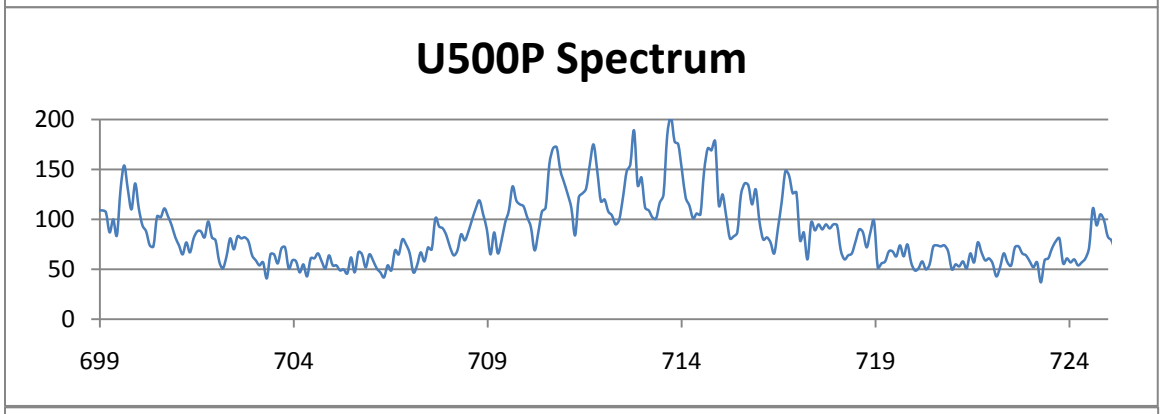

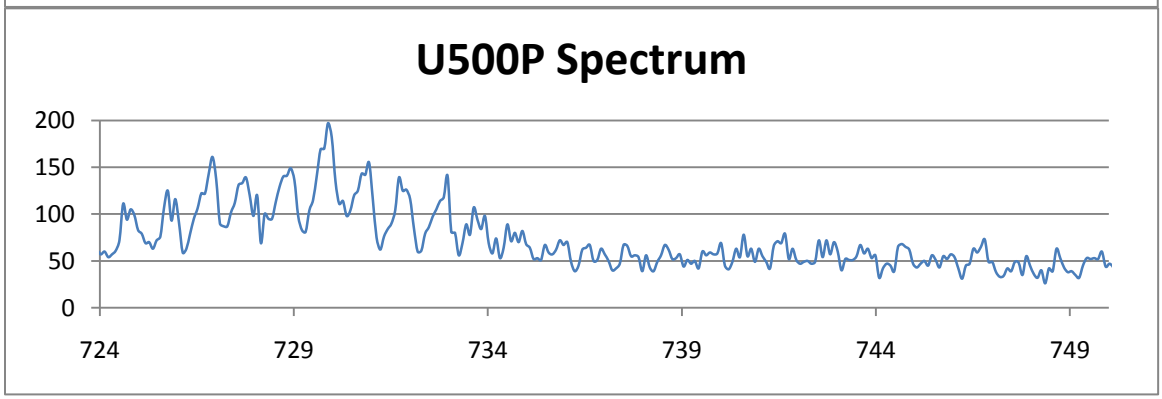

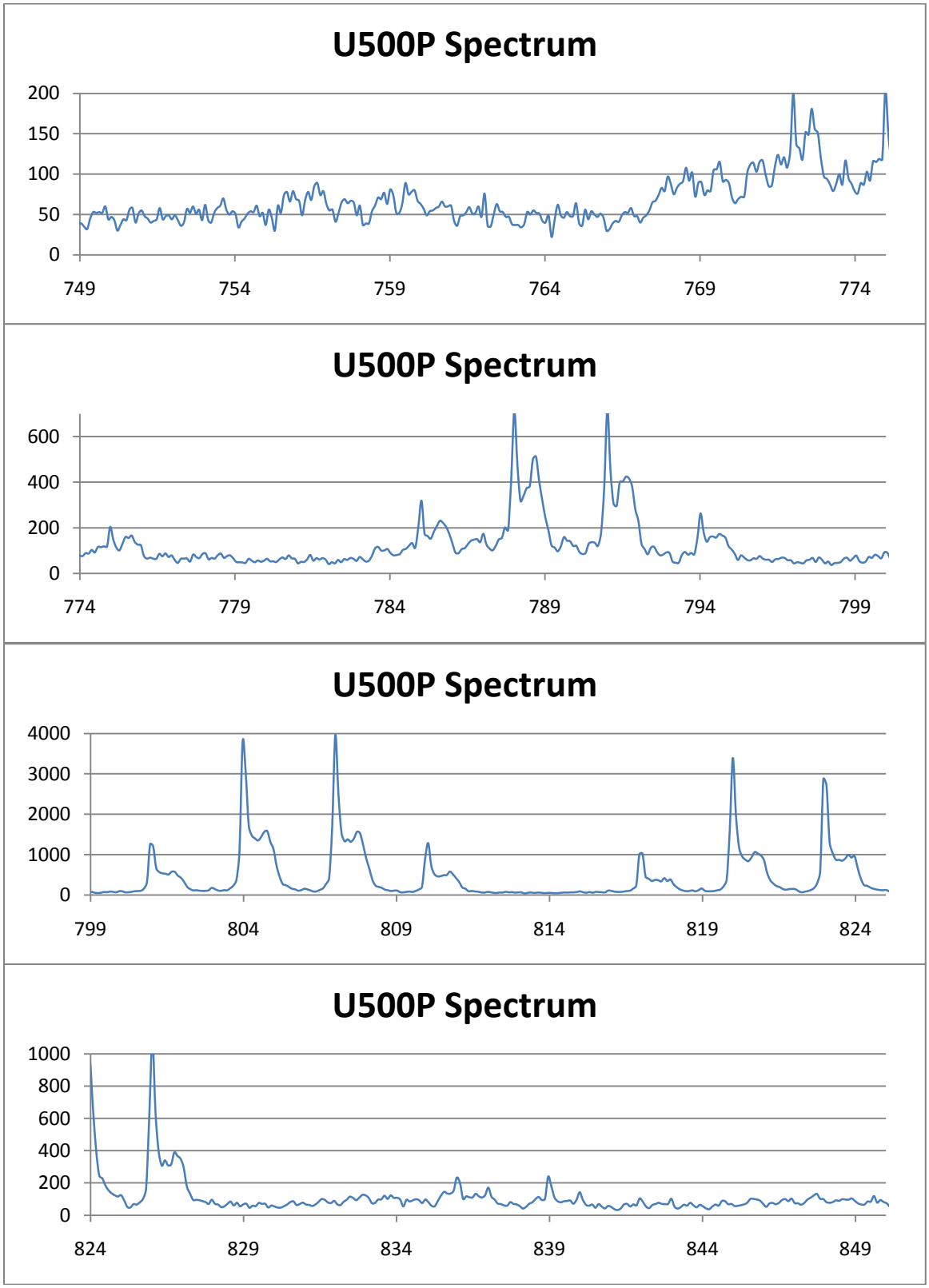

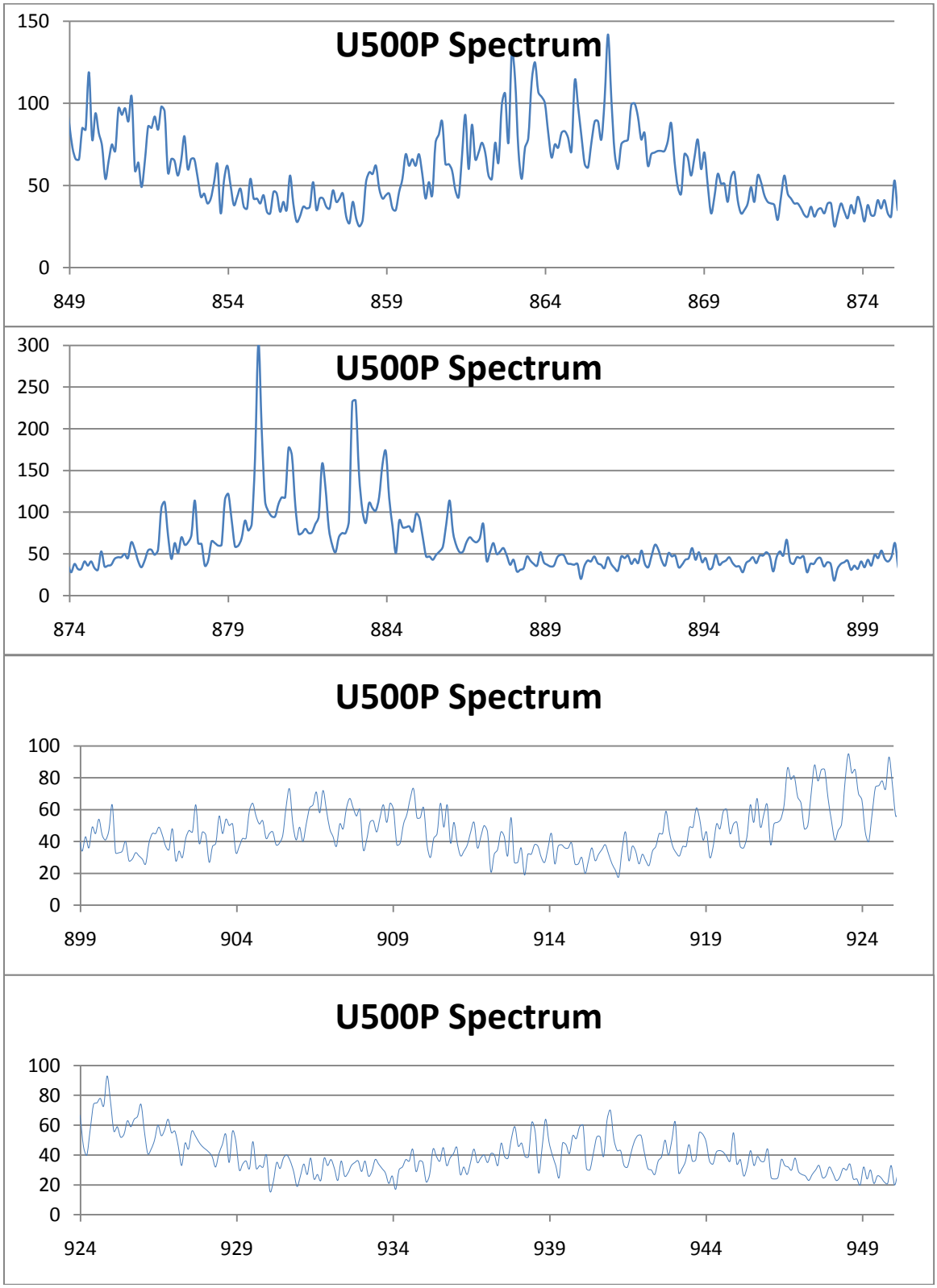

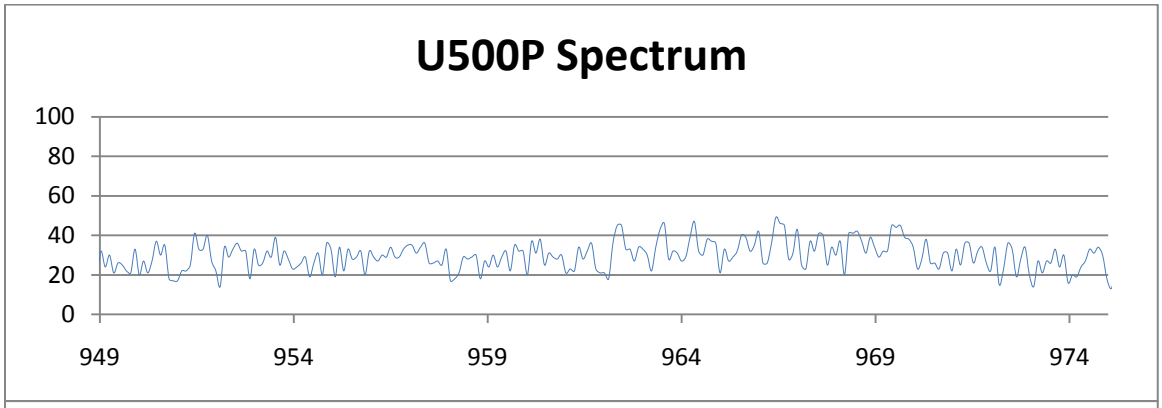

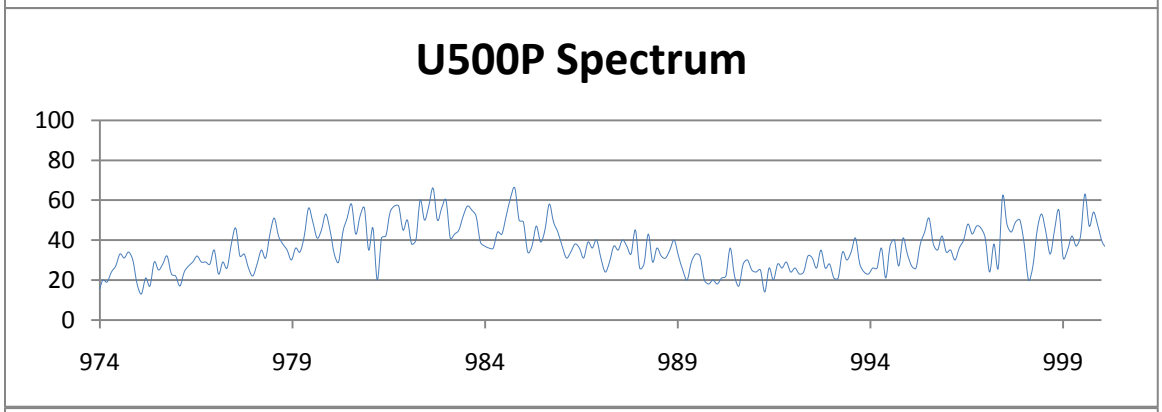

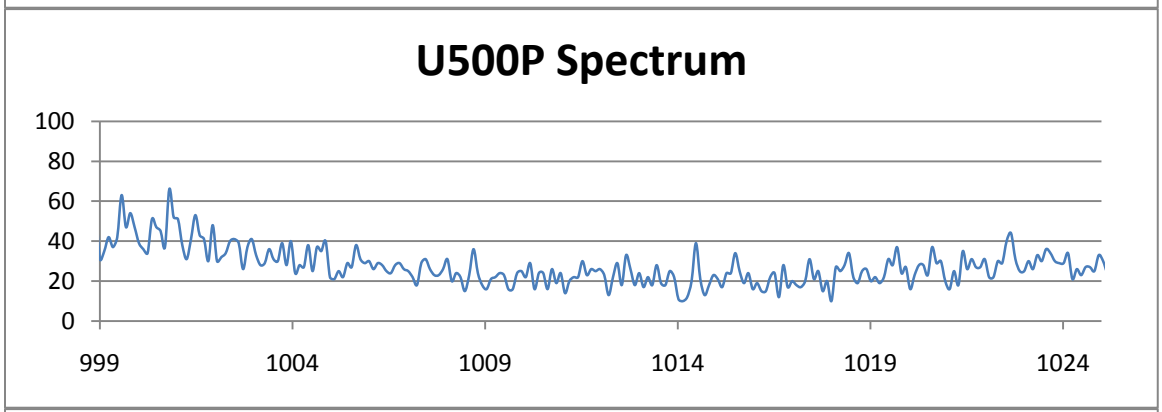

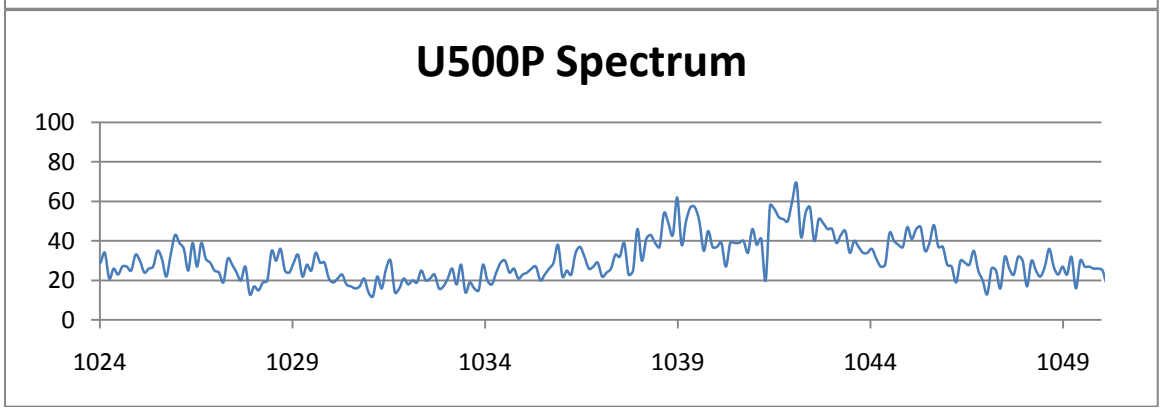

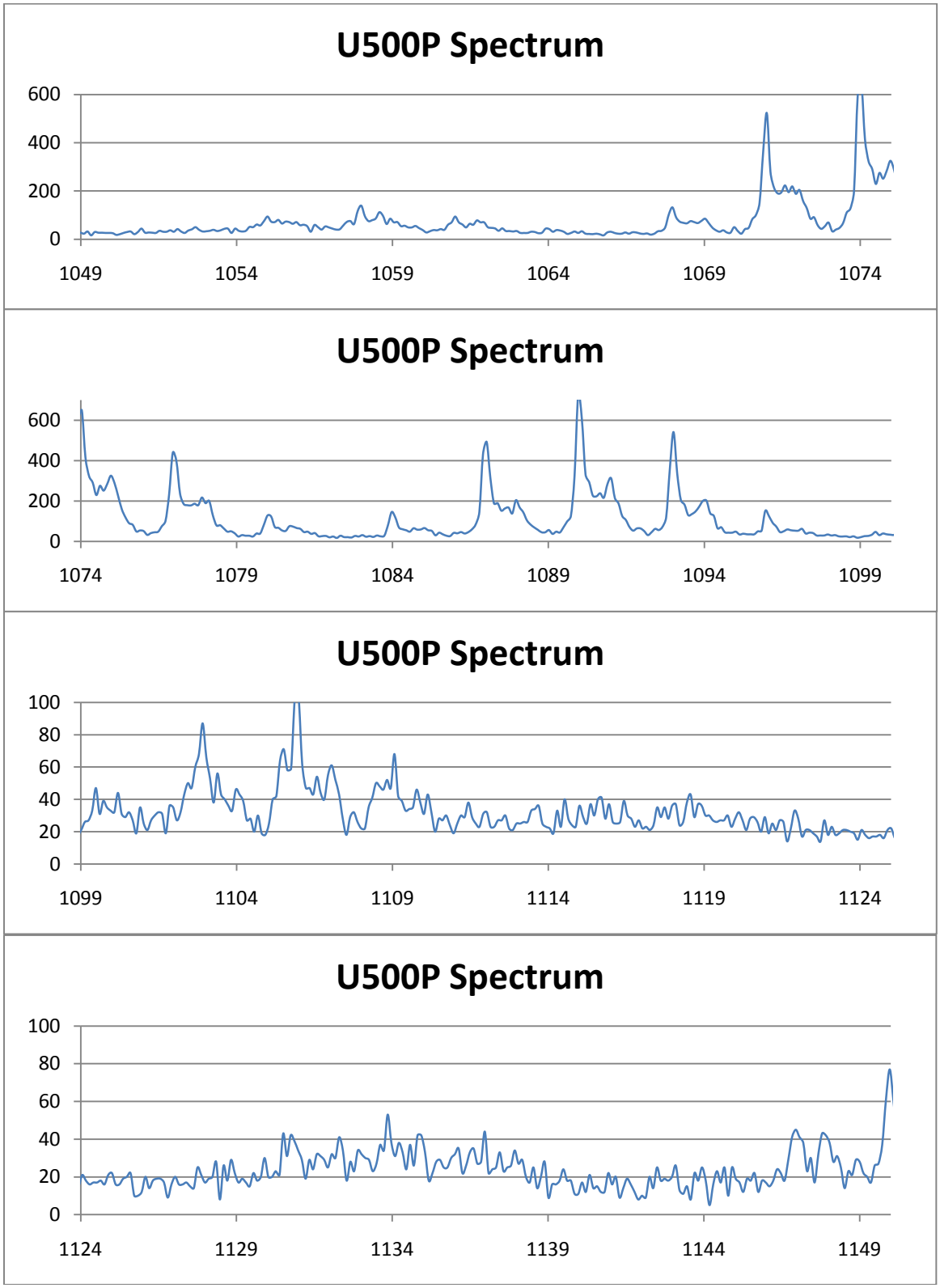

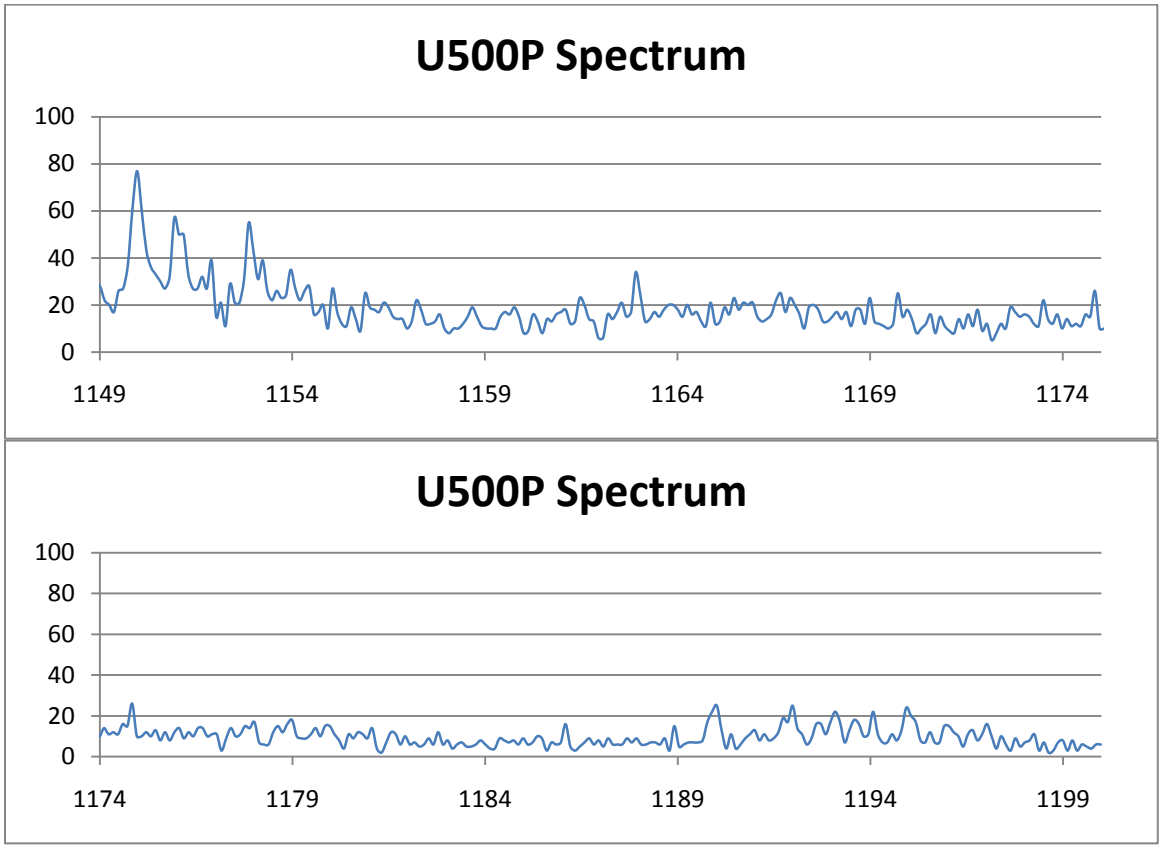

Appendix M. Sample Ion Images

This appendix contains ion images for the highest intensity spectrum collected for each sample. The color bar goes from black, the lowest intensity to white, the highest intensity.

T10001P

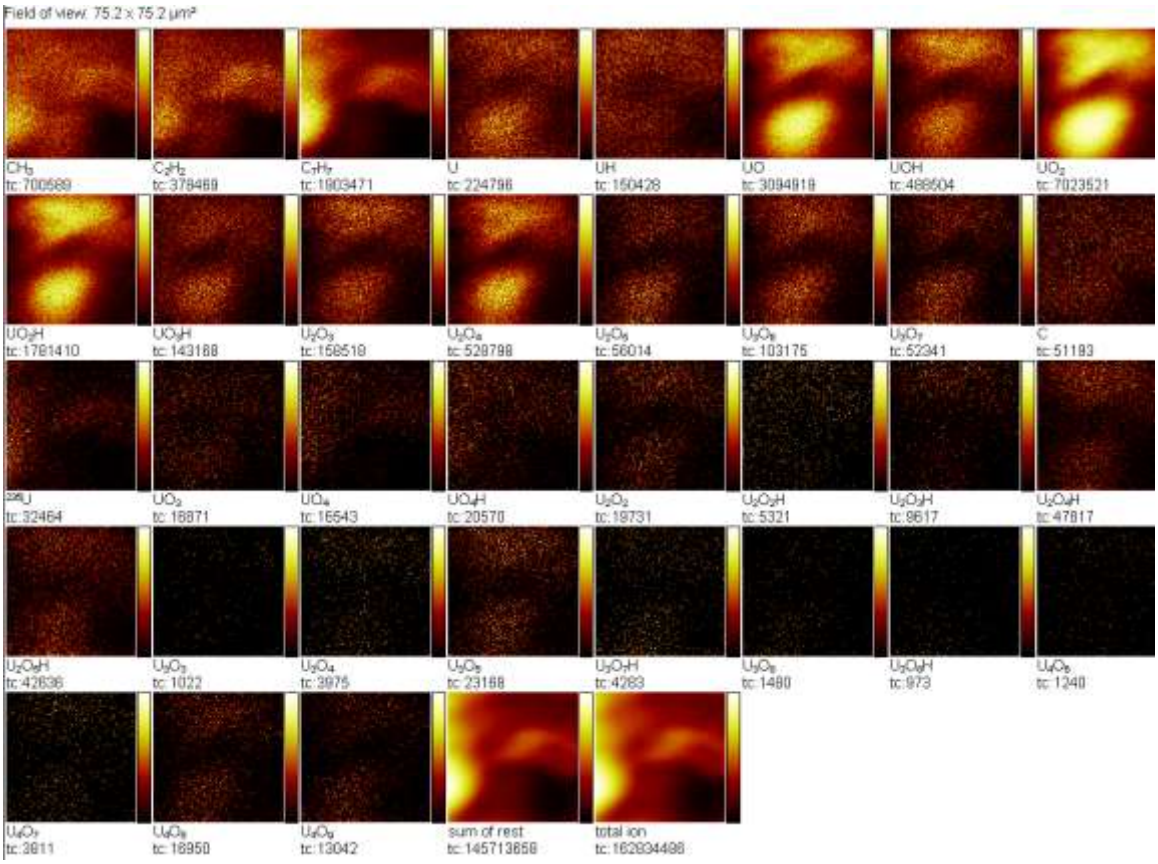

Figure 46. Sample T100 positive ion image.

T10101P

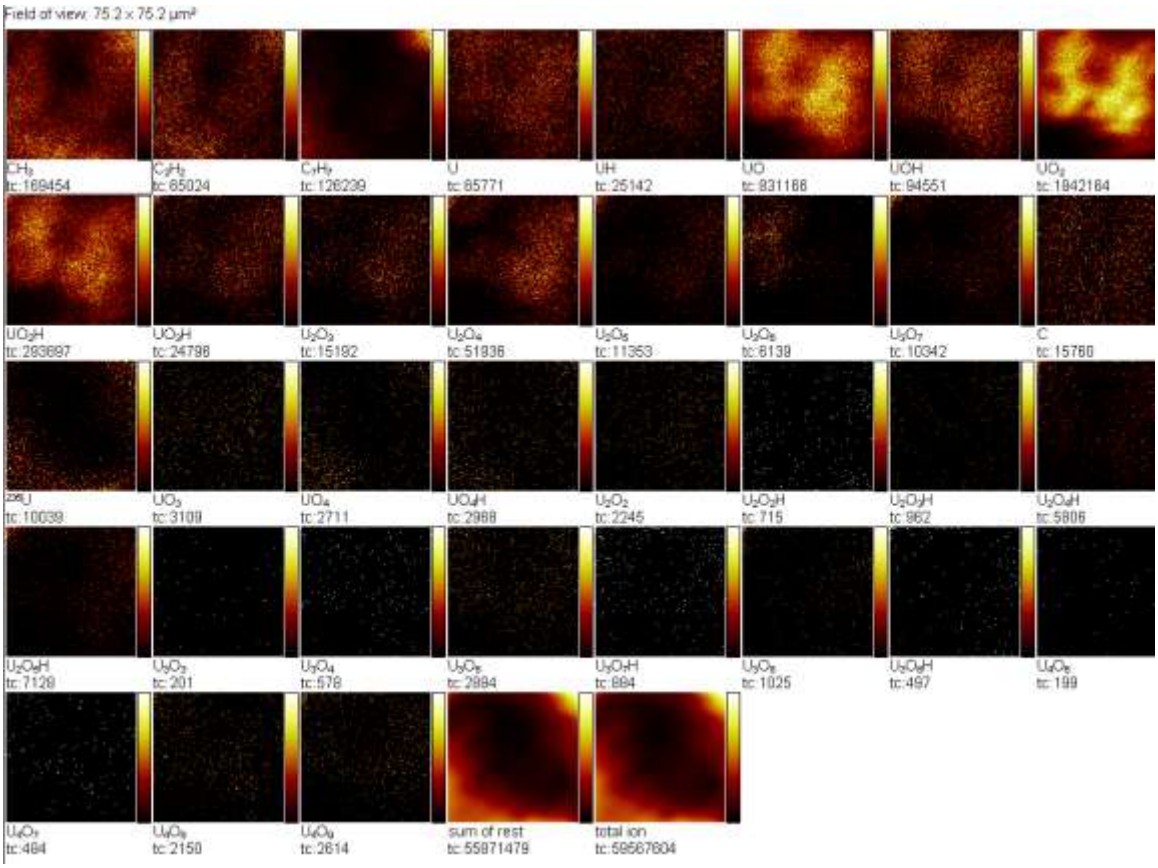

Figure 47. Sample T101 positive ion image.

T10201P

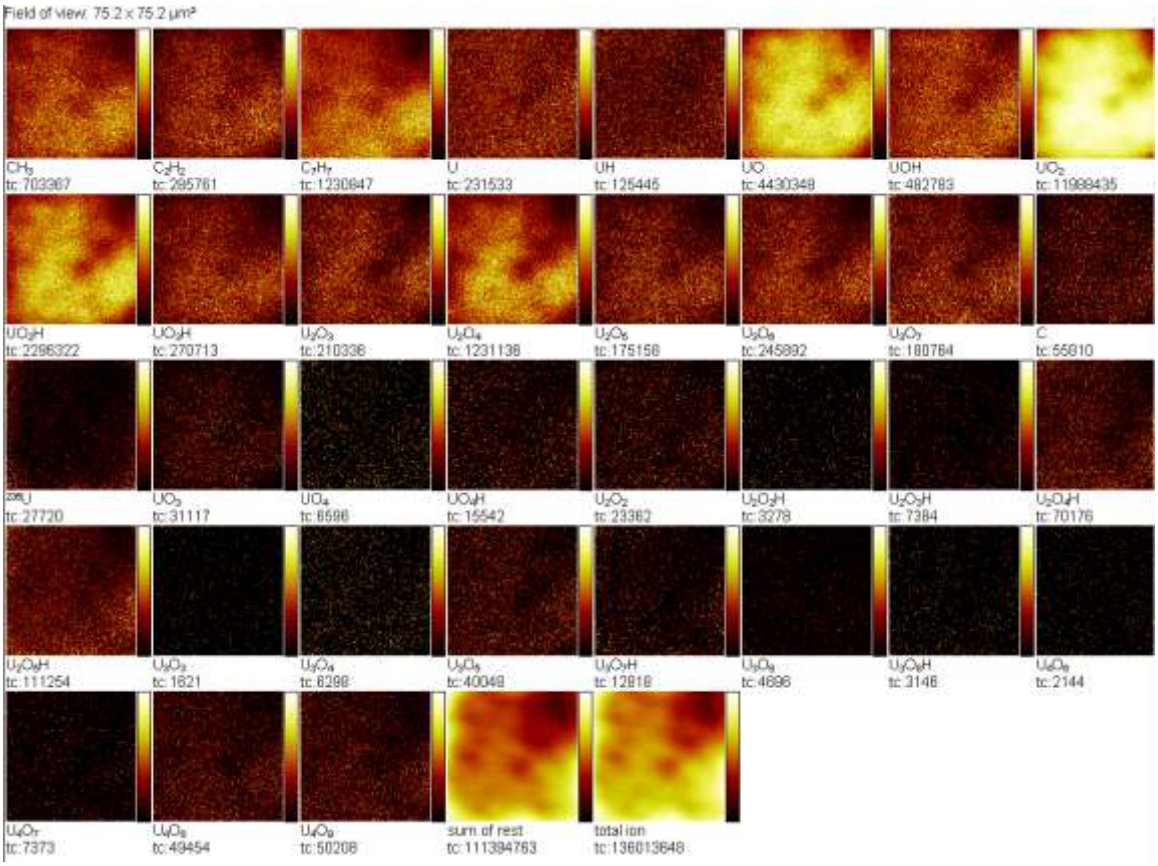

Figure 48. Sample T102 positive ion image.

U00505P

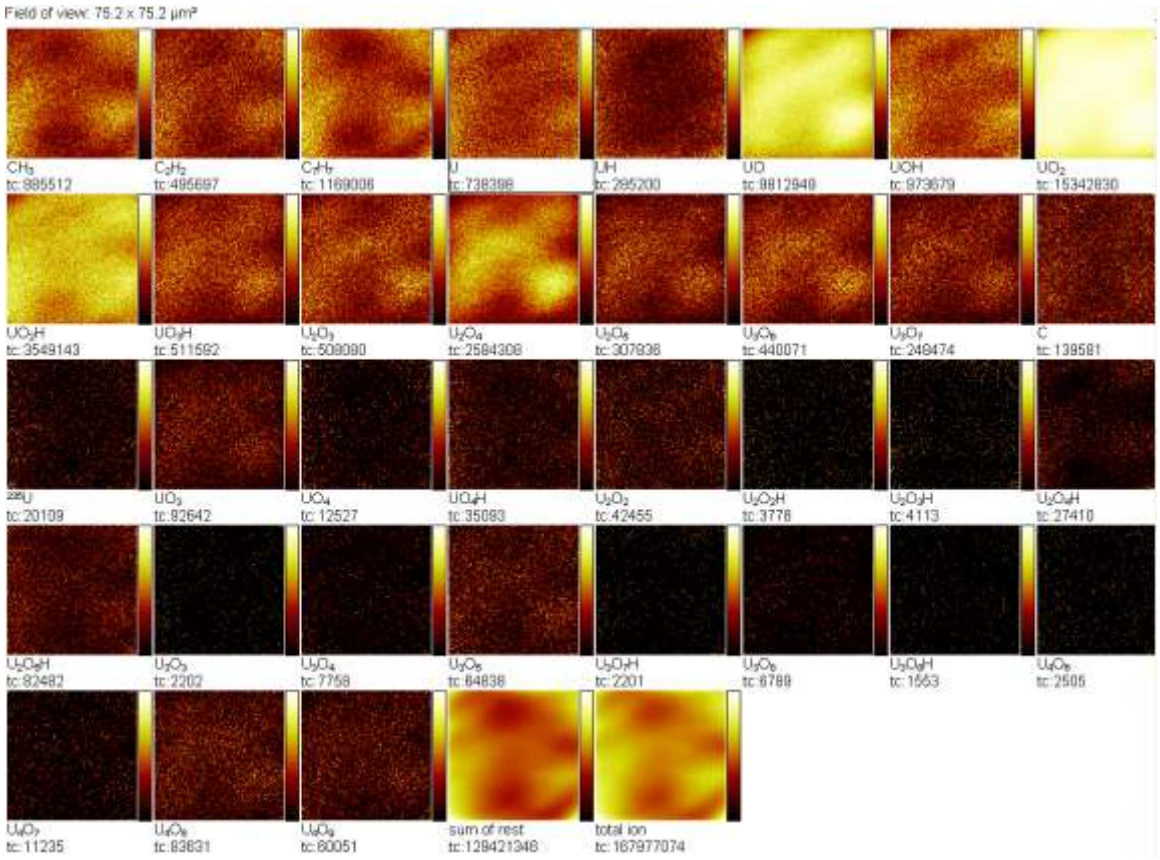

Figure 49. Sample U005 positive ion image.

U1802P

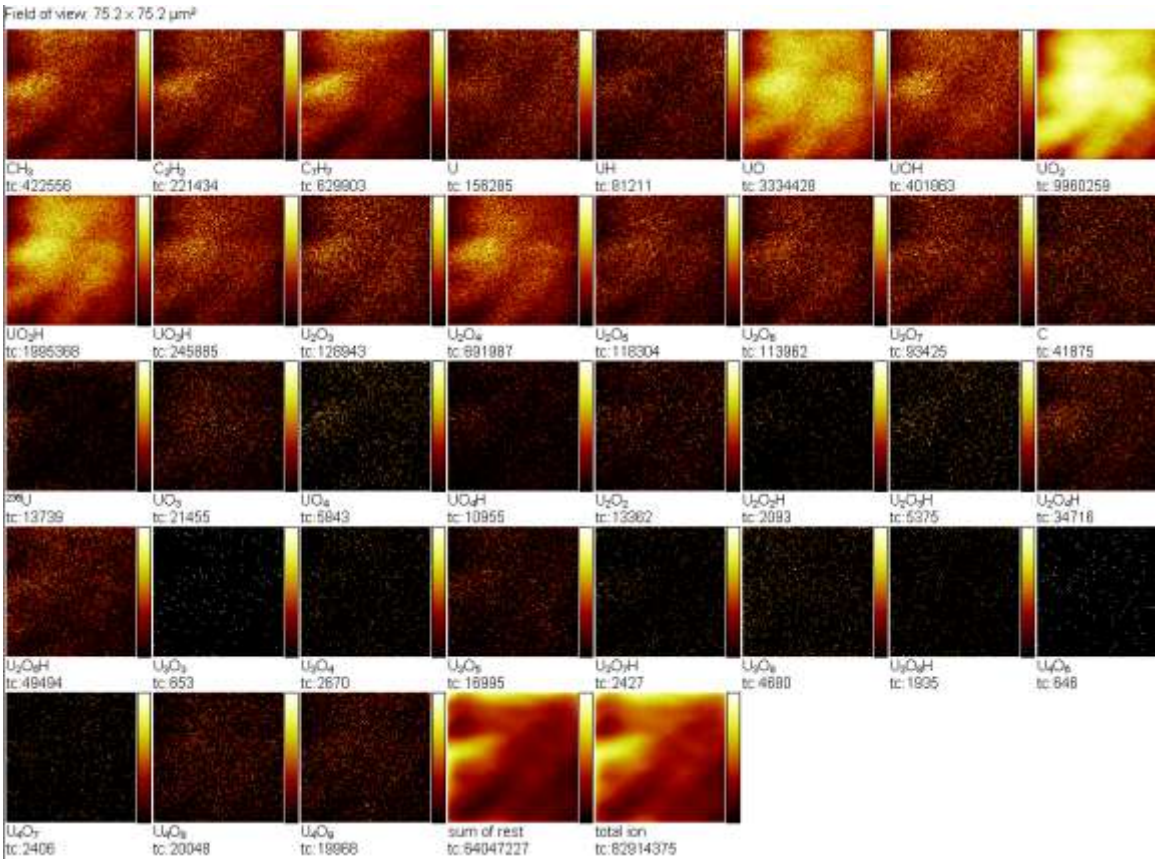

Figure 50. Sample U18 positive ion image.

U12901P

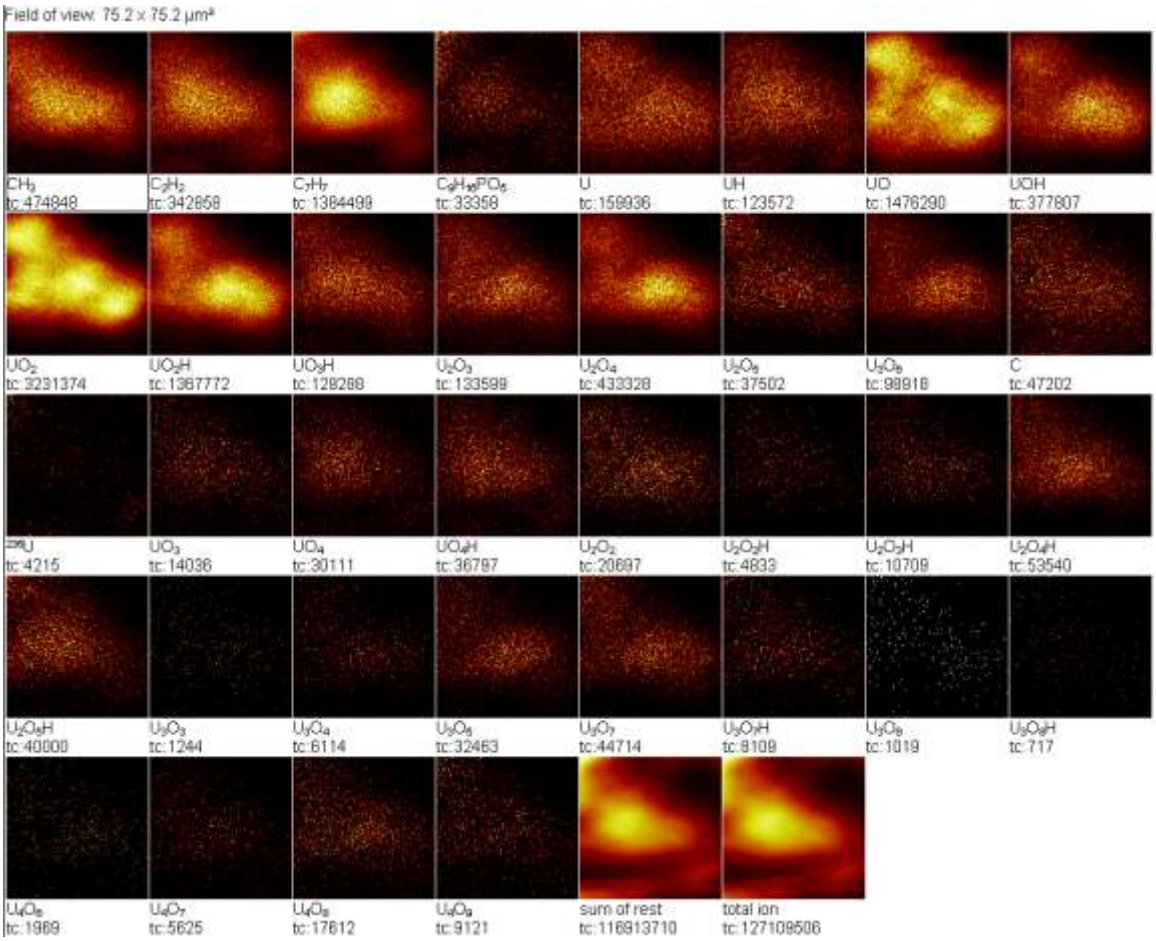

Figure 51. Sample U129 positive ion image.

U50001P

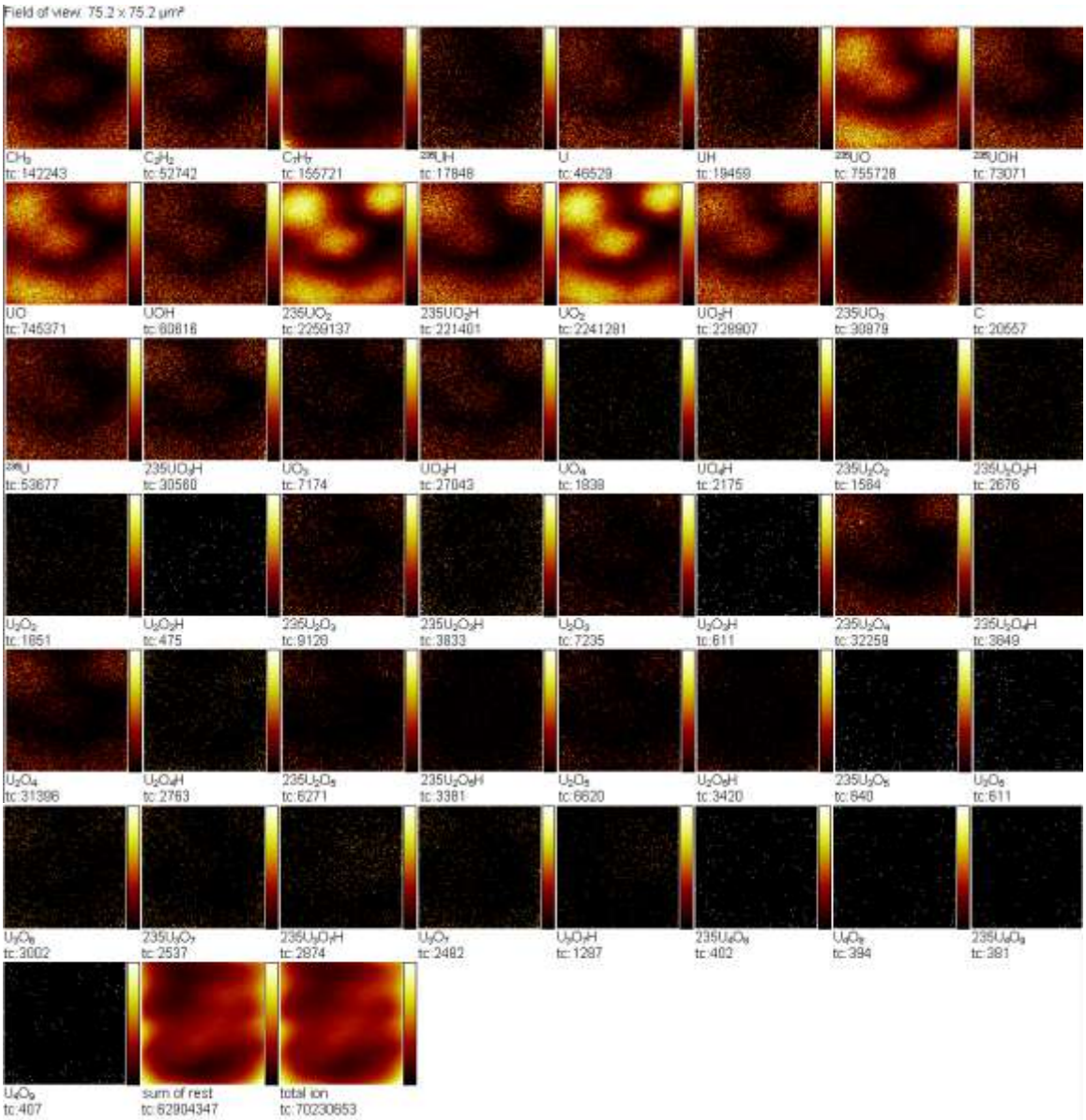

Figure 52. Sample U500 positive ion image.

U90003P

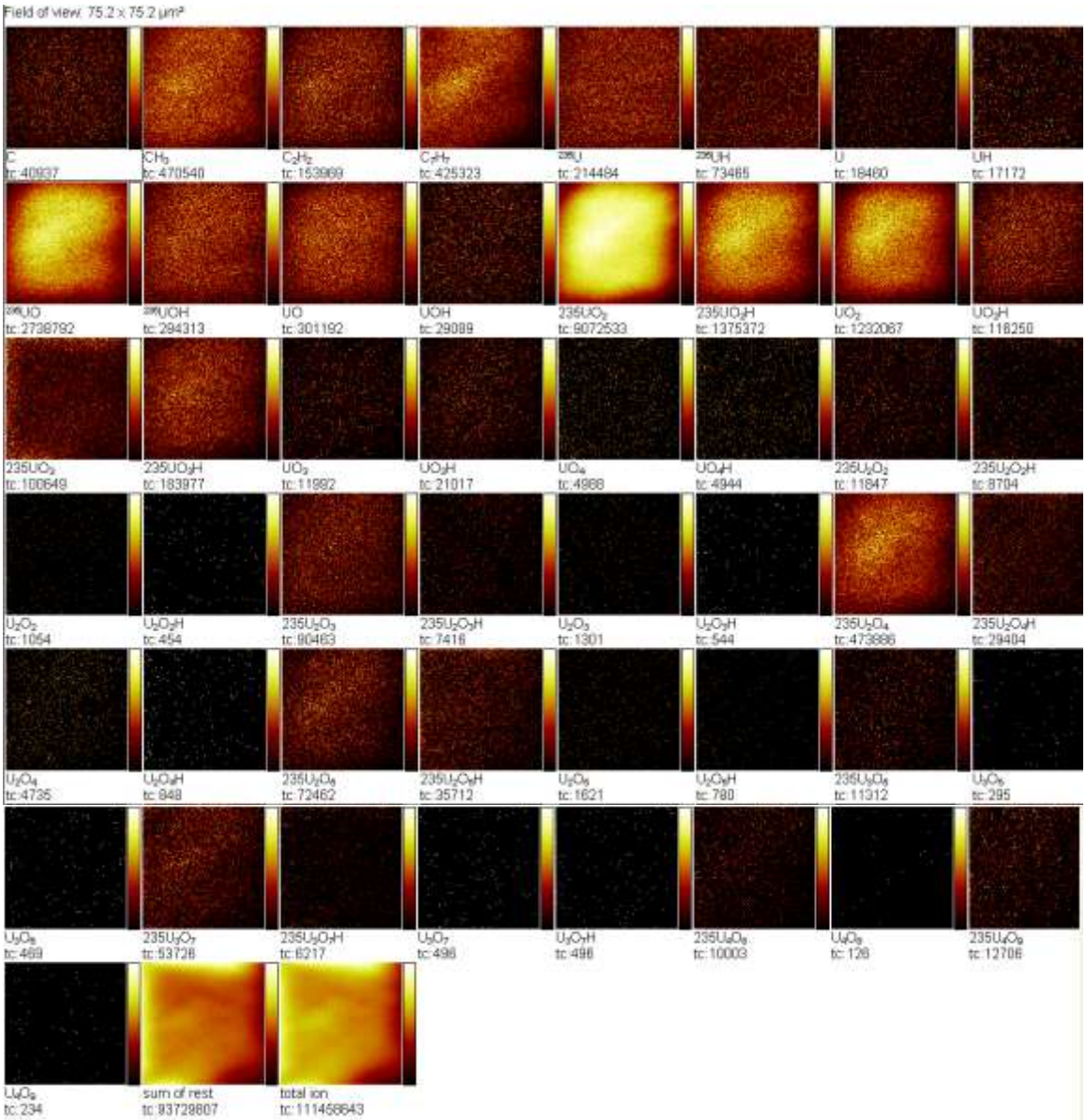

Figure 53. Sample U900 positive ion image.

Appendix N. Lists of Peaks of Interest

This appendix contains lists of peaks of interest calculated from the isotopic abundances of each atom in each cluster. The order of each of the specific isotopes is as follows: $^{16}O^+ - ^{18}O^+ - ^{235}U^+ - ^{238}U^+$. Results of the calculations are provided according to cluster in Table 32 and as a consolidated list in Table 33.

Table 32. Peak list of all possible combinations of isotopes for various uranium oxide ions separated by cluster ion species.

UO	Mass	Order	Mass
1-0-1-0	251.0388	0-1-1-0	253.0431
1-0-0-1	254.0457	0-1-0-1	256.0499

UO_2	Mass	Order	Mass	Order	Mass
2-0-1-0	267.0338	1-1-1-0	269.038	0-2-1-0	271.0422
2-0-0-1	270.0406	1-1-0-1	272.0449	0-2-0-1	274.0491

UO_3	Mass	Order	Mass	Order	Mass	Order	Mass
3-0-1-0	283.0287	2-1-1-0	285.0329	1-2-1-0	287.0372	0-3-1-0	289.0414
3-0-0-1	286.0355	2-1-0-1	288.0398	1-2-0-1	290.044	0-3-0-1	292.0483

UO_4	Mass	Order	Mass	Order	Mass	Order	Mass	Order	Mass
4-0-1-0	299.0236	3-1-1-0	301.0278	2-2-1-0	303.0321	1-3-1-0	305.0363	0-4-1-0	307.0406
4-0-0-1	302.0304	3-1-0-1	304.0347	2-2-0-1	306.0389	1-3-0-1	308.0432	0-4-0-1	310.0474

U_2O_3	Mass	Order	Mass	Order	Mass	Order	Mass
3-0-2-0	518.0726	2-1-2-0	520.0768	1-2-2-0	522.0811	0-3-2-0	524.0853
3-0-1-1	521.0794	2-1-1-1	523.0837	1-2-1-1	525.0879	0-3-1-1	527.0922
3-0-0-2	524.0863	2-1-0-2	526.0906	1-2-0-2	528.0948	0-3-0-2	530.099

U_2O_4	Mass	Order	Mass	Order	Mass	Order	Mass	Order	Mass
4-0-2-0	534.0675	3-1-2-0	536.0718	2-2-2-0	538.076	1-3-2-0	540.0802	0-4-2-0	542.0845
4-0-1-1	537.0744	3-1-1-1	539.0786	2-2-1-1	541.0829	1-3-1-1	543.0871	0-4-1-1	545.0913
4-0-0-2	540.0812	3-1-0-2	542.0855	2-2-0-2	544.0897	1-3-0-2	546.094	0-4-0-2	546.094

U_2O_5	Mass	Order	Mass	Order	Mass
5-0-2-0	550.0624	4-1-2-0	552.0667	3-2-2-0	554.0709
2-3-2-0	556.0752	1-4-2-0	558.0794	0-5-2-0	560.0836
5-0-1-1	553.0693	4-1-1-1	555.0735	3-2-1-1	557.0778
2-3-1-1	559.082	1-4-1-1	561.0863	0-5-1-1	563.0905
5-0-0-2	556.0761	4-1-0-2	558.0804	3-2-0-2	560.0846
2-3-0-2	562.0889	1-4-0-2	562.0889	0-5-0-2	564.0931

U_3O_3	Mass	Order	Mass	Order	Mass	Order	Mass
3-0-3-0	753.1165	2-1-3-0	755.1208	1-2-3-0	757.125	0-3-3-0	759.1293
3-0-2-1	756.1234	2-1-2-1	758.1276	1-2-2-1	760.1319	0-3-2-1	762.1361
3-0-1-2	759.1302	2-1-1-2	761.1345	1-2-1-2	763.1387	0-3-1-2	765.143
3-0-0-3	762.1371	2-1-0-3	764.1413	1-2-0-3	766.1456	0-3-0-3	768.1498

U_30_4	Mass	Order	Mass	Order	Mass	Order	Mass	Order	Mass
4-0-3-0	769.1114	3-1-3-0	771.1157	2-2-3-0	773.1199	1-3-3-0	775.1242	0-4-3-0	777.1284
4-0-2-1	772.1183	3-1-2-1	774.1225	2-2-2-1	776.1268	1-3-2-1	778.131	0-4-2-1	780.1353
4-0-1-2	775.1251	3-1-1-2	777.1294	3-1-1-2	779.1336	1-3-1-2	781.1379	0-4-1-2	783.1421
4-0-0-3	778.132	3-1-0-3	780.1363	3-1-0-3	782.1405	1-3-0-3	784.1447	0-4-0-3	786.149

U_3O_5	Mass	Order	Mass	Order	Mass
5-0-3-0	785.1063	4-1-3-0	787.1106	3-2-3-0	789.1148
2-3-3-0	791.1191	1-4-3-0	793.1233	0-5-3-0	795.1276
5-0-2-1	788.1132	4-1-2-1	790.1174	3-2-2-1	792.1217
2-3-2-1	794.1259	1-4-2-1	796.1302	0-5-2-1	798.1344
5-0-1-2	791.1201	4-1-1-2	793.1243	3-2-1-2	795.1286
2-3-1-2	797.1328	1-4-1-2	799.137	0-5-1-2	801.1413
5-0-0-3	794.1269	4-1-0-3	796.1312	3-2-0-3	798.1354
2-3-0-3	800.1397	1-4-0-3	802.1439	0-5-0-3	804.1481

U_3O_6	Mass	Order	Mass	Order	Mass	Order	Mass
6-0-3-0	801.1013	5-1-3-0	803.1055	4-2-3-0	805.1097	3-3-3-0	807.114
2-4-3-0	809.1182	1-5-3-0	811.1225	0-6-3-0	813.1267		
6-0-2-1	804.1081	5-1-2-1	806.1124	4-2-2-1	808.1166	3-3-2-1	810.1209
2-4-2-1	812.1251	1-5-2-1	814.1293	0-6-2-1	816.1336		
6-0-1-2	807.115	5-1-1-2	809.1192	4-2-1-2	811.1235	3-3-1-2	813.1277
2-4-1-2	815.132	1-5-1-2	817.1362	0-6-1-2	819.1405		
6-0-0-3	810.1218	5-1-0-3	812.1261	4-2-0-3	814.1303	3-2-0-3	816.1346
2-4-0-3	818.1388	1-5-0-3	820.1431	0-6-0-3	822.1473		

U_3O_7	Mass	Order	Mass	Order	Mass	Order	Mass
7-0-3-0	817.0962	6-1-3-0	819.1004	5-2-3-0	821.1047	4-3-3-0	823.1089
3-4-3-0	825.1132	2-5-3-0	827.1174	1-6-3-0	829.1216	0-7-3-0	831.1259
7-0-2-1	820.103	6-1-2-1	822.1073	5-2-2-1	824.1115	4-3-2-1	826.1158
3-4-2-1	828.12	2-5-2-1	830.1243	1-6-2-1	832.1285	0-7-2-1	834.1328
7-0-1-2	823.1099	6-1-1-2	825.1141	5-2-1-2	827.1184	4-3-1-2	829.1226
3-4-1-2	831.1269	2-5-1-2	833.1311	1-6-1-2	835.1354	0-7-1-2	837.1396
7-0-0-3	826.1168	6-1-0-3	828.121	5-2-0-3	830.1252	4-3-0-3	832.1295
3-4-0-3	834.1337	2-5-0-3	836.138	1-6-0-3	838.1422	0-7-0-3	840.1465

U_4O_6	Mass	Order	Mass	Order	Mass	Order	Mass
6-0-4-0	1036.145	5-1-4-0	1038.149	4-2-4-0	1040.154	3-3-4-0	1042.158
2-4-4-0	1044.162	1-5-4-0	1046.166	0-6-4-0	1048.171		
6-0-3-1	1039.152	5-1-3-1	1041.156	4-2-3-1	1043.161	3-3-3-1	1045.165
2-4-3-1	1047.169	1-5-3-1	1049.173	0-6-3-1	1051.178		
6-0-2-2	1042.159	5-1-2-2	1044.163	4-2-2-2	1046.167	3-3-2-2	1048.172
2-4-2-2	1050.176	1-5-2-2	1052.18	0-6-2-2	1054.184		
6-0-1-3	1045.166	5-1-1-3	1047.17	4-2-1-3	1049.174	3-3-1-3	1051.178
2-4-1-3	1053.183	1-5-1-3	1055.187	0-6-1-3	1057.191		
6-0-0-4	1048.173	5-1-0-4	1050.177	4-2-0-4	1052.181	3-3-0-4	1054.185
2-4-0-4	1056.19	1-5-0-4	1058.194	0-6-0-4	1060.198		

U_4O_7	Mass	Order	Mass	Order	Mass	Order	Mass
7-0-4-0	1052.14	6-1-4-0	1054.144	5-2-4-0	1056.149	4-3-4-0	1058.153
3-4-4-0	1060.157	2-5-4-0	1062.161	1-6-4-0	1064.166	0-7-4-0	1066.17
7-0-3-1	1055.147	6-1-3-1	1057.151	5-2-3-1	1059.155	4-3-3-1	1061.16
3-4-3-1	1063.164	2-5-3-1	1065.168	1-6-3-1	1067.172	0-7-3-1	1069.177
7-0-2-2	1058.154	6-1-2-2	1060.158	5-2-2-2	1062.162	4-3-2-2	1064.167
3-4-2-2	1066.171	2-5-2-2	1068.175	1-6-2-2	1070.179	0-7-2-2	1072.184
7-0-1-3	1061.161	6-1-1-3	1063.165	5-2-1-3	1065.169	4-3-1-3	1067.173
3-4-1-3	1069.178	2-5-1-3	1071.182	1-6-1-3	1073.186	0-7-1-3	1075.19
7-0-0-4	1064.168	6-1-0-4	1066.172	5-2-0-4	1068.176	4-3-0-4	1070.18
3-4-0-4	1072.185	2-5-0-4	1074.189	1-6-0-4	1076.193	0-7-0-4	1078.197

U_4O_8	Mass	Order	Mass	Order	Mass	Order	Mass	Order	Mass
8-0-4-0	1068.135	7-1-4-0	1070.139	6-2-4-0	1072.144	5-3-4-0	1074.148	4-4-4-0	1076.152
3-5-4-0	1078.156	2-6-4-0	1080.16	1-7-4-0	1082.165	0-8-4-0	1084.169		
8-0-3-1	1071.142	7-1-3-1	1073.146	6-2-3-1	1075.15	5-3-3-1	1077.155	4-4-3-1	1079.159
3-5-3-1	1081.163	2-6-3-1	1083.167	1-7-3-1	1085.172	0-8-3-1	1087.176		
8-0-2-2	1074.149	7-1-2-2	1076.153	6-2-2-2	1078.157	5-3-2-2	1080.161	4-1-2-2	1082.166
3-5-2-2	1084.17	2-6-2-2	1086.174	1-7-2-2	1088.178	0-8-2-2	1090.183		
8-0-1-3	1077.156	7-1-1-3	1079.16	6-2-1-3	1081.164	5-3-1-3	1083.168	4-1-1-3	1085.173
3-5-1-3	1087.177	2-6-1-3	1089.181	1-7-1-3	1091.185	0-8-1-3	1093.19		
8-0-0-4	1080.162	7-1-0-4	1082.167	6-2-0-4	1084.171	5-3-0-4	1086.175	5-3-0-4	1088.179
3-5-0-4	1090.184	2-6-0-4	1092.188	1-7-0-4	1094.192	0-8-0-4	1096.196		

U_4O_9	Mass	Order	Mass	Order	Mass	Order	Mass	Order	Mass
9-0-4-0	1084.13	8-1-4-0	1086.134	7-2-4-0	1088.138	6-3-4-0	1090.143	5-4-4-0	1092.147
4-5-4-0	1094.151	3-6-4-0	1096.155	2-7-4-0	1098.16	1-8-4-0	1100.164	0-9-4-0	1102.168
9-0-3-1	1087.137	8-1-3-1	1089.141	7-2-3-1	1091.145	6-3-3-1	1093.15	5-4-3-1	1095.154
4-5-3-1	1097.158	3-6-3-1	1099.162	2-7-3-1	1101.167	1-8-3-1	1103.171	0-9-3-1	1105.175
9-0-2-2	1090.144	8-1-2-2	1092.148	7-2-2-2	1094.152	6-3-2-2	1096.156	5-4-2-2	1098.161
4-5-2-2	1084.17	3-6-2-2	1102.169	2-7-2-2	1104.173	1-8-2-2	1106.178	0-9-2-2	1108.182
9-0-1-3	1093.151	8-1-1-3	1095.155	7-2-1-3	1097.159	6-3-1-3	1099.163	5-4-1-3	1101.167
4-5-1-3	1103.172	3-6-1-3	1105.176	2-7-1-3	1107.18	1-8-1-3	1109.184	0-9-1-3	1111.189
9-0-0-4	1096.157	8-1-0-4	1098.162	7-2-0-4	1100.166	6-3-0-4	1102.17	5-4-0-4	1104.174
4-5-0-4	1106.179	3-6-0-4	1108.183	2-7-0-4	1110.187	1-8-0-4	1112.191	0-9-0-4	1114.196

Table 33 . Peak list of all possible combinations of isotopes for various uranium oxide ions separated by mass.

Order	Mass	Order	Mass	Order	Mass	Order	Mass
1-0-1-0	251.0388377	4-0-0-3	778.1320062	0-7-0-3	840.1464706	6-2-4-0	1072.143501
0-1-1-0	253.0430835	3-1-1-2	779.1336383	4-4-3-0	841.1080693	0-7-2-2	1072.183534
1-0-0-1	254.0456972	0-4-2-1	780.1352704	7-1-1-2	841.1090509	3-4-0-4	1072.184516
0-1-0-1	256.049943	3-1-0-3	780.136252	5-3-2-1	842.110683	7-1-3-1	1073.146115
2-0-1-0	267.0337523	1-3-1-2	781.1378841	8-0-0-3	842.1116646	1-6-1-3	1073.186148
1-1-1-0	269.0379981	3-1-0-3	782.1404978	3-5-3-0	843.1123151	5-3-4-0	1074.147747
2-0-0-1	270.0406118	0-4-1-2	783.1421299	6-2-1-2	843.1132967	8-0-2-2	1074.148728
0-2-1-0	271.0422439	1-3-0-3	784.1447436	4-4-2-1	844.1149288	2-5-0-4	1074.188762
1-1-0-1	272.0448576	5-0-3-0	785.1063423	7-1-0-3	844.1159104	6-2-3-1	1075.15036
0-2-0-1	274.0491034	0-4-0-3	786.1489894	2-6-3-0	845.1165609	0-7-1-3	1075.190394
3-0-1-0	283.0286669	4-1-3-0	787.1105881	5-3-1-2	845.1175425	4-4-4-0	1076.151992
2-1-1-0	285.0329127	5-0-2-1	788.1132018	3-5-2-1	846.1191746	7-1-2-2	1076.152974

3-0-0-1	286.0355264	3-2-3-0	789.1148339	6-2-0-3	846.1201562	1-6-0-4	1076.193007
1-2-1-0	287.0371585	4-1-2-1	790.1174476	1-7-3-0	847.1208067	5-3-3-1	1077.154606
2-1-0-1	288.0397722	2-3-3-0	791.1190797	4-4-1-2	847.1217883	8-0-1-3	1077.155588
0-3-1-0	289.0414043	5-0-1-2	791.1200613	2-6-2-1	848.1234204	3-5-4-0	1078.156238
1-2-0-1	290.044018	3-2-2-1	792.1216934	5-3-0-3	848.124402	6-2-2-2	1078.15722
0-3-0-1	292.0482638	1-4-3-0	793.1233255	0-8-3-0	849.1250525	0-7-0-4	1078.197253
4-0-1-0	299.0235815	4-1-1-2	793.1243071	3-5-1-2	849.1260341	4-4-3-1	1079.158852
3-1-1-0	301.0278273	2-3-2-1	794.1259392	1-7-2-1	850.1276662	7-1-1-3	1079.159834
4-0-0-1	302.030441	5-0-0-3	794.1269208	4-4-0-3	850.1286478	2-6-4-0	1080.160484
2-2-1-0	303.0320731	0-5-3-0	795.1275713	2-6-1-2	851.1302799	5-3-2-2	1080.161466
3-1-0-1	304.0346868	3-2-1-2	795.1285529	0-8-2-1	852.131912	8-0-0-4	1080.162447
1-3-1-0	305.0363189	1-4-2-1	796.130185	3-5-0-3	852.1328936	3-5-3-1	1081.163098
2-2-0-1	306.0389326	4-1-0-3	796.1311666	1-7-1-2	853.1345257	6-2-1-3	1081.164079
0-4-1-0	307.0405647	2-3-1-2	797.1327987	2-6-0-3	854.1371394	1-7-4-0	1082.16473
1-3-0-1	308.0431784	0-5-2-1	798.1344308	0-8-1-2	855.1387715	4-1-2-2	1082.165711
0-4-0-1	310.0474242	3-2-0-3	798.1354124	1-7-0-3	856.1413852	7-1-0-4	1082.166693
3-0-2-0	518.07259	1-4-1-2	799.1370445	0-8-0-3	858.145631	2-6-3-1	1083.167344
2-1-2-0	520.0768358	2-3-0-3	800.1396582	6-0-4-0	1036.14518	5-3-1-3	1083.168325
3-0-1-1	521.0794495	6-0-3-0	801.1012569	5-1-4-0	1038.149426	9-0-4-0	1084.129924
1-2-2-0	522.0810816	0-5-1-2	801.1412903	6-0-3-1	1039.15204	0-8-4-0	1084.168976
2-1-1-1	523.0836953	1-4-0-3	802.143904	4-2-4-0	1040.153672	3-5-2-2	1084.169957
0-3-2-0	524.0853274	5-1-3-0	803.1055027	5-1-3-1	1041.156285	4-5-2-2	1084.169957
3-0-0-2	524.086309	6-0-2-1	804.1081164	3-3-4-0	1042.157917	6-2-0-4	1084.170939
1-2-1-1	525.0879411	0-5-0-3	804.1481498	6-0-2-2	1042.158899	1-7-3-1	1085.171589
2-1-0-2	526.0905548	4-2-3-0	805.1097485	4-2-3-1	1043.160531	4-1-1-3	1085.172571
0-3-1-1	527.0921869	5-1-2-1	806.1123622	2-4-4-0	1044.162163	8-1-4-0	1086.13417
1-2-0-2	528.0948006	3-3-3-0	807.1139943	5-1-2-2	1044.163145	2-6-2-2	1086.174203
0-3-0-2	530.0990464	6-0-1-2	807.1149759	3-3-3-1	1045.164777	5-3-0-4	1086.175185
4-0-2-0	534.0675046	4-2-2-1	808.116608	6-0-1-3	1045.165759	9-0-3-1	1087.136783
3-1-2-0	536.0717504	2-4-3-0	809.1182401	1-5-4-0	1046.166409	0-8-3-1	1087.175835
4-0-1-1	537.0743641	5-1-1-2	809.1192217	4-2-2-2	1046.167391	3-5-1-3	1087.176817
2-2-2-0	538.0759962	3-3-2-1	810.1208538	2-4-3-1	1047.169023	7-2-4-0	1088.138415
3-1-1-1	539.0786099	6-0-0-3	810.1218354	5-1-1-3	1047.170004	1-7-2-2	1088.178449
1-3-2-0	540.080242	1-5-3-0	811.1224859	0-6-4-0	1048.170655	5-3-0-4	1088.17943
4-0-0-2	540.0812236	4-2-1-2	811.1234675	3-3-2-2	1048.171636	8-1-3-1	1089.141029
2-2-1-1	541.0828557	2-4-2-1	812.1250996	6-0-0-4	1048.172618	2-6-1-3	1089.181063
0-4-2-0	542.0844878	5-1-0-3	812.1260812	1-5-3-1	1049.173269	6-3-4-0	1090.142661
3-1-0-2	542.0854694	0-6-3-0	813.1267317	4-2-1-3	1049.17425	9-0-2-2	1090.143643
1-3-1-1	543.0871015	3-3-1-2	813.1277133	2-4-2-2	1050.175882	0-8-2-2	1090.182695

2-2-0-2	544.0897152	1-5-2-1	814.1293454	5-1-0-4	1050.176864	3-5-0-4	1090.183676
0-4-1-1	545.0913473	4-2-0-3	814.130327	0-6-3-1	1051.177514	7-2-3-1	1091.145275
1-3-0-2	546.093961	2-4-1-2	815.1319591	3-3-1-3	1051.178496	1-7-1-3	1091.185308
0-4-0-2	546.093961	0-6-2-1	816.1335912	7-0-4-0	1052.140095	5-4-4-0	1092.146907
5-0-2-0	550.0624192	3-2-0-3	816.1345728	1-5-2-2	1052.180128	8-1-2-2	1092.147889
4-1-2-0	552.066665	7-0-3-0	817.0961715	4-2-0-4	1052.18111	2-6-0-4	1092.187922
5-0-1-1	553.0692787	1-5-1-2	817.1362049	2-4-1-3	1053.182742	6-3-3-1	1093.149521
3-2-2-0	554.0709108	2-4-0-3	818.1388186	6-1-4-0	1054.14434	9-0-1-3	1093.150502
4-1-1-1	555.0735245	6-1-3-0	819.1004173	0-6-2-2	1054.184374	0-8-1-3	1093.189554
2-3-2-0	556.0751566	0-6-1-2	819.1404507	3-3-0-4	1054.185355	4-5-4-0	1094.151153
5-0-0-2	556.0761382	7-0-2-1	820.103031	7-0-3-1	1055.146954	7-2-2-2	1094.152134
3-2-1-1	557.0777703	1-5-0-3	820.1430644	1-5-1-3	1055.186988	1-7-0-4	1094.192168
1-4-2-0	558.0794024	5-2-3-0	821.1046631	5-2-4-0	1056.148586	5-4-3-1	1095.153767
4-1-0-2	558.080384	6-1-2-1	822.1072768	2-4-0-4	1056.189601	8-1-1-3	1095.154748
2-3-1-1	559.0820161	0-6-0-3	822.1473102	6-1-3-1	1057.1512	3-6-4-0	1096.155399
0-5-2-0	560.0836482	4-3-3-0	823.1089089	0-6-1-3	1057.191233	6-3-2-2	1096.15638
3-2-0-2	560.0846298	7-0-1-2	823.1098905	4-3-4-0	1058.152832	9-0-0-4	1096.157362
1-4-1-1	561.0862619	5-2-2-1	824.1115226	7-0-2-2	1058.153814	0-8-0-4	1096.196414
2-3-0-2	562.0888756	3-4-3-0	825.1131547	1-5-0-4	1058.193847	4-5-3-1	1097.158012
1-4-0-2	562.0888756	6-1-1-2	825.1141363	5-2-3-1	1059.155446	7-2-1-3	1097.158994
0-5-1-1	563.0905077	4-3-2-1	826.1157684	3-4-4-0	1060.157078	2-7-4-0	1098.159644
0-5-0-2	564.0931214	7-0-0-3	826.11675	6-1-2-2	1060.158059	5-4-2-2	1098.160626
3-0-3-0	753.1165131	2-5-3-0	827.1174005	0-6-0-4	1060.198093	8-1-0-4	1098.161608
2-1-3-0	755.1207589	5-2-1-2	827.1183821	4-3-3-1	1061.159692	3-6-3-1	1099.162258
3-0-2-1	756.1233726	3-4-2-1	828.1200142	7-0-1-3	1061.160673	6-3-1-3	1099.16324
1-2-3-0	757.1250047	6-1-0-3	828.1209958	2-5-4-0	1062.161324	1-8-4-0	1100.16389
2-1-2-1	758.1276184	1-6-3-0	829.1216463	5-2-2-2	1062.162305	7-2-0-4	1100.165853
0-3-3-0	759.1292505	4-3-1-2	829.1226279	3-4-3-1	1063.163937	2-7-3-1	1101.166504
3-0-1-2	759.1302321	2-5-2-1	830.12426	6-1-1-3	1063.164919	5-4-1-3	1101.167486
1-2-2-1	760.1318642	5-2-0-3	830.1252416	1-6-4-0	1064.165569	0-9-4-0	1102.168136
2-1-1-2	761.1344779	0-7-3-0	831.1258921	4-3-2-2	1064.166551	3-6-2-2	1102.169118
0-3-2-1	762.13611	3-4-1-2	831.1268737	7-0-0-4	1064.167533	6-3-0-4	1102.170099
3-0-0-3	762.1370916	1-6-2-1	832.1285058	2-5-3-1	1065.168183	1-8-3-1	1103.17075
1-2-1-2	763.1387237	4-3-0-3	832.1294874	5-2-1-3	1065.169165	4-5-1-3	1103.171731
2-1-0-3	764.1413374	8-0-3-0	833.0910861	0-7-4-0	1066.169815	2-7-2-2	1104.173363
0-3-1-2	765.1429695	2-5-1-2	833.1311195	3-4-2-2	1066.170797	5-4-0-4	1104.174345
1-2-0-3	766.1455832	0-7-2-1	834.1327516	6-1-0-4	1066.171778	0-9-3-1	1105.174996
0-3-0-3	768.149829	3-4-0-3	834.1337332	1-6-3-1	1067.172429	3-6-1-3	1105.175977
4-0-3-0	769.1114277	7-1-3-0	835.0953319	4-3-1-3	1067.173411	1-8-2-2	1106.177609

3-1-3-0	771.1156735	1-6-1-2	835.1353653	8-0-4-0	1068.135009	4-5-0-4	1106.178591
4-0-2-1	772.1182872	8-0-2-1	836.0979456	2-5-2-2	1068.175043	2-7-1-3	1107.180223
2-2-3-0	773.1199193	2-5-0-3	836.137979	5-2-0-4	1068.176024	0-9-2-2	1108.181855
3-1-2-1	774.122533	6-2-3-0	837.0995777	0-7-3-1	1069.176675	3-6-0-4	1108.182837
1-3-3-0	775.1241651	0-7-1-2	837.1396111	3-4-1-3	1069.177656	1-8-1-3	1109.184469
4-0-1-2	775.1251467	7-1-2-1	838.1021914	7-1-4-0	1070.139255	2-7-0-4	1110.187082
2-2-2-1	776.1267788	1-6-0-3	838.1422248	1-6-2-2	1070.179288	0-9-1-3	1111.188715
0-4-3-0	777.1284109	5-3-3-0	839.1038235	4-3-0-4	1070.18027	1-8-0-4	1112.191328
3-1-1-2	777.1293925	8-0-1-2	839.1048051	8-0-3-1	1071.141869	0-9-0-4	1114.195574
1-3-2-1	778.1310246	6-2-2-1	840.1064372	2-5-1-3	1071.181902		

Appendix O. Hydrocarbon Intensity Calculations

This appendix contains values for each the intensities for the 259^+, 260^+, 261^+, 304^+, 308^+, and 318^+ peaks. Averages and standard deviations were calculated for each sample. All of the results are provided in Table 34.

Table 34. Hydrocarbon intensities, average values, and standard deviations for selected samples.

Sample	Natural UO_3	Depleted U_3O_8	Natural UO_3	Natural U_3O_8	Enriched U_3O_8	Enriched U_3O_8
Cts. 259	83509	275263	104386	18964	11119	53431
Cts. 260	85298	280492	108622	19925	11732	56350
Cts. 261	84232	276543	105290	19434	11278	54240
Cts. 304	76393	266428	94241	17637	3820	50688
Cts. 308	79238	271268	98047	18180	5995	52997
Cts. 318	75201	267910	95501	17862	4906	48562
Avg.	80645.17	272984	101014.5	18667	11376.33	52711.33
σ	4299.204	5401.882	5875.475	917.0775	318.1106	2738.141

Appendix P. Assumptions

It was assumed that the counts in each of the peaks are Poisson distributed with a standard deviation equal to the square root of the number of counts. This assumption was based upon the fact that the relative error is small. The maximum error from any of the peaks was calculated to be 3,055. All of the peak intensities used for data analysis were well above this level therefore, the assumption is justified.

There were two assumptions made in regards to the TOF-SIMS instrument used for this research:

1. The mass analyzer does not have a mass bias and that ion intensities are directly related to the number of ions that struck the detector.
2. The spectra are constructed from the total ion count for each peak of interest with no fitting algorithm applied.

Both of these assumptions were later verified through contact with the instrument manufacturer.

Appendix Q. Determination of α, β, and γ Values

This appendix contains the table of values of ion intensities used in Matlab code to determine values of α, β, and γ.

Table 35. Ion intensities used in Matlab code to determine α, β, and γ values for each sample.

Depleted UO_2	UO^+
Mass	Intensity
270	7023521
254	3088398
255	498041
256	48043

Depleted UO_2	UO_2^+
Mass	Intensity
270	7023521
271	1781410
271	193926

Depleted UO_2	UO_3^+
Mass	Intensity
270	7023521
286	26731
287	181404
288	65238
289	112797

Natural UO_3	UO^+
Mass	Intensity
270	1842164
254	834232
255	98755
256	6912

Natural UO_3	UO_2^+
Mass	Intensity
270	1842164
271	287863
271	25899

Natural UO_3	UO_3^+
Mass	Intensity
270	1842164
286	6460
287	36903
288	11411
289	17798

Depleted U_3O_8	UO^+
Mass	Intensity
270	11988435
254	4386772
255	503340
256	31212

Depleted U_3O_8	UO_2^+
Mass	Intensity
270	11988435
271	2435970
271	211782

Depleted U_3O_8	UO_3^+
Mass	Intensity
270	11988435
286	33837
287	271923
288	26417
289	46430

Depleted U_3O_8	UO^+
Mass	Intensity
270	15342830
254	9890311
255	1018851

Depleted U_3O_8	UO_2^+
Mass	Intensity
270	15342830
271	3834661
271	465272

Depleted U_3O_8	UO_3^+
Mass	Intensity
270	15342830
286	108148
287	515988

256	58728

288	35448
289	63853

Natural UO_3	UO^+
Mass	Intensity
270	9960259
254	3484409
255	426512
256	33283

Natural UO_3	UO_2^+
Mass	Intensity
270	9960259
271	2206992
271	187675

Natural UO_3	UO_3^+
Mass	Intensity
270	9960259
286	28492
287	247091
288	36312
289	41990

Natural U_30_8	UO^+
Mass	Intensity
270	3231374
254	1095084
255	8443
256	4402

Natural U_30_8	UO_2^+
Mass	Intensity
270	3231374
271	1367772
271	124836

Natural U_30_8	UO_3^+
Mass	Intensity
270	3231374
286	8783
287	18215
288	3922
289	4903

Enriched U_30_8	UO^+
Mass	Intensity
270	2241281
254	912844
255	66608
256	5134

Enriched U_30_8	UO_2^+
Mass	Intensity
270	2241281
271	248020
271	45555

Enriched U_30_8	UO_3^+
Mass	Intensity
270	2241281
286	11197
287	32738
288	4900
289	10319

Enriched U_30_8	UO^+
Mass	Intensity
270	1232067
254	301192
255	29089
256	1621

Enriched U_30_8	UO_2^+
Mass	Intensity
270	1232067
271	116250
271	22586

Enriched U_30_8	UO_3^+
Mass	Intensity
270	1232067
286	11992
287	16017
288	2764
289	4516

Appendix R. Gaussian Curves for All Samples

This appendix contains the information used to calculate oxidation state values for each of the samples. Table 36 provides all of the values used to create Gaussian curves for each of the samples. Each of the curves generated by Sigmaplot is also provided in Figures 54-61.

Table 36. Values used to generate Gaussian curves for oxidation state calculations.

Sample	Depleted UO_2	Natural UO_3	Depleted U_3O_8	Depleted U_3O_8	Natural UO_3	Natural U_30_8	Enriched U_30_8	Enriched U_30_8
UO	2376	1746	1223	912	2633	1627	350	1697
$U0_2$	27695	19403	21962	3716	28236	17975	2160	5238
UO_3	209651	335705	321172	33978	533727	123684	31298	48992
UO_4	47271	195007	93772	10029	199398	24415	15121	21638
U_2O_4	374	167	102	117	307	760	155	149
U_2O_5	2065	1242	6091	616	2109	4453	260	216
U_2O_6	10207	14412	27440	3300	23500	8667	1082	4041
U_2O_7	311	185	741	160	354	960	140	189
U_3O_5	15381	44211	20578	1414	8359	4305	263	5448
U_3O_6	61557	242848	160619	6397	51387	32200	1285	32647
U_3O_7	33269	144228	98391	5381	41593	14788	1086	24377
U_3O_8	777	3630	2482	438	2268	330	104	1064
K (UO_y)	5.01	5.68	5.21	5.11	5.49	4.97	5.58	5.49
K (U_2O_y)	5.25	5.22	5.28	5.31	5.34	5.19	5.31	5.45
G-	5.13	5.45	5.245	5.21	5.415	5.08	5.445	5.47
K (U_3O_y)	3.82	3.85	3.83	3.94	3.93	3.83	3.95	3.91
K Average	4.48	4.65	4.54	4.58	4.67	4.46	4.70	4.69

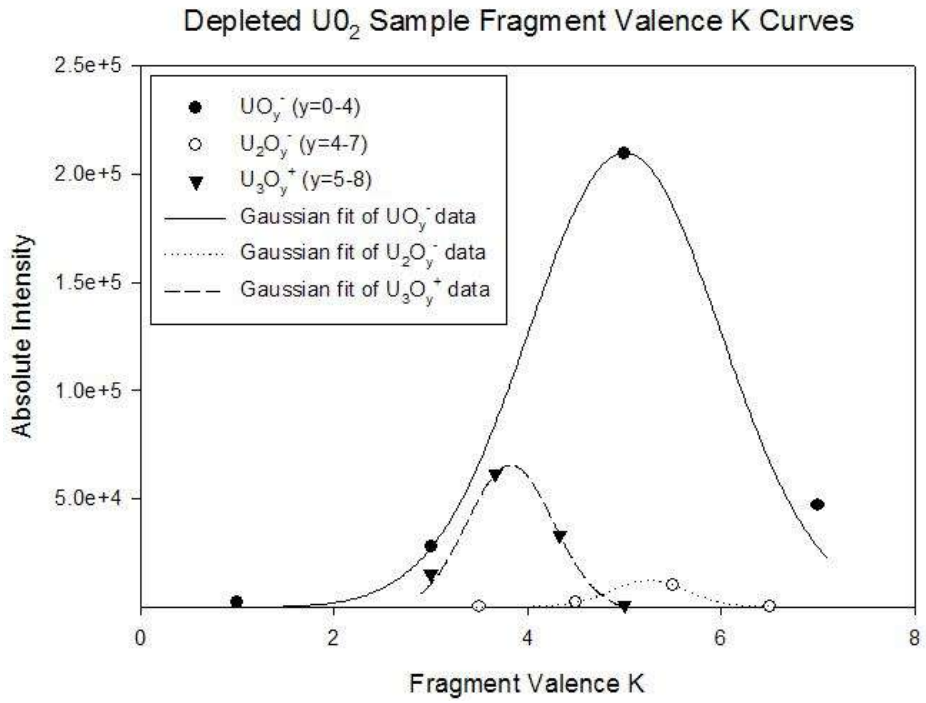

Figure 54. System of Gaussian curves used to calculate average oxidation state for a depleted UO_2 sample.

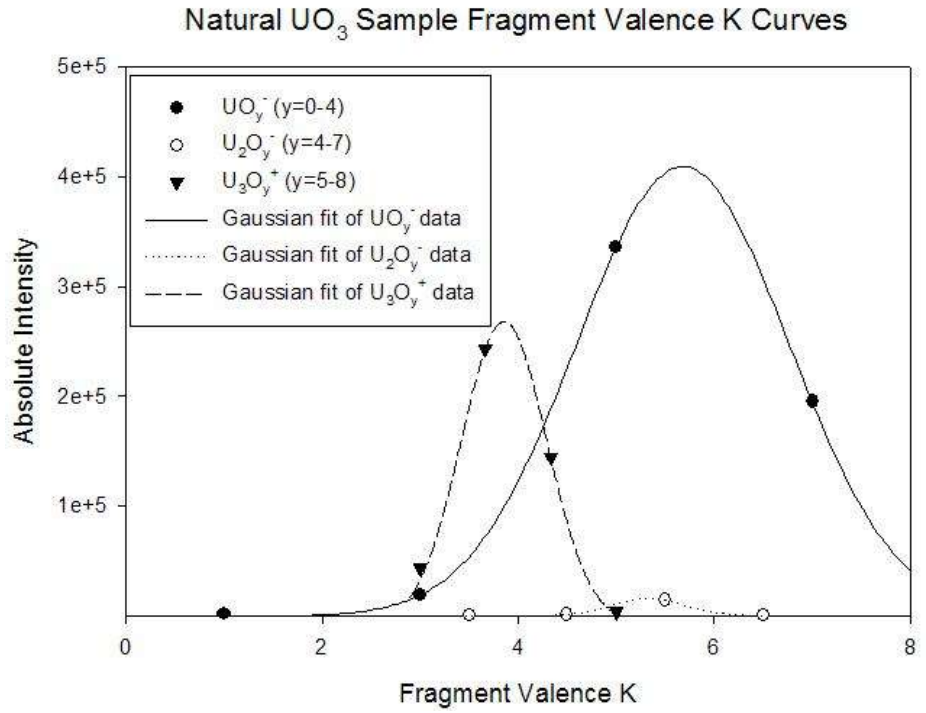

Figure 55. System of Gaussian curves used to calculate average oxidation state for a natural UO_3 sample.

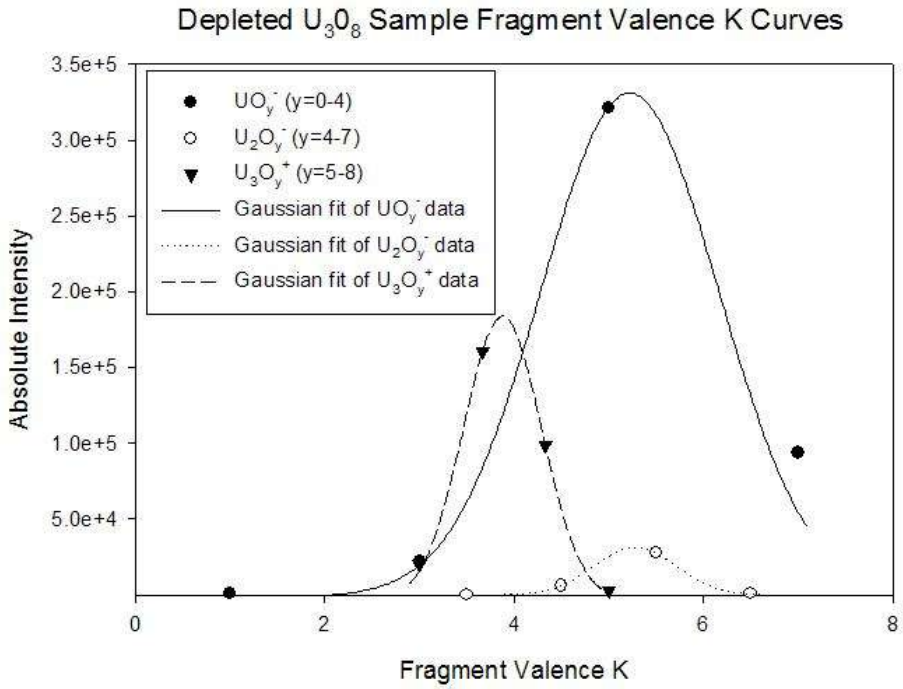

Figure 56. System of Gaussian curves used to calculate average oxidation state for a depleted U_3O_8 sample.

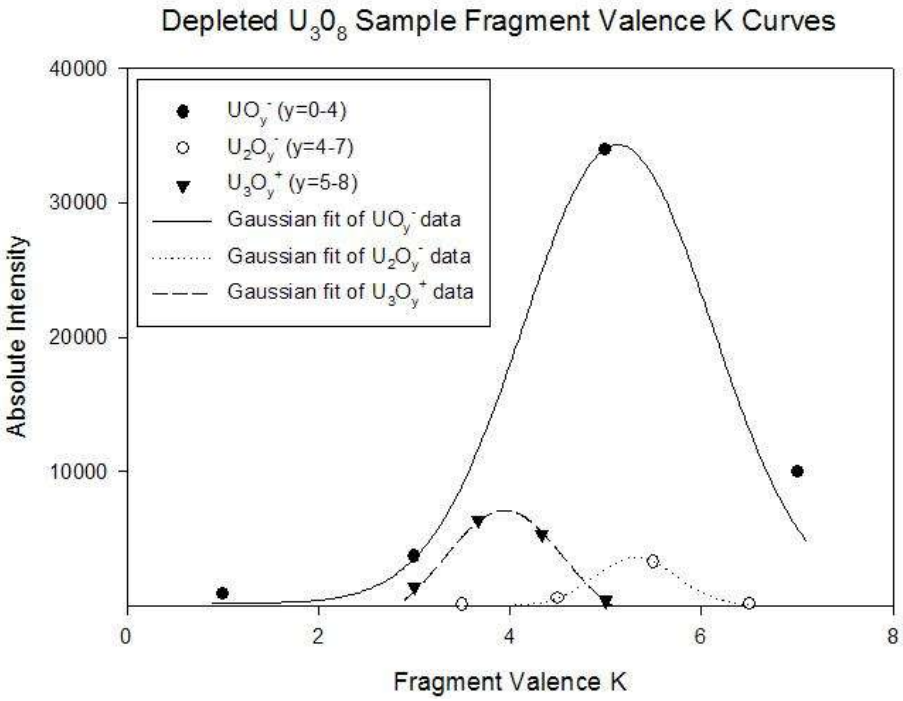

Figure 57. System of Gaussian curves used to calculate average oxidation state for a depleted U_3O_8 sample.

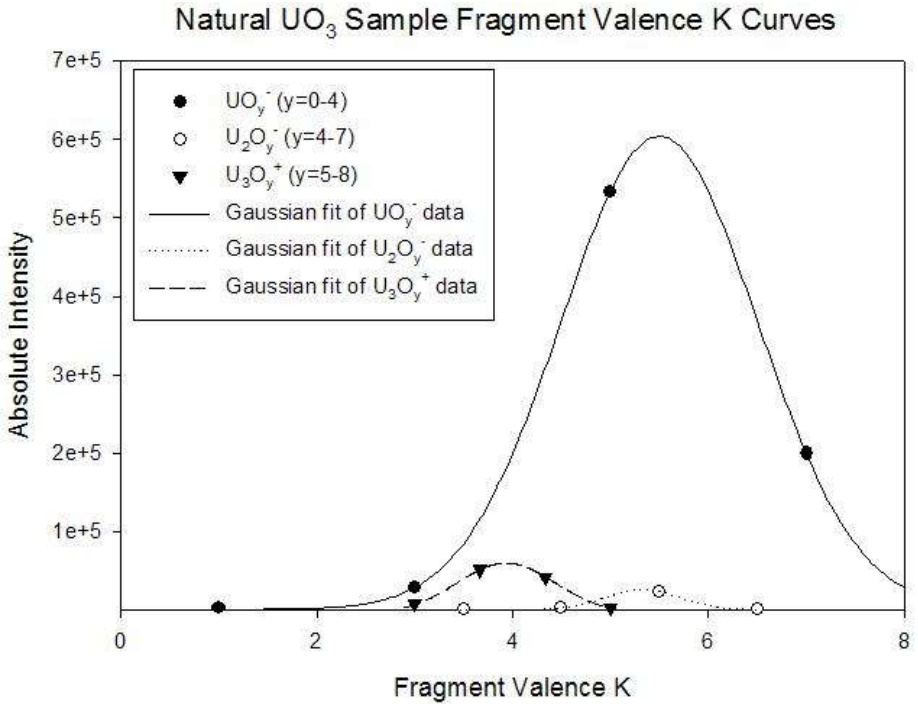

Figure 58. System of Gaussian curves used to calculate average oxidation state for a natural UO_3 sample.

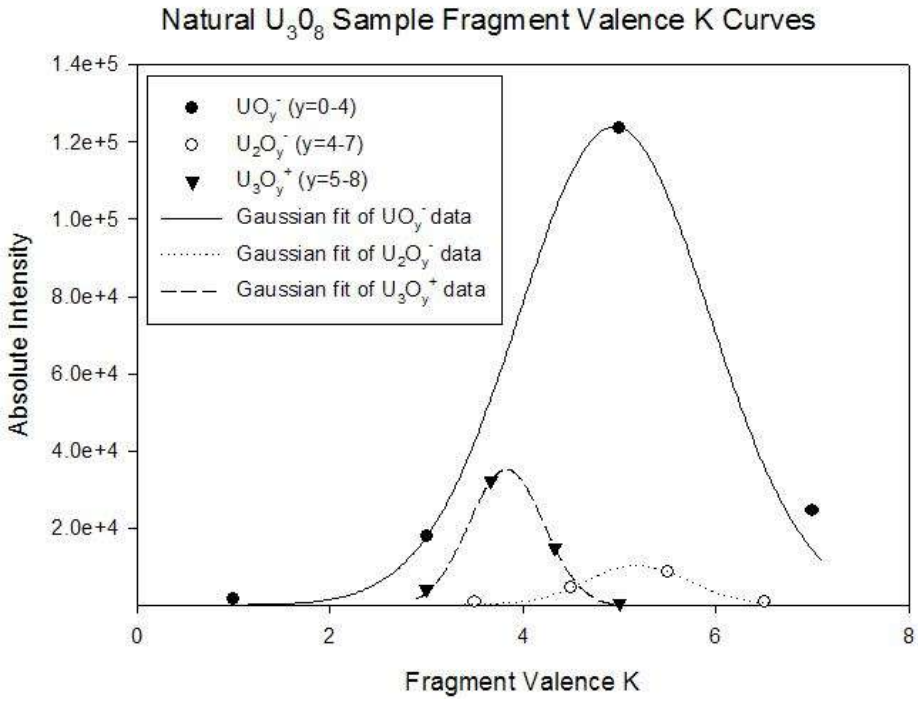

Figure 59. System of Gaussian curves used to calculate average oxidation state for a natural U_3O_8 sample.

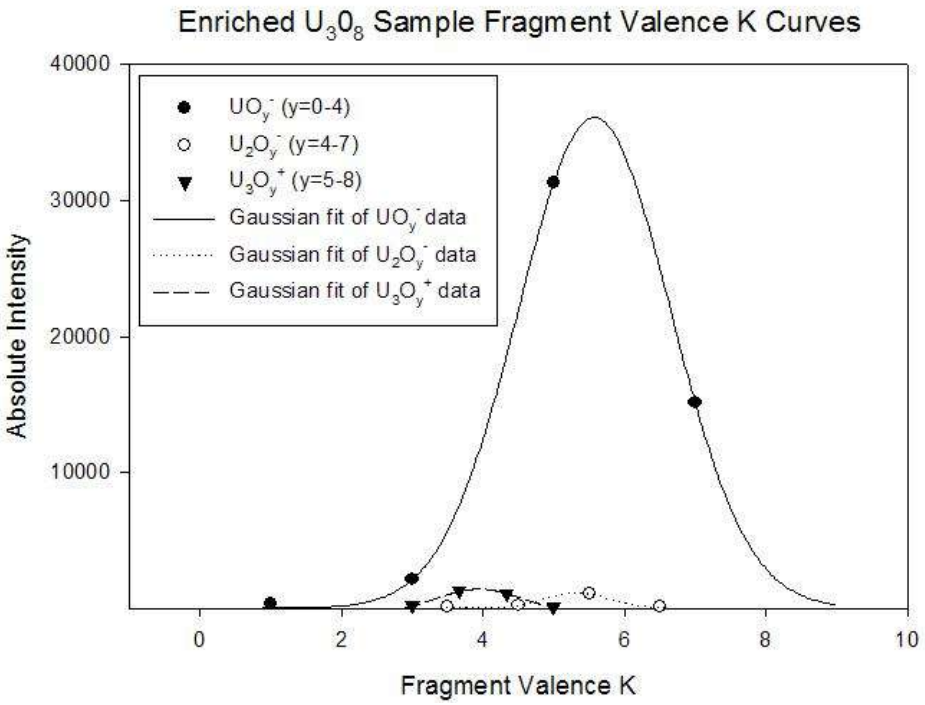

Figure 60. System of Gaussian curves used to calculate average oxidation state for an enriched U_3O_8 sample.

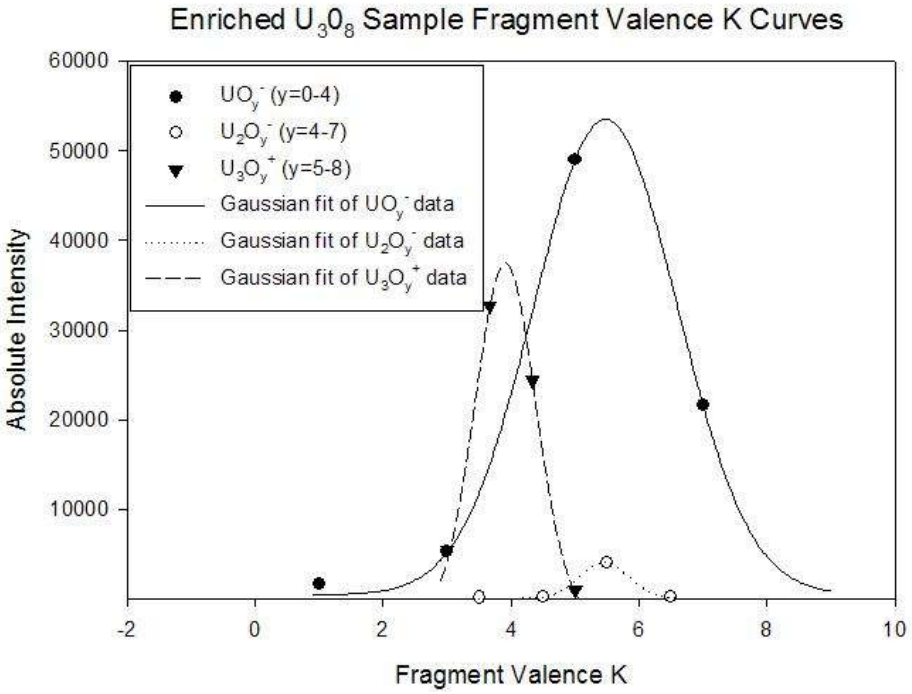

Figure 61. System of Gaussian curves used to calculate average oxidation state for an enriched U_3O_8 sample.

Appendix S. Project Schedule

This appendix contains the timeline for the research conducted in this project.

Table 37. Project schedule of research.

Timeline	Activity
22-Jun-09	Begin independent study
14-Aug-09	Literature review/outline methodology
25-Aug-09	Submit prospectus
4-Sep-09	Submit safety review for UYQT
16-Oct-09	Complete method for sample preparation
22-Oct-09	Prospectus defense
28-Oct-09	Training for use of balance
30-Oct-09	Prepare CeO_2 samples
31-Oct-09	Mass samples on balance
3-Nov-09	Collect SEM images of CeO2 samples
6-Nov-09	Training for use of alpha/beta counter and background measurements
9-Nov-09	Compute activity and mass measurements for uranium samples
10-Nov-09	Prepare uranium oxide samples
15-Nov-09	Take samples to SUNY for measurements
22-Nov-09	Return from SUNY with uranium samples
23-Nov-09	Begin data analysis
19-Jan-10	Submit draft thesis
16-Feb-10	Submit revised thesis
TBD	Defend thesis
25-Mar10	Graduation

Bibliography

Allison, Graham. "Nuclear Accountability," *Technology Review*, 108(7): 43 (July 2005).

American Physical Society. *Nuclear Forensics: Role, State of the Art, Program Needs.* Washington: GPO, 2008.

Aubriet, Frédéric, Claude Poleunis and Patrick Bertrand. "Capabilities of Static TOF-SIMS in the Differentiation of First-row Transition Metal Oxides," *Journal of Mass spectrometry*, 36:641-651 (2001).

Becker, J. Sabine and Hans-Joachim Dietze. "Inorganic Mass Spectrometric Methods for Trace, Ultratrace, Isotope, and Surface Analysis," *International Journal of Mass Spectrometry*, 197:1-35 (2000).

Becker, Johanna Sabine. "Mass Spectrometry of Long-lived Radionuclides," *Spectrochimica Acta Part B*, 58:1757-1784 (2003).

Becker, J. Sabine and Hans-Joachim Dietze. "State-of-the-art in Inorganic Mass Spectrometry for Analysis of High-purity Materials," *International Journal of Mass Spectrometry*, 228:127–150 (2003).

Benninghoven, A., Rüdenauer, F. G. and Werner, H. W. *Secondary Ion Mass Spectrometry: Basic Concepts, Instrumental Aspects, Applications and Trends.* New York: John Wiley & Sons, Inc, 1987.

Betti, Maria. "Isotope Ratio Measurements by Secondary Ion Mass Spectrometry (SIMS) and Glow Discharge Mass Spectrometry (GDMS)," *International Journal of Mass Spectrometry*, 242:169-182 (2005).

Betti, Maria, Gabriele Tamborini, and Lothar Koch. "Use of Secondary Ion Mass Spectrometry in Nuclear Forensic Analysis for the Characterization of Plutonium and Highly Enriched Uranium Particles," *Analytical Chemistry*, 71:2616-2622 (1999).

Bonino, O., O. Dugne, C. Merlet, E. Gat, Ph. Holliger and M. Lahaye. "Study of Surface Modification of Uranium and UFe_2 by Various Surface Analysis Techniques," *Journal of Nuclear Materials*, 294:305-314 (2001).

Boudjadar, S., F. Haranger, T. Jalowy, A. Robin, B. Ban d'Etat, T. Been, Ph. Boduch, H. Lebius, B. Manil, L. Maunoury, and H. Rothard. "Contribution of Ion Emission to Sputtering of Uranium Dioxide by Highly Charged Ions," *The European Physical Journal D*, 32:19-24 (2005).

Broczkowski, Michael E., R. Zhu, Z. Ding, J. J. Noël, and D. W. Shoesmith. "Electrochemical, SECM, and XPS Studies of the Influence of H_2 on UO_2 Nuclear Fuel Corrosion," *Material Research Society Symposium Proceedings*, 932:449-456 (2006).

Bürger, S., L.R. Riciputi, S. Turgeon, D. Bostick, E. McBay and M. Lavelle. "A High Efficiency Cavity Ion Source Using TIMS for Nuclear Forensic Analysis," *Journal of Alloys and Compounds*, 444-445:660-662 (2007).

Bürger, S. and L.R. Riciputi. "A Rapid Isotope Ratio Analysis Protocol for Nuclear Solid Materials Using Nano-second Laser-ablation Time-of-flight ICP-MS," *Journal of Environmental Radioactivity*, doi:10.1016/j.jenvrad.2009.07.009 (2009).

Bürger, S., L.R. Riciputi, D.A. Bostick, S. Turgeon, E.H. McBay and M. Lavelle. "Isotope Ratio Analysis of Actinides, Fission Products, and Geolocators by High-efficiency Multi-collector Thermal Ionization Mass Spectrometry," *International Journal of Mass Spectrometry*, doi:10.1016/j.ijms.2009.06.010 (2009).

Chivers, Daniel H., Bethany F. Lyles Goldblum, Brett H. Isselhardt, and Jonathan S. Snider. "Before the Day After: Using Pre-Detonation Nuclear Forensics to Improve Fissile Material Security," *Arms Control Today*, (July/August 2008). 8 January 2010 http://www.armscontrol.org/act/2008_07-08/NuclearForensics.

Christian, Gary D. *Analytical Chemistry* (4th Edition). New York: John Wiley and Sons, 1986.

Christian, Gary D. and James E. O'Reilly. *Instrumental Analysis* (2nd Edition). Newton, MA:Allyn and Bacon, Inc., 1986.

Coakley, Kevin J., David S. Simons, Andrew M. Leifer. "Secondary Ion Mass Spectrometry Measurements of Isotopic Ratios: Correction for Time Varying Count Rate," *International Journal of Mass Spectrometry*, 240:107-120 (2005).

Crompton, T. R. *Characterisation of Polymers*. Shropshire, U. K.: Smithers Rapra Technology Limited, 2008.

Cuynen, Erik, Luc Van Vaeck and Pierre Van Espen. "Speciation of Oxides with Static Secondary Ion Mass Spectrometry," *Rapid Communications in Mass Spectrometry*, 13:2287-2301 (1999).

Delegard, C. H., A. J. Schmidt, and J. W. Chenault. *Mechanical Properties of K Basin Sludge Constituents and Their Surrogates*. PNNL-14947. Pacific Northwest National Laboratory, November, 2004.

Donohue, D., A. Ciurapinski, J. Cliff III, F. Rüdenauer, T. Kuno, and J. Poths. "Microscopic Studies of Spherical Particles for Nuclear Safeguards," *Applied Surface Science*, 255:2561-2568 (2008).

Eisenbud, Merril and Thomas Gesell. *Environmental Radioactivity from Natural, Industrial, and Military Sources* (4th Edition). San Diego: Academic Press, 1997.

Erdmann, N., J.-V. Kratz, N. Trautmann, and G. Passler. "Resonance Ionization Mass Spectrometry of Ion Beam Sputtered Neutrals for Element- and Isotope-Selective Analysis of Plutonium in Micro-particles," *Analytical and Bioanalytical Chemistry*, DOI 10.1007/s00216-009-2906-6 (June, 2009).

Esaka, F., M. Magara, C.G. Lee, S. Sakurai, S. Usuda, and N. Shinohara. "Comparison of ICP-MS and SIMS Techniques for Determining Uranium Isotope Ratios in Individual Particles," *Talanta*, 78:290-294 (2009).

Esaka, Fumitaka, Kazuo Watanabe, Hiroyasu Fukuyama, Takashi Onodera, Konomi T. Esaka, Masaaki Magara, Satoshi Sakuraiand, and Shigekazu Usuda. "Efficient Isotope Ratio Analysis of Uranium Particles in Swipe Samples by Total-Reflection X-ray Fluorescence Spectrometry and Secondary Ion Mass Spectrometry," *Journal of Nuclear Science and Technology*, 41:1027-1032 (November 2004).

Esaka, F, K.T. Esaka, C.G. Lee, M. Magara, S. Sakurai, S. Usuda, and K. Watanabe. "Particle isolation for analysis of uranium minor isotopes in individual particles by secondary ion mass spectrometry," *Talanta*, 71:1011-1015 (2007).

Fahey, A. J., and S. Messenger. "Isotopic ratio measurements by time-of-flight secondary ion Mass Spectrometry," *International Journal of Mass Spectrometry*, 208:227–242 (2001).

Ferguson, Charles. "Can Nuclear Forensics Trace a Detonated Nuclear Weapon to its Source?" *Paper presented at the annual meeting of the American Political Science Association, Marriott, Loews Philadelphia, and the Pennsylvania Convention Center, Philadelphia, PA*, (Aug 31, 2006).

Fischer, David. *History of the International Atomic Energy Agency: the first Forty Years.* Vienna: The International Atomic Energy Agency (IAEA), 1997.

Francis, J.T., A. M. Brennenstü, S. Ramamurthy, and N. S. McIntyre. "Use of ToF-SIMS in the Study of Corrosion Processes: Monel 400 Steam Generator Tubing under CANDU Start-up Conditions," *Surface and Interface Analysis*, 34:189-191 (2002).

Gale Group. "The International Atomic Energy Agency (IAEA)," *Worldmark Encyclopedia of Nations*, 2007. 29 September 2009 http://www.encyclopedia.com/doc/1G2-2586700051.html.

Gerstmann, Udo C., Wilfried Szymczak, Vera Höllriegl, Wei Bo Li, Paul Roth, Peter Schramel, Shinji Takenaka And Uwe Oeh. "Investigations on the Solubility of Corrosion Products on Depleted Uranium Projectiles by Simulated Body Fluids and the Consequences on Dose Assessment," *Radiation and Environmental Biophysics*, 47(Gale, 2007):205-212 (2008).

Gibson, John K. and Richard G. Haire. "Synthesis and Investigation of Plutonium Oxide Cluster Ions: $Pu_xO_y^+$ ($x \leq 18$)," *Journal of Alloys and Compounds*, 322:143-152 (2001).

Gilbert, Richard O. *Statistical Methods for Environmental Pollution Monitoring*. New York: Van Nostrand Reinhold Co., 1987.

Gnos, Edwin, Beda A. Hofmann, All Al-Kathiri, Silvio Lorenzetti, Otto Eugster, Martin J. Whitehouse, Igor M. Villa, A. J. Timothy Jull, Jost Eikenberg, Bernhard Spettel, Urs Krähenbühl, Ian A. Franchi, Richard C. Greenwood. "Pinpointing the Source of a Lunar Meteorite: Implications for the Evolution of the Moon," *Science*, 305(5684):657-659 (July 2004).

Government Accountability Office (GAO). *United States Government Accountability Office*. GAO-09-527R. Washington: GPO, June 1, 2009.

Grant, P.M., K.J. Moody, I.D. Hutcheon, D.L. Phinney, R.E. Whipples, J.S. Haas, A. Alcarez, J.E. Andrews, G.L. Klunder, R.E. Russo, T.E. Fickies, G.E. Pelkey, B.D. Andresen, D.A. Kruchten, S. Cantlin. "Nuclear Forensics in Law Enforcement Applications," *Journal of Radioanalytical and Nuclear Chemistry*, 235:129-132 (1998).

Gunther, J. *Hohlraum Characterization Milestones.* UCRL-TR-210899. Washington: GPO, March 29, 2005.

Halverson, J.E. and D.M. Beals. *Trace Analytical Techniques for Nuclear Forensics*. WSRC-MS-99-00357. Springfield, VA: Office of Scientific and Technical Information, 1999.

Hou, Xiaolin, and Per Roos. "Critical Comparison of radiometric and Mass Spectrometric Methods for the Determination of Radionuclides in environmental, Biological and Nuclear Waste Samples." *Analytica Chimica Acta*, 608:105-139 (2008).

Inn, Kenneth G.W., Hiromu Kurosaki, Carole Frechou, Chris Gilligan, Robert Jones, Stephen LaMont, Jeff Leggitt, Chunshen Li, Keith McCroan, Ronald Swatski. "A Blueprint for Radioanalytical Metrology CRMs, Intercomparisons, and PE," *Applied Radiation and Isotopes*, 66:835-840 (2008).

Jakopič, Rožle, Stephan Richter, Heinz Kuhn, Ljudmila Benedik, Boris Pihlar, Yetunde Aregb. "Isotope Ratio Measurements of pg-size Plutonium Samples Using TIMS in Combination with "Multiple Ion Counting" and Filament Carburization," *International Journal of Mass Spectrometry*, 279:87-92 (2009).

Keegan, Elizabeth, Stephan Richter, Ian Kelly, Henri Wong, Patricia Gadd, Heinz Kuehn, and Adolfo Alonso-Munoz. "The Provenance of Australian Uranium Ore Concentrates by Elemental and Isotopic Analysis," *Applied Geochemistry*, 23:765-777 (2008).

Kips, Ruth, Ann Leenaers, Gabriele Tamborini, Maria Betti, Sven Van den Berghe, Roger Wellum, and Philip Taylor. "Characterization of Uranium Particles Produced by Hydrolysis of UF_6 Using SEM and SIMS," *Microscopy and Microanalysis*, 13:156-164 (2007).

Kohli, Rajiv and K. L. Mittal. *Developments in Surface Contamination and Cleaning: Fundamentals and Applied Aspects*. Norwich, NY: William Andrew Inc., 2008.

LaMont, Stephen P., Robert E. Steiner, Kenneth Inn, Stephen Goldberg and Jeffrey Liggett. "Reference Materials for Nuclear Forensics Quality Assurance," *Transactions of the American Nuclear Society*, 98:822-823 (2008).

Massila, K., R. D. Stein, S. M. Suhaizan, and A. A. Azlianor. "Theoretical Isotope Generator: An Alternative towards Isotope Pattern Calculator," *World Academy of Science, Engineering and Technology*, 27:146-149 (2007).

Mayer, K., M. Wallenius and T. Fanghänel. "Nuclear Forensic Science-From Cradle to Maturity," *Journal of Alloys and Compounds*, 444-445:50-56 (2007).

Montana State University (MSU), "Thermal Ionization Mass Spectrometry (TIMS)," Technical information provided on MSU web page. http://serc.carleton.edu/research_education/geochemsheets/techniques/TIMS.html. 10 Jul 2009.

Montana State University (MSU), "Time-of-Flight Secondary Ion Mass Spectroscopy (ToF-SIMS) ," Technical information provided on MSU web page. http://serc.carleton.edu/research_education/geochemsheets/techniques/ToFSIMS.html. 25 June 2009.

Morrall, P., D. W. Price, A. J. Nelson, W.J. Siekhaus, E. Nelson, K. J. Wu, M. Stratman and W. McLean II. "TOF-SIMS Characterization of Uranium Hydride." *Philosophical Magazine Letters*, 87(8):541-547 (August 2007).

Morrall, P., D. Price, A. Nelson, W. Siekhaus, E. Nelson, K. J. Wu, M. Stratman, B. McLean. *ToF-SIMS Study of Polycrystalline Uranium after Exposure to Deuterium*. UCRL-JRNL-218359. Lawrence Livermore National Laboratory, January 24, 2006.

Nagy, G. and A.V. Walker. "Enhanced Secondary Ion Emission with a Bismuth Cluster Ion Source," *International Journal of Mass Spectrometry*, 262:144-153 (2007).

Nelson, A., W. Moberlychan, R. A. Bliss, W. Siekhaus, T. Felter, and J. Denliner. *Comparative experimental study of x-ray absorption spectroscopy and electron energy loss spectroscopy on passivated U surfaces*. UCRL-PROC-226789. Lawrence Livermore National Laboratory, December 13, 2006.

Nelson, A. J., T. E. Felter, K. J. Wu, C. Evans, J. L. Ferreira, W. J. Siekhaus and W. McLean. "Uranium Passivation by C^+ Implantation: A Photoemission and Secondary Ion Mass Spectrometry Study," *Surface Science*, 600:1319-1325 (2006).

Nicolaou, G. "Determination of the Origin of Unknown Irradiated Nuclear Fuel." *Journal of Environmental Radioactivity*, 86:313-318 (2006).

Nittler, Larry R. and Alexander, Conel M. O'D. "Automated Isotopic Measurements of Micron-sized Dust: Application to Meteoritic Presolar Silicon Carbide," *Geochimica et Cosmochimica Acta*, 67(24):4961-4980 (2003).

Ohashi, Hiroshi, Etsuzo Noda and Takahashi Morozumi. "Oxidation of Uranium Dioxide," *Journal of Nuclear Science and Technology*, 11(10):445-451 (October 1974).

Pajo, L., G. Tamborini, G. Rasmussen, K. Mayer and L. Koch. "A Novel Isotope Analysis of Oxygen in Uranium Oxides: Comparison of Secondary Ion Mass Spectrometry, Glow Discharge Mass Spectrometry and Thermal Ionization Mass Spectrometry," *Spectrochimica Acta Part B*, 56:541-549 (2001).

Pajo, Leena K. UO_2 Pellet Impurities, Pellet Surface Roughness and $n(^{18}O)/n(^{16}O)$ Ratios, Applied to Nuclear Forensic Science. Doctoral Dissertation AAIC806683, University of Helsinki (2001).

Phinney, Douglas. "Quantitative Analysis of Microstructures by Secondary Ion Mass Spectrometry," *Microscopy and Microanalysis*, 12:352-355 (2006).

Physical Electronics Incorporated (PHI), "PHI nano-TOF Product Brochure," Technical information provided on PHI web page. https://www.phi.com/products/nanoTOF/nanotof-brochure.pdf. 9 July 2009.

Physical Electronics Incorporated (PHI), "TOF-SIMS Surface Analysis," Technical information provided on PHI web page. http://www.phi.com/techniques/tof-sims.html. 25 June 2009.

Plog, C., L. Wiedmann, and A. Benninghoven. "Empirical Formula for the Calculation of Secondary Ion Yields from Oxidized Metal Surfaces and Metal Oxides," *Surface Science*, 67:565-580 (1977).

Portier, S., S. Brémier, and C.T. Walker. "Secondary Ion Mass Spectrometry of Irradiated Nuclear Fuel and Cladding: An Overview," *International Journal of Mass Spectrometry*, 263:113-126 (2007).

Ravanel, X., C. Trouiller, M. Juhel, C. Wyon, L. F. Tz. Kwakman, and D. Léonard. "Static time-of-flight secondary ion mass spectrometry analysis of microelectronics related substrates using a polyatomic ion source," *Applied Surface Science*, 255:1440-1442 (2008).

Sandia National Laboratories. *Optimization of Thermochemical, Kinetic, and Electrochemical Factors Governing Partitioning of Radionuclides During Melt Decontamination of Radioactively Contaminated Stainless Steel*. Project ID No. 60363; Year 2. Sandia National Laboratories, June 15, 1999.

Schueneman, Richard A. Oxidation at Surfaces of Uranium Oxide Particles. Master's Thesis AFIT/GNE/ENP/01M-05, Air Force Institute of Technology (2001).

Schueneman, R. A., A.I. Khaskelis, D. Eastwood, W.J. van Ooij, and L.W. Burggraf. "Uranium oxide weathering: spectroscopy and kinetics," *Journal of Nuclear Materials*, 323:8-17 (2003).

Simons, D. S., G. Gillen, C. J. Zeissler, R. H. Fleming and P. J. McNitt, P. J. "Automated SIMS for determining Isotopic Distributions in Particle Populations," in *Secondary Ion Mass Spectrometry SIMS XI*. Ed. G. Gillen, R. Lareau, J. Bennett and F. Stevie. Hoboken NJ: John Wiley and Sons, Inc., 1998.

Skoog, Douglas A., Holler, James F. and Crouch, Stanley R. *Principles of Instrumental Analysis* (6th Edition). Fort Worth: Saunders College Publishing, 2006.

Tamborini, G., D. Phinney, O. Bildstein, and M. Betti. "Oxygen Isotopic Measurements by Secondary Ion Mass Spectrometry in Uranium Oxide Microparticles: A Nuclear Forensic Diagnostic," *Analytical Chemistry*, 74:6098-6101 (2002)

U.S. Nuclear Regulatory Commission (NRC). "Special Nuclear Material," (February, 2007). 1 October 2009 http://www.nrc.gov/materials/sp-nucmaterials.html

Vickerman, John C., Alan Brown, and Nicola M. Reed. *Secondary Ion Mass Spectrometry Principles and Application*. New York: Oxford University Press, 1989.

Wallenius, M., K. Mayer and I. Ray. "Nuclear Forensic Investigations: Two Case Studies," *Forensic Science International*, 156:55-62 (2006).

Wilson, R. G., F. A. Stevie, and C.W. Magee. *Secondary Ion Mass Spectrometry: A Practical Handbook for Depth Profiling and Bulk Impurity Analysis*. New York: John Wiley and Sons, 1989.

Wucher, A. "Molecular secondary ion formation under cluster bombardment: A fundamental review," *Applied Surface Science*, 252:6482-6489 (2006).

Yang, Hee-Chul, Jae-Hee Lee, Jung-Guk Kim, Jae-Hyung Yoo, and Joon-Hyung Kim. "Behavior of Radioactive Metal Surrogates Under Various Waste Combustion Conditions," *Journal of the Korean Nuclear Society*, 34(Fischer, 2007):80-89 (February, 2002).

Zhu, Ying-Jie, Neal Olson and Thomas P. Beebe, Jr. "Surface Chemical Characterization of 2.5μm Particulates ($PM_{2.5}$) from Air Pollution in Salt Lake City Using TOF-SIMS, XPS and FTIR," *Environmental Science and Technology*, 35:3113-3121 (2001)

REPORT DOCUMENTATION PAGE

Form Approved
OMB No. 074-0188

PLEASE DO NOT RETURN YOUR FORM TO THE ABOVE ADDRESS.

1. REPORT DATE *(DD-MM-YYYY)*	**2. REPORT TYPE**	**3. DATES COVERED** *(From – To)*
25-03-2010	Master's Thesis	March 2009 – March 2010

4. TITLE AND SUBTITLE
Nuclear Forensics: Measurements of Uranium Oxides Using Time-of-Flight Secondary Ion Mass Spectrometry (TOF-SIMS)

5a. CONTRACT NUMBER
5b. GRANT NUMBER
5c. PROGRAM ELEMENT NUMBER

6. AUTHOR(S)
Schuler, Wesley A., MSgt, USAF

5d. PROJECT NUMBER
5e. TASK NUMBER
5f. WORK UNIT NUMBER

7. PERFORMING ORGANIZATION NAMES(S) AND ADDRESS(S)
Air Force Institute of Technology
Graduate School of Engineering and Management (AFIT/EN)
2950 Hobson Way, Building 640
WPAFB OH 45433-8865

8. PERFORMING ORGANIZATION REPORT NUMBER
AFIT/GWM/ENP/10-M03

9. SPONSORING/MONITORING AGENCY NAME(S) AND ADDRESS(ES)
Sponsor requested to be unnamed.

10. SPONSOR/MONITOR'S ACRONYM(S)

11. SPONSOR/MONITOR'S REPORT NUMBER(S)

12. DISTRIBUTION/AVAILABILITY STATEMENT
APPROVED FOR PUBLIC RELEASE; DISTRIBUTION UNLIMITED.

13. SUPPLEMENTARY NOTES

14. ABSTRACT

Over the past decade, law enforcement, governmental and public agencies have been stymied by the threat of the trafficking of nuclear materials. During this time span, reports from the International Atomic Energy Agency of illicit trafficking have increased eightfold from 20 to 160. For this reason, nuclear forensics is a burgeoning science focused on the identification of seized special nuclear materials. Identification of these materials is based upon the wealth of information that can be obtained by applying multiple analytical and measurement technologies. All of the information gained from each sample can then be used to further characterize other samples culminating in the inclusion of all of the collected data into a central database. Information must be reported in a timely manner as actionable results need to be presented as quickly as possible if there is to be any attribution for trafficking of nuclear material. Identification parameters such as uranium content, isotopic composition, and levels of impurities can be measured simultaneously in an effort to completely characterize a sample. All of these measurements combined can offer information as to the source of the material and its intended use. Many of the current analytical techniques used in nuclear forensics require extensive sample preparation and offer minimal amounts of information about the sample. Time-of-Flight Secondary Ion Mass Spectrometry (TOF-SIMS) is presented as a rapid analytical technique that provides many of these identification parameters with minimal sample preparation. TOF-SIMS spectra were collected on eight different standard reference materials covering a range of stoichiometries and levels of enrichment. Samples included UO_2, UO_3 and U_3O_8 stoichiometries ranging from slightly depleted (0.5% ^{235}U) to highly enriched (90.0% ^{235}U) uranium. Spectra were simulated in an effort to deconvolve composite peaks resulting from the protonation of cluster ions. The levels of protonation were quantified through the solutions of series of simultaneous equations. Spectra were then reassessed with a hydrocarbon subtraction from the $^{235}UO_2$+ and $^{238}UO_2$+ peaks to provide extremely accurate isotopic measurements. Analysis of the results revealed that actionable information could be determined rapidly with minimal sample preparation.

15. SUBJECT TERMS
Nuclear, forensics, uranium, time-of-flight, secondary ion mass spectrometry, nonproliferation

16. SECURITY CLASSIFICATION OF:			**17. LIMITATION OF ABSTRACT**	**18. NUMBER OF PAGES**	**19a. NAME OF RESPONSIBLE PERSON**
a. REPORT	**b. ABSTRACT**	**c. THIS PAGE**			Larry Burggraf, Ph.D, AFIT
U	**U**	**U**	**UU**	188	**19b. TELEPHONE NUMBER** *(Include area code)* 785-3636 x4507 Larry.Burggraf@afit.af.mil

Standard Form 298 (Rev. 8-98)
Prescribed by ANSI Std. Z39-18